2014-01-14

Automated Control for Oil Sands SAGD Operations

Guo, Tao

UNIVERSITY OF CALGARY

Automated Control for Oil Sands SAGD Operations

By

Tao Guo

A THESIS

SUBMITTED TO THE FACULTY OF GRADUATE STUDIES

IN PARTIAL FULFILMENT OF THE REQUIREMENT FOR THE

DEGREE OF MASTER OF SCIENCE

DEPARTMENT OF CHEMICAL AND PETROLEUM ENGINEERING

CALGARY, ALBERTA

JANUARY, 2014

Abstract

The Steam Assisted Gravity Drainage (SAGD) process is widely used in the Athabasca oil sands deposit to recover extra heavy oil, also referred to as bitumen. Since the viscosity of bitumen is high, typically over 1 million cP, at original reservoir conditions, heat is required to lower its viscosity to the point it becomes mobile enough to be recovered under gravity drainage. To heat the reservoir, steam is injected into the formation and thus SAGD is energy intense – on average, the steam-to-oil ratio (SOR) is equal to about 3.5 m^3 (expressed as cold water equivalent) of steam injected per m^3 of bitumen produced. Given that the fuel used to generate steam is the largest operating cost, the SOR is a key control on the economics of any SAGD project. The target for many SAGD operations is a SOR lower than $2.5m^3/m^3$. However, very few field operations have achieved this threshold. Here, the use of dynamic distributed steam injection within a pad of SAGD wellpairs controlled via a Proportional-Integral-Derivative (PID) feedback controller to lower the SOR is explored, a concept we refer to as Smart Pad. The Smart Pad is designed to dynamically distribute steam injection along multiple well pairs so that over a period of operation, the pad-scale cSOR is lowered as the process evolves. First, a method to condition the PID control gains is described and second, the controller is applied to a multiple well pair SAGD pad in a typical Athabasca oil sands reservoir. The results demonstrate that automated control can lead to improvements of the SOR over that of constant pressure. The results show that automated PID control is able to detect “sweet spots” (oil zones with better geological properties) in the reservoir and dynamically deliver more steam to that region. Meanwhile, it reduces the steam injection towards relatively worse quality zones, i.e. shale barriers, to lower the local SOR. In this manner, the PID feedback controller provides an effective method to control SAGD operations, especially over the first 7 to 10 years of operation, where for the same amount of steam injection, it helps to achieve reduced cSOR and increased oil recovery. Also, since the PID controller dynamically controls the process according to its performance, the method appears to reduce the degree of dependence of SAGD operation on knowledge of the geological conditions of the reservoir. The algorithm described could be applied to any operating or new SAGD pad.

Acknowledgements

First of all, I would like to give my hearty appreciate to my supervisor Dr. Ian D. Gates, who has provided the opportunity for such an interesting and exciting research topic. I really enjoyed the work for the two years of my M.Sc. study. Ian has been a great mentor and supported me when I need it the most. I also liked his humor, which makes meeting a happy time. I also like to thank Jacky Wang, my co-author and colleague. He has provided me invaluable help at the beginning stage of my research work and that was a time when I have no much clue what I was doing. I also like to share opinions and discuss on various topics with Jacky, be it academia, life in general, investment or automobiles (we both love cars). I appreciate his knowledge and ideas which often inspired me on my work. I would say that without Ian and Jacky, I would not be able to finish this thesis. Also my thanks to Carbon Management Canada (CMC), I appreciate their funds on my study. I am proud that my research may help to reduce CO2 emission. I have made effort to a green planet.

What's more, I would like to thank my mother and father for their love and understanding. I highly doubt they have any clue what I am doing here in Calgary, but they show their support and care in their own ways. I would also like to specially thank my girlfriend, soon to be my fiancée, Jaclyn Wang. In all, they motivate me to finish my work. Without their support, this thesis would neither be possible.

Table of Contents

List of Tables

List of Figures and Illustrations

List of Symbols, Abbreviations and Nomenclature

Symbol	Definition
SAGD	Steam assisted gravity drainage
CSS	Cyclic Steam Stimulation
cSOR	Cumulative Steam to Oil Ratio
iSOR	Instantaneous Steam to Oil Ratio
ICV	Inflow Control Valve
ICD	Inflow Control Device
FCV	Flow Control Valve
PICD	Passive Inflow Control Device
PID	Proportional Integral Derivative Control
POCD	Passive Outflow Control Device
FDC	Flow Distribution Control
Kp	Proportional control gain
TI	Integral control gain
TD	Derivative control gain
t	time
e	error between actual and target iSOR, m^3/m^3
CWE	Cold Water Equivalent
DTS	Distributed Temperature Sensor
Q	Pressure differential between the upstream and downstream flow
ΔP	Derivative control gain
K	Permeability of the flow media
u	Fluid viscosity
A	The cross section area of the flow pathway
OOIP	Original oil in place

Chapter One: **Introduction**

1.1 Alberta Crude Bitumen Deposit

Western Canada hosts over 1.7 trillion barrels of unconventional crude oil in the form of heavy oil and extra heavy oil (Alberta Energy Regulator 2013). Of this resource, about 10% is recoverable with existing technology from oil sands reservoirs. The majority of the unconventional oil is extra heavy oil (often referred to as bitumen) with API gravity lower than 10°API and viscosities greater than 1 million cP. In other words, in its natural state, the oil flows very slowly – if left to flow from a coffee cup, it might take weeks for part of the bitumen to flow to the edge of the cup. This means that the oil is not producible from underground reservoirs under natural conditions.

Figure 1-1 displays an example of the bitumen viscosity versus temperature. For most oil sands reservoirs, the original reservoir temperature is between about 7 and 14°C and thus, the viscosity of the oil is typically greater than 100,000 and often in the millions of cP. Thus, one of the main challenges for producing this oil is first the task of mobilizing the oil, in other words, reducing its viscosity so that it can be produced to surface with existing drive forces. If a target is to get the oil viscosity below about 10 cP, this implies that the temperature required is equal to about 200°C.

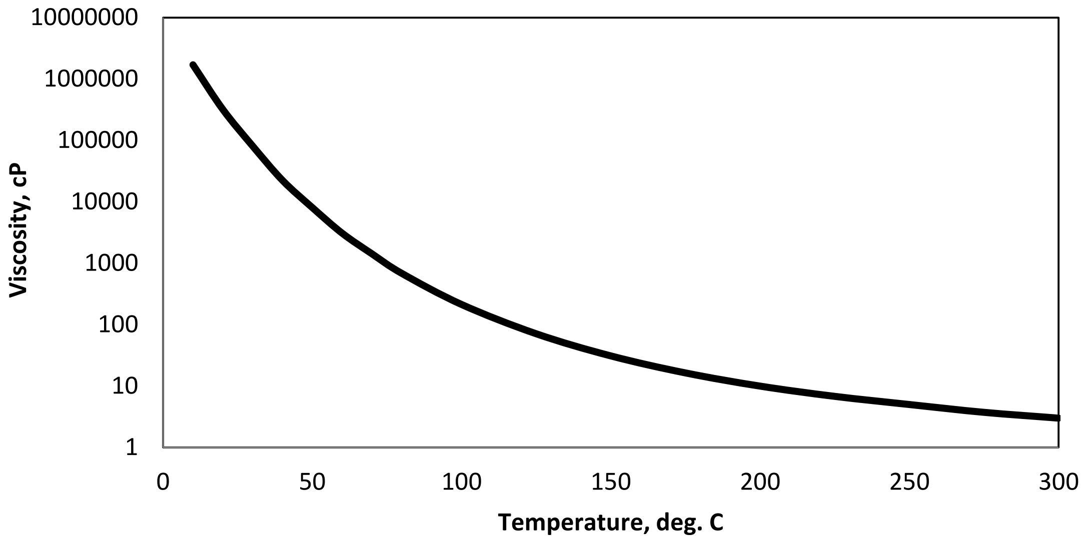

Figure 1-1: Effect of temperature on viscosity of Athabasca crude bitumen (modified from Mehrotra and Svrcek, 1986).

In the Western Canadian Sedimentary Basin, the majority of the crude bitumen is contained in three main deposits in northern Alberta: the Athabasca Wabiskaw, the Cold Lake and Peace River deposits, as shown in Figure 1-2 below. The main oil sands formations for the Athabasca, Cold Lake, and Peace River deposits are the McMurray, Clearwater, and Bluesky Formations, respectively.

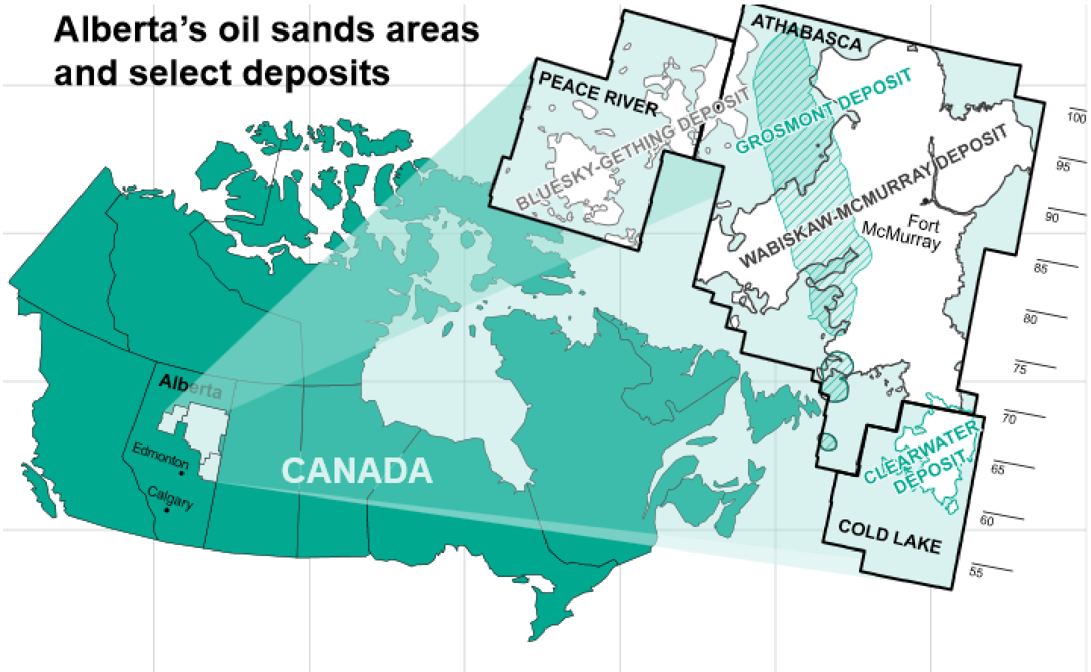

Figure 1-2: Location of the three major crude bitumen deposit in northern Alberta: Athabasca, Cold Lake and Peace River (ST98-2013 Alberta Energy Regulator).

For oil sands reservoirs hosted in the Athabasca, Cold Lake, and Peace River areas, there are currently three main methods for producing heavy and extra heavy oil: cold production, Cyclic Steam Stimulation (CSS) and Steam Assisted Gravity Drainage (SAGD) (Alberta Energy Regulator 2013). Cold production is commonly used in lower viscosity heavy oil reservoirs, typically between 1,000 and 50,000 cP. The process typically recoveries about 10% of the oil in place and thus follow-up processes such as water or polymer or solvent injection are being used to raise the recovery factor. These follow-up processes are non-thermal because cold production reservoirs tend to be relatively thin and thermal recovery technologies would suffer excessive heat losses if used. In 2012, roughly 25 per cent of in situ recovered unconventional crude oil was accomplished by cold and non-thermal production.

CSS, also known as the Huff and Puff method, consists of three stages: 1. steam injection, 2. soak, and 3. production. Steam is first injected to heat bitumen in the reservoir. The injection pressure is usually higher than rock fracture pressure threshold and thus the reservoir is steam-fractured to enhance injectivity. After the desired amount of steam has been injected into the formation, the well is usually shut in for a few days for the heat to distribute within the formation from the steam-fractured zone, in other words, the heat 'soaks' into the reservoir. Thereafter, oil production is started on the same well, at first by natural flow and then by artificial lift. Production rates decline as the reservoir pressure falls and the oil cools down. At some point, production is stopped when the oil rate reaches an economic limit. Next, another cycle is started and the cycles are repeated until the overall process becomes uneconomic. CSS is most used in reservoirs where there is a thick caprock (to withstand the high steam injection pressures required for fracturing the reservoir) and where solution gas content is sufficient to drive oil to the well during the production interval. These types of reservoirs are most found in the Cold Lake and Peace River deposits. In 2012, roughly 26 per cent of in situ oil sands production was recovered by CSS (Alberta Energy Regulator 2013).

1.2 Steam Assisted Gravity Drainage (SAGD)

SAGD was an oil sand recovery process originally proposed by Roger Butler while at Imperial Oil in the late 1970's (Butler, 1982). This technology was then tested in several phases at the Alberta Oil Sands Technical Research Authority (AOSTRA) Underground Test Facility (UTF) with success. It has been commercially in use since 2001 on most new thermal projects in the Athabasca oil sands deposit since it can be operated at relatively low pressure in reservoirs with very low solution gas content. The SAGD process, shown in Figure 1-3, consists of two horizontal wells, one atop the other. The top well is the steam injection well whereas the bottom well is the fluid production well. In typical practice, the wells are separated by about 5 meters (Butler, 1997). Steam, typically of quality higher than 90 per cent, is continuously injected into the top well and reservoir fluids are continuously produced from the lower production well.

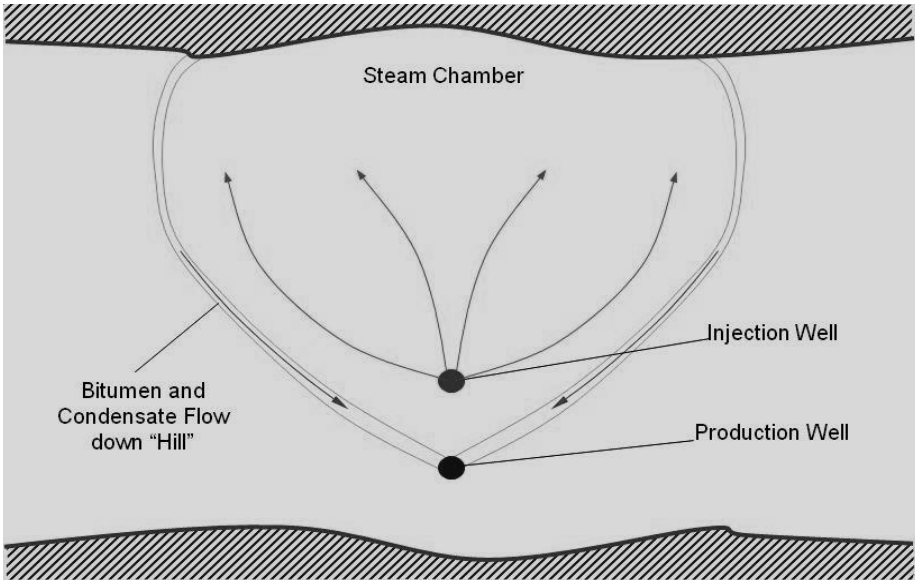

Figure 1-3: Cross-section view of the Steam Assisted Gravity Drainage process. The wells are horizontal wells that go into the page.

In SAGD, the injection steam flows into a steam chamber, a region depleted of oil. The injected steam flows to the edge of the chamber and releases its latent heat to the cold bitumen, which in turn becomes hot, mobile (lower viscosity), and flows through and along the edges of the chamber, under the action of gravity, to the production well located at the bottom of the steam chamber (Gates, 2011). A typical SAGD operation usually involves several stages. The first stage is referred to as the pre-heating or steam circulation stage. During this period (normally between 3 and 6 months long), steam is circulated through both the injection and production wells so as to establish thermal communication between the two wells. In circulation, steam is often injected into both wells at reservoir pressure through tubing strings and produced back to surface through both wells. In this manner, the wells act like line heaters within the reservoir. The purpose of the pre-heat stage is to heat the bitumen between the top and bottom wells so that when SAGD starts, the oil between the wells is mobilized enough to drain into the production well to create the steam chamber (Gates, 2011). Following the pre-heat stage is the steam chamber growth. During this period, steam is continuously injected into formation and steam rises to heat the surrounding oil sands and oil drains to the production well. Here, the initial steam chamber grows both vertically and laterally. In this stage, the oil rate increases as the steam chamber grows and more oil is mobilized and drains to the production well. The injection pressure at this stage is often maintained higher than the reservoir pressure to promote steam chamber growth but lower than formation fracture limit to protect formation integrity. During this stage, all heat losses from the injected steam are to the oil sands reservoir. Depending on the thickness of pay zone, sooner or later, SAGD operation enters into the plateau stage where the steam chamber reaches the top of the pay zone. During this stage, as more steam is injected into the formation, the steam chamber only extends laterally across the reservoir. A portion of the heat injected is now lost to the overburden. Thus, the thermal efficiency of the process declines. In SAGD, the single most important factor to evaluate thermal efficiency is the Steam-to-Oil Ratio (SOR), which measures the amount of steam required (this is a cost since fuel is consumed to generate steam) to produce a unit amount of oil. The steam injection pressure is often lowered during the plateau stage to improve thermal efficiency. At the end of the plateau stage, adjacent steam chambers may eventually meet each other and merge to form a conglomerate steam chamber. The operation life of a SAGD project can be as long as 30 years (ConocoPhillips Canada, 2010). Because of the increased oil recovery ratio and thermal efficiency, SAGD technology is becoming the major choice of in situ production method in Athabasca oil sands recovery. In 2012, 49 per cent of in situ oil sands production was recovered by SAGD (Alberta Energy Regulator 2013).

The SAGD process is energy-intensive. To produce each cubic meter of bitumen, from field data, between 2 and 5+ cubic meters of steam (in cold water equivalent, CWE) are required (Gates, 2011). Thus, steam generation costs and recycling in SAGD operation is an essential concern. In field operations, there are several reasons why injected steam does not deliver heat energy efficiently to bitumen leading to reduced thermal efficiency. One of the main reasons is the underlying geology of oil sands formations and their heterogeneity. One other reason is due to well placement – they are not perfectly horizontal and may have significant undulations along their trajectories. Another reason is due to the operation strategy itself. For example, as steam reaches the overburden, a fraction of the injected heat is lost to the caprock which despite its energy investment, returns no oil for production. Water-saturated shale barriers imbedded in pay zone also consume heat of steam without producing oil. Furthermore, if the shale barriers are laterally extensive and/or located close enough to the injection wells, these barriers retard or even stop vertical propagation of the steam chamber (Bois et al, 2011; Hubbard et al. 2011; Su et al. 2013). In field operations, in the absence of subcool steam-trap control, it is also observed that injected steam can be produced by the production well without delivering heat energy to the oil sands formation. (Ito and Suzuki, 1999; Edmunds, 1998; Gates and Leskiw, 2010).

Many SAGD operators have hot and cold spots along the wellpairs arising from heterogeneity of the reservoir. This leads to poor wellpair utilization and thus, there is a need to improve the operating performance of SAGD especially in the context of its energy and greenhouse gas emissions intensities and water consumption as well as the perception that oil sands recovery processes are 'dirty oil' recovery processes. Although there have been many different approaches pursued to achieve lower steam-to-oil ratios and improved water consumption including steam-non-condensable gas methods, steam-solvent methods, multiple tubing string injection and production points, improvements in well liner design, use of limited entry perforations (also referred to as in-flow/out-flow devices), in/out flow control devices, it remains unclear which is the final answer although it will most likely be a combination of several approaches. Here, the focus of this thesis is on automated control strategies for SAGD.

1.3 Research Questions

This thesis documents an investigation on applying Proportional-Integral-Derivative (PID) feedback control to a pad-scale SAGD operation. The research questions are as follows:

1. What instruments and devices can help improve steam conformance in SAGD?
2. Can automated control by using a PID controller improve SAGD performance? How does a PID feedback controller maintain a target SOR in SAGD?
3. How does PID feedback controller dynamically distribute steam among well pairs to improve steam efficiency?

1.4 Organization of Thesis

The thesis is divided into five Chapters. Chapter 2 is a literature review that includes a brief introduction to SAGD, issues confronted by SAGD, the Surmont SAGD operation, an introduction of the PID feedback control and ICV and how they are used to improve steam conformance in SAGD, and a review of automated control for in situ SAGD operations. Chapter 3 describes a detailed numerical simulation study to evaluate the impact of PID feedback control on SAGD. Chapter 4 further explores the benefits of PID feedback control on SAGD operation, but this time focus on its functionality of dynamically distributing steam to improve steam efficiency. In the end, conclusions and recommendations from this study are listed in Chapter 5.

Chapter Two: **Literature Review**

2.1 The Challenge of SAGD

SAGD is a complicated operation that involves heat exchange and multiple-phase fluid flow. In addition, reservoir heterogeneity affects SAGD performance. For example, imbedded shale layers could change steam flow path and reduce thermal efficiency. In addition, the long horizontal well pairs face issues in the uniformity of flow profile along wellbores. For example, steam would lose thermal load as it travels down the well and inflow fluid would become more difficult to flow as it becomes far from wellhead, due to friction pressure drop. Live steam production is another challenge in SAGD, where injected steam is produced directly from producer, without doing heat exchange with the bitumen.

In SAGD, the fundamental challenge is to efficiently utilize steam. If sufficient steam is provided and the cost of steam is not considered, then eventually most oil will be recovered. However, the recovered bitumen may not justify the cost of steam generation, which is the single biggest expenditure in SAGD. Steam-to-oil ratio (SOR) is a good indicator of thermal efficiency. It measures the amount of steam needed to recovery a unit amount of oil. Thus, lower SOR indicates better thermal efficiency.

Since SAGD requires steam injection and steam is mostly generated by burning natural gas, CO2 emission is another issue. The solution of less CO2 emission also ties to the SOR of SAGD, since a lower SOR means less steam injection for the same amount of oil produced. This is also a motivation of this thesis, which is to reduce CO2 emission in SAGD by improving thermal efficiency, or the SOR.

For an ideal SAGD well pair, steam would be uniformly injected along the well length and a uniform steam chamber would form surrounding the wellbore. However, in reality, rarely can steam be uniformly injected along the well, thus steam conformance can not be achieved. The main challenge is the reservoir heterogeneity and fluid dynamics along long pipes. Steam naturally follows the least-resistance path to flow. Thus, if a portion of the well length is surrounded by shale barrier, which is ultra-low in permeability, then steam simply not flows there. Also, for an 800 meter long well with continuous perforation, as steam is injected at the wellhead, more steam exits the tubing at the heel than at the toe, leaving the toe end temperature low while the heel end producing live steam. Steam conformance is important to SAGD efficiency, since worse conformance means less steam-bitumen contact areas, which reduces the effective well length.

2.2 Proportional Integral and Derivative (PID) Feedback Control

2.2.1 Control Theory

Control theory is an interdisciplinary branch of engineering and mathematics that deals with the behavior of dynamics systems with inputs. A controller manipulates the input to a system to obtain the desired effect on the output of the system. The usual objective of a control theory is to calculate solutions for the proper corrective action from the controller that result in system stability, that is, the system will hold the set point and not oscillate around it (William, 1996). A control system may be thought of as having four functions: measure, compare, compute and correct.

A controller can be divided into two categories: open-loop controller and closed-loop controller. An open-loop controller, also called a non-feedback controller, is a type of controller that computes its input into a system using only the current state and its model of the system (Kuo, 1991). An open-loop controller is often used in simple process because of its simplicity and low cost, especially when feedback is not critical. Open-loop control is useful for well-defined systems where the relationship between input and the resultant state can be modeled by a mathematical formula. For example, determining the voltage to be fed to an electric motor that drives a constant load, in order to achieve a desired speed would be a good application of open-loop control (Christophe, 2012). A closed-loop controller uses feedback to control states or output of a dynamical system (Franklin, 2002).

Control systems with feedback controllers are useful in reservoir simulation as they enable the maintenance of desired operating conditions of a field. This in turn helps establish automated mechanism in the field, and also in determining long term field operating strategies (Guyaguler, 2009).

2.2.2 PID Controller

The PID controller is one of the most-used feedback control design (Graham, 2001). The PID stands for Proportional, Integral and Derivative. A PID controller calculates an error value as the difference between a measured process variable and a desired set-point. The PID controller remained the most widely used controller in process control until today. An investigation performed in 1989 in Japan indicated that more than 90 per cent of the controllers used in process industries are PID controllers (Araki, 2009). In the absence of knowledge of the underlying process, a PID controller has historically been considered to be the best controller (Stuart, 1993).

The controller attempts to minimize the error by adjusting the process control inputs. The PID controller calculation algorithm involves three separate constant parameters, the proportional, the integral and the derivative values, denoted P, I and D. These values can be interpreted in terms of time and error: proportional constant depends on the present error, integral constant on the accumulation of past errors, and derivative constant depends on rate of change of error. The weighted sum of these three actions is used to adjust the process via a control element, in this study, the steam injection rate at each injection point.

The first published PID controller was proposed by an engineer, Nicolas Minorsky, in 1922. Minorsky was designing an automatic steering system for the US Navy, and based his analysis on observation of a helmsman, observing that the helmsman controlled the ship not only based on the current error, but also on past error and current rate of change (Stuart, 1984). A typical example of PID feedback control loop is the action of maintaining water temperature in a bath. The process often involves adjusting hot and cold water valves to mix the two streams. At certain point of process, the temperature of the mixed water is measured. Based on this feedback, a control action of either adjusting the hot or cold water valves will be performed until the water temperature stabilizes at the desired value. During this process, the sensed water temperature is the process variable or process value. The desired temperature is called the setpoint. The input into the process (the position of hot and cold water valve) is called the manipulated variable. The difference between the temperature measurement and the setpoint is the error and quantifies how far away the bath temperature is from the setpoint (Araki, 2009). The PID feedback controller speeds up the process of approaching the desired bath temperature.

The general PID feedback controller has the following form (Astrom and Hagglund, 1995):

$$u(t) = K_P \left[e(t) + \frac{1}{T_I} \int_0^t e(t)dt + T_D \frac{de(t)}{dt} \right] \tag{1}$$

Where t is time, u(t) is the manipulated variable, e(t) is the observed error between the process variable and the setpoint at time t, K_p is the proportional gain, K_p/T_I is the integral gain, and K_pT_D is the derivative gain. The performance of PID controller depends on three parameters, the proportional gain (K_p), the integral gain (Kp/T_I) and the derivative gain (K_pT_D). The proportional term produces an output that is proportional to the current error. A high proportional gain results in a large change in the output for a given change in the error. If the proportional gain is higher than the optimal gain (or even too low) the system can become unstable. In contrast, a small gain results in a small output response to the same given error, and it results in a less responsive or less sensitive controller. The integral gain is the sum of the instantaneous error over time and gives the accumulated offset that should have been corrected previously. In other words, it represents the cumulative error of the past. It can cause the system to oscillate around the setpoint with decreasing amplitude based on the gain value. The derivative term can reduce the oscillation. However, a derivative gain which is not optimal may drive the system towards instability.

2.3 **Wellbore completion technologies in SAGD**

Since the beginning of SAGD concept, the wellbore completion has seen a gradual change in design to improve SAGD efficiency. SAGD well usually involves open-hole completion with slotted liner installed.

2.3.1 Single Tubing

In the first SAGD wells, steam was typically injected into the heel of the well and fluids were produced from the heel of the well. As steam is injected at the heel, it travels the entire length of the horizontal well (usually between 500 and 1000 m, and typically about 700 m) to reach the far end of the well bore (the toe). The heterogeneity of the reservoir leads to variable injectivity of the steam along the well which leads to non-uniform steam chamber development in the reservoir. This implies poor well utilization – that is, steam is not able to spread evenly along the horizontal well, from the heel to toe. Thus, the SAGD wellpair length that achieves effective steam conformance may be only a fraction of the total well length. This has been observed from seismic interpretation of SAGD Steam chambers (ConocoPhillips Canada, 2013). For the production well where production of fluid occurs only at the heel of the well, the fluid at the toe of the wellbore experiences much higher pressure drop due to friction, as compared to the fluid at the heel, which is much closer to the tubing and the lift system. Thus, the fluid at the heel flows much easier as compared to the fluid at the toe. A consequence will be water coning at the heel, if the production well sits on top of a water zone. Also due to the non-uniform inflow in the wellbore, a steam trap control will be hard to apply along the well, since the liquid level above the producer is rarely uniform. In such case, steam injected from the injection tubing may directly enter the production tubing and being brought to the surface, instead of doing its job of heating up the bitumen and thus SAGD efficiency for delivering steam energy to the oil sand is low.

2.3.2 Dual-Tubing

To improve steam conformance along injection wells and fluid production along production wells, many operators have used multiple tubing strings where for example a tubing string delivers steam to the heel of the well and a second tubing string, landed at the toe of the horizontal well, injects steam at the toe of the well. There are two configuration options for placing the second tubing within the slotted liner: The first one would be to place the toe tubing parallel to the heel tubing, as shown in Figure 2-1. The second option is to make concentric tubing with the toe tubing inside the heel tubing, as depicted in Figure 2-2.

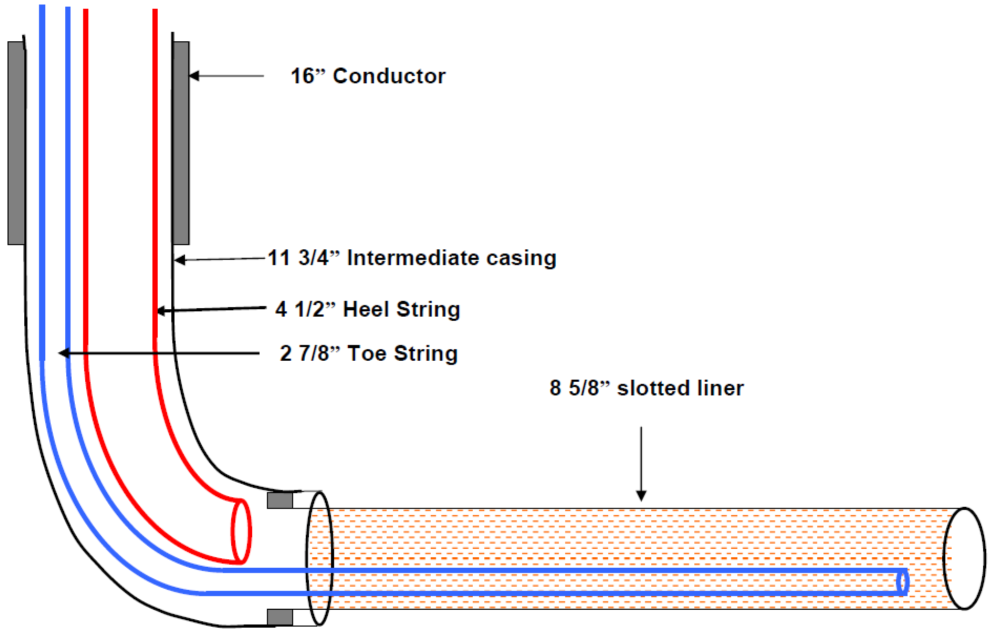

Figure 2-1: Dual tubing injector completion with the heel and the toe tubing placed parallel to each other. (courtesy of ConocoPhillips Canada, 2009).

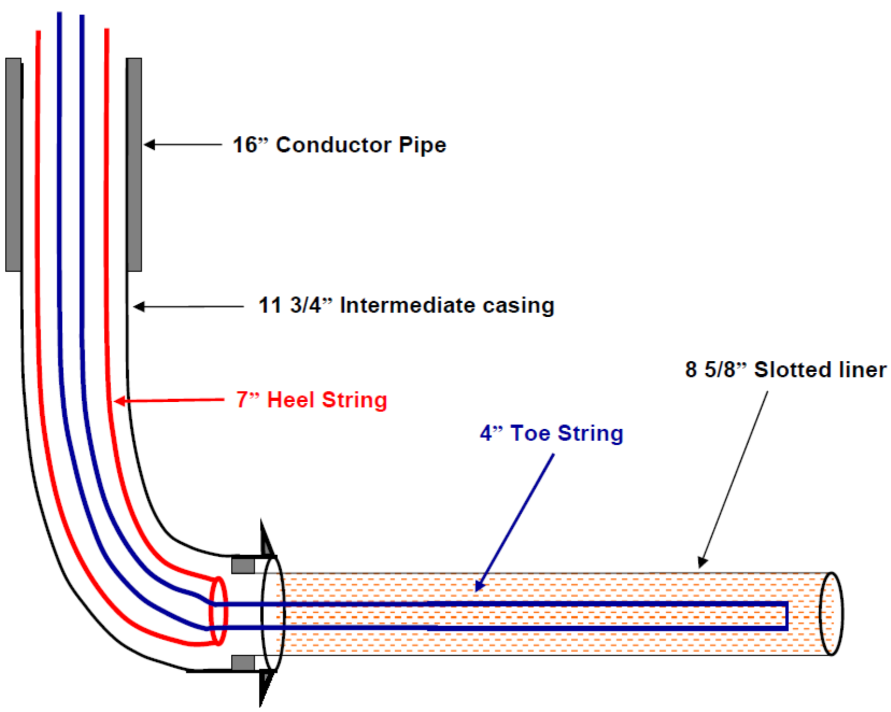

Figure 2-2: Dual tubing injector completion with the heel and the toe tubing concentric to each other (courtesy of ConocoPhillips Canada, 2009).

For many operators, the dual tubing design has become well configuration of choice in current SAGD projects. The benefits of the second tubing landed at the toe are obvious: for injection, steam is now able to be instantaneously injected at both the heel and toe and this can be done with different volumes into each to attempt to balance the steam profile in the injection well to achieve uniform conformance along the wellpair. As a result, the steam conformance at the toe end is significantly improved over the heel-only injection. As mentioned before, an improvement in steam conformance in the toe end quickly increase the effective length of the SAGD well, thus increase oil rate. A second benefit is that with two injection points along the well bore to manipulate, steam trap control becomes easier and more effective. This will be discussed in detail later when introducing the dual tubing injection via PID controller.

For production, the benefit of dual tubing is that fluid is drawn from both ends of the well bore. Thus fluid withdrawing rate increases and inflow becomes more uniform along the horizontal well. Although dual tubing well bore has made improvement over the heel-only tubing, there are still issues involving steam conformance and inflow uniformity. In dual tubing injection, steam conformance usually exhibits a dumbbell-shape, as shown in Figure 2-3. It is because steam transportation from either heel or toe to the middle regions of the horizontal well still faces quality decline and heat loss during the process. Thus, even though steam at the heel and toe injection regions is uniform, it is hardly the same in the middle regions. A simple solution, following the logic will be adding even more tubing in the well bore. However, there is a limitation on the number of tubing that can be placed in the wellbore. If triple tubing are placed in the wellbore, being either side by side or concentric, the volume left for fluid to flow will be less and the fluid volumetric rate will decrease. If a larger well bore is used to accommodate the increasing number of tubing, then the total length of the horizontal well will probably be reduced to ensure drill and completion can still be done within budget and shorter well length means reduced oil rate. Also, the incremental complexity of triple or even more tubing all placed within the same slotted liner may raise reliability and maintenance concern in long-term operation. All in all, for now, dual-tubing design appears to be the majority choice for SAGD projects.

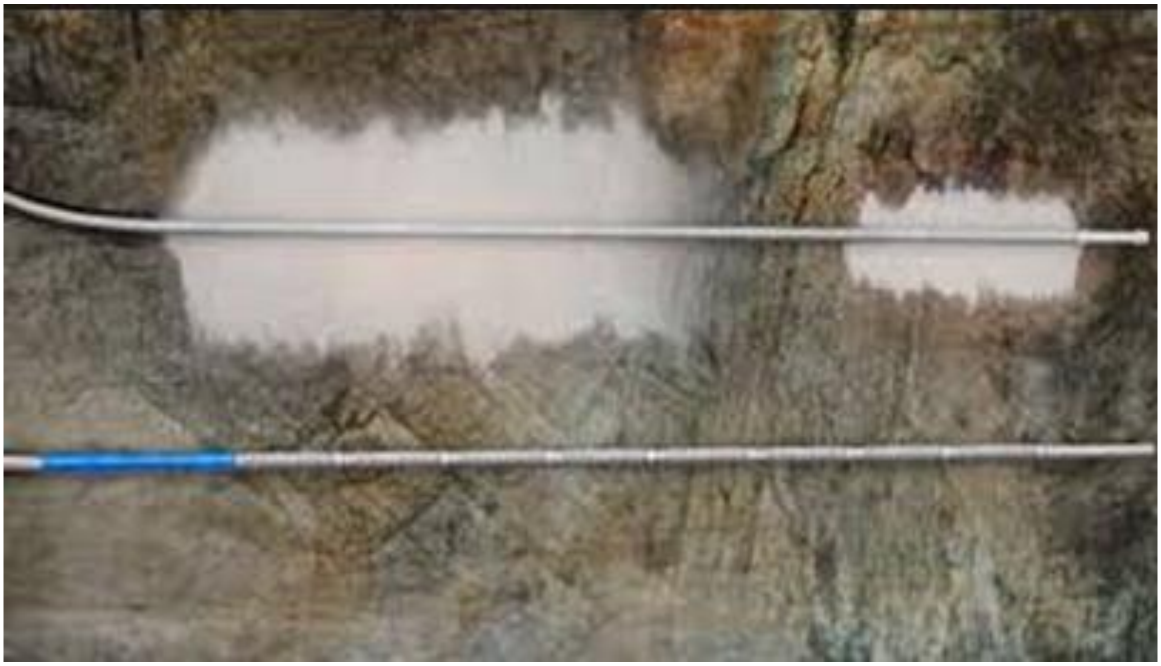

Figure 2-3: Dumbbell-shaped steam conformance in dual tubing injection design (courtesy of Halliburton).

The top well is the dual-tubing injector and the bottom well is the producer in SAGD. It is observed that a large region achieved uniform steam conformance at the heel tubing and a small region at the toe tubing. However, the middle-range area is not contacted by steam.

2.3.3 Slotted Liners

The most common completion design for SAGD wells has been the slotted liner as shown below in Figure 2-4. Slotted liners are used in the horizontal sections as a sand control device. Slotted liners are manufactured by cutting a series of longitudinal slots, typically 0.30–0.46 mm (0.012–0.018 inch) wide by about 50–70 mm (2–2.75 inch) long. Slot width is selected, based on the formation's grain-size distribution, to restrict sand production and allow fluid inflow (Xie, 2007)

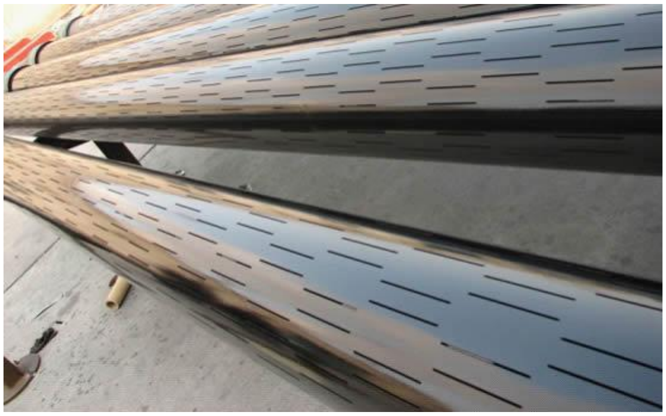

Figure 2-4: Slotted liner in gang pattern or staggered pattern (courtesy of Pioneer Well Screen Co. Ltd).

In general, there are three types of slotted liners, straight pattern, staggered pattern and the gang pattern, as shown below in Figure 2-5.

Figure 2-5 Three different slotted liner patterns (courtesy of Pioneer Well Screen Co. Ltd).

2.3.4 Passive Flow Control – Inflow Control Device (ICD)

To further improve thermal efficiency and SAGD performance, more complex completion designs are being tested in numerical experiments and field pilots. Among those instruments are inflow control devices (ICDs) and Flow Control Valves (FCVs). The names of the devices vary from supplier to supplier, but the essential function remains the same.

Inflow control devices are well completion technologies deployed along the length of the well aimed at distributing the inflow evenly along the length of the well. ICDs usually consist of a choke, orifice, or valve that restricts flow and create additional pressure drop across the device to balance or equalize well bore pressure drop to create a more evenly distributed flow profile along the horizontal well. A schematic plot of an ICD on production well is show in Figure 2-6.

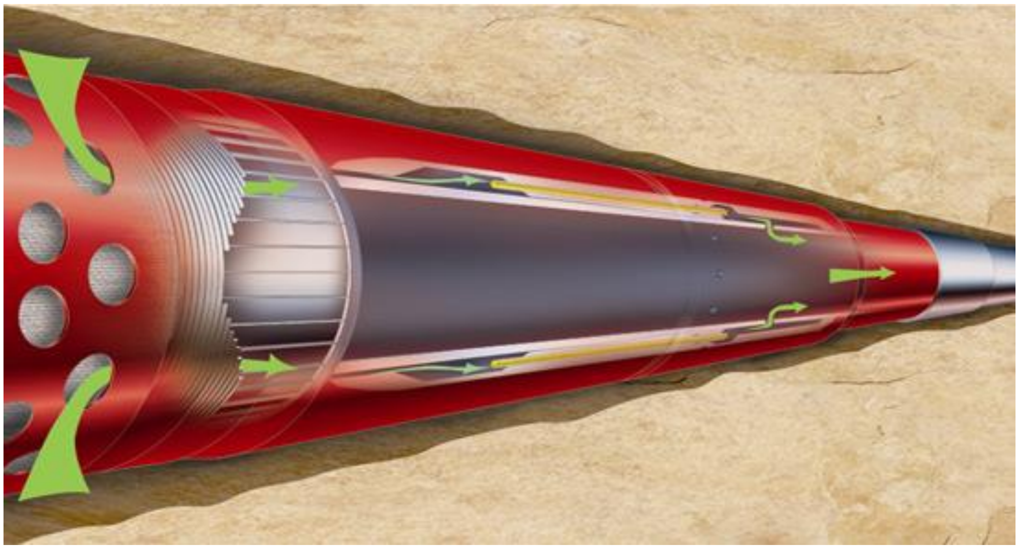

Figure 2-6: A schematic plot of an inflow control device on the production well (courtesy of Halliburton).

For a standard completion, if the drawdown pressure drop is uniform along the well, the flow into the well is controlled by the flow resistance – this in turn is comprised of the flow resistance across the well and the reservoir permeability profile along the well. For the ICD displayed in Figure 2-6, fluid inflow has a limited entrance area through which to flow into the wellbore and tubing. Each ICD can be designed (choke diameter) so that the inflow profile along the well is defined leading to a more uniform flow profile along the well.

ICDs are usually pre-configured on surface and after the deployment, it is not possible to adjust the chokes to alter the flow profile into the well unless a work over is performed where the completion is withdrawn from the well and replaced. When used in a steam injection well, ICDs are able to make more evenly distributed steam injection along the well bore. When used in a SAGD production well, ICDs are able to balance the flow profile along the well and to balance well bore pressure; thus to prevent steam breakthrough and help to achieve steam trap control.

Since ICDs are able to improve inflow profile along production wells and steam conformance along injection wells, additional tubing strings within the wellbore may not be necessary. A single tubing string with multiple ICDs deployed along its length would do the same if not a better job (Stalder, 2013).

2.3.5 Active Flow Control – Flow Control Valve (FCV)

Flow Control Valves (FCVs), also called Interval Control Valves (ICVs), refer to surface controlled down-hole flow control valve – these are adjustable flow valves that can be tuned to make the inflow or outflow from a well along its length more uniform. In general, there are simpler FCVs where the operation is either open or closed and more complex ones where the openings can be varied to alter flow rates through the devices. Whereas ICDs are considered passive flow control device where no adjustment is possible after the ICD is placed in the well, FCVs are active control devices where adjustments can be made as the recovery process evolves. Regardless the structure of various FCV devices, the common principle is that the flow restrictor deployed on the tubing string communicates with the surface for specific adjustments in its setting. FCVs have been used only in a few cases in SAGD injection well to distribute steam injection along horizontal well.

2.3.5.1 On-and-Off mode FCV

One example of a commercial FCV configuration is the sliding sleeve arrangement shown in Figure 2-7. The sliding sleeve FCV has two modes, open or closed. The opening action of the FCV is controlled by a hydraulic line connected to the surface whereas the closing action is controlled by a common hydraulic line that also controls closure of other FCVs along the injection well. In other words, in the configuration shown in Figure 2-7, communication between the FCVs and surface requires a total of n+ 1 hydraulic lines where n is the number of FCVs. An example of an injection well completion with four FCVs is shown below in Figure 2-8.

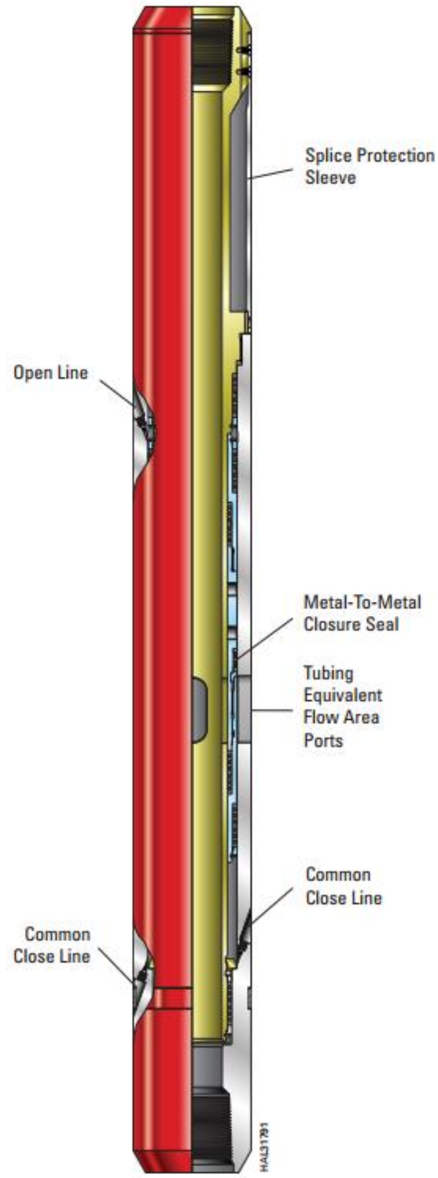

Figure 2-7: The schematic plot of a typical sliding sleeve Flow Control Valve (courtesy of Halliburton).

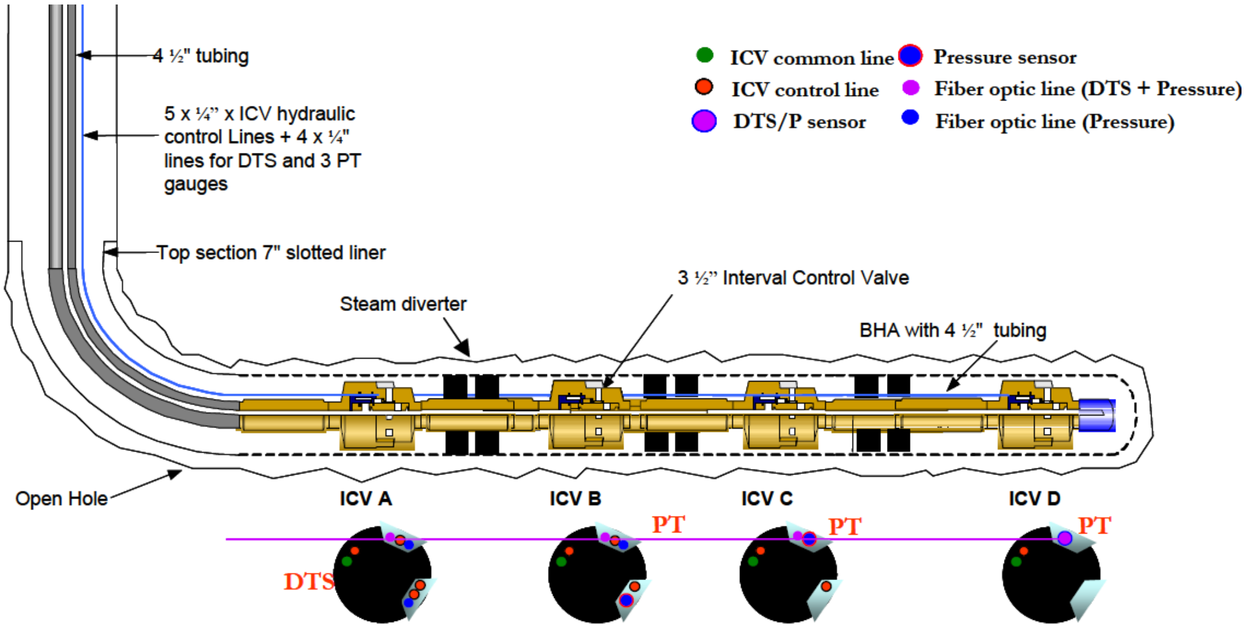

Figure 2-8: Intelligent injection well completion with 4 FCVs. Here, the FCV are referred to as interval control valves (ICVs) (courtesy of Halliburton).

In Figure 2-8, four FCVs are deployed along the 4 ½ inch injection tubing string. A 7 inch slotted liner is used in the completion. Five ¼ inch FCV hydraulic control lines and four ¼ inch distributed temperature sensor (DTS) lines also run through the tubing connecting the FCVs. In this well completion design, three steam diverters (packers specially designed for steam isolation) are placed between each pair of FCVs. The steam diverter divides the horizontal well into four isolated intervals. The steam injected through each FCV flows to its associated interval. In this manner, operators at surface is able to choose steam injection in one or more specific well intervals, based on the temperature and pressure data, to enhance steam conformance along the whole well length. The device has been tested at Shell Orion SAGD field. The results from the field tests demonstrate that a 20 to 40 per cent reduction in cSOR and a 5 to 10 per cent increase in oil recovery can be been achieved by using these devices (Clark, 2013).

2.3.5.2 Multiple position FCV

Some FCV devices have multiple discrete valve positions each one controllable at surface. In this way, steam injection into each well interval can be customized in a continuous and variable manner. Thus, this permits a greater degree of control of flow in or out of the well. Multiple setting FCV devices have been used in conventional oil recovery operations (Clark, 2013).

2.4 Simulation Studies on Flow Control in SAGD

In 2009, Gotawala and Gates published their study on SAGD Smart injection wells. They proposed to use multiple injection points along the injection well, with each injection point deployed with an internal control valve (ICV), which is a similar device to the multiple-valve-position FCV that has been introduced previously. The ICV is controlled by a proportional-integral-derivative (PID) feedback controller to enforce subcool between the injection and production wells. The injection well is divided into six equal intervals, each being controlled by an Internal Control Valve (ICV). The ICV controls steam injection into each well interval so operator has the ability to purposely distribute steam along the well pair to improve steam conformance. In the study, the PID is used to control the steam injection pressure in each well interval so as to enforce a specific subcool. The following equation is used in the study as PID control function:

$$P_i^{new} = P_i^{old} + K_p \varepsilon_i + K_D \frac{d\varepsilon_i}{dt} + K_I \int_{t=0}^{t_{new}} \varepsilon_i(\tau) d\tau \qquad 2$$

Where P_i is the steam injection pressure of interval i, K_p is the proportional control gain, K_D is the derivative control gain, and K_I is the integral control gain. In their study, the values of the control parameters K_p, K_D and K_I were set equal to 1.0, 20.0 and 0.01, respectively. The error, ε, is the difference between the subcool temperature difference (the temperature difference between the steam injection temperature and the produced fluids temperature) and the setpoint value. If the subcool temperature difference is too large, this implies that there is excessive liquid hold-up in the steam, chamber whereas if the difference is too low, then live steam could be produced at the production well (Gates and Leskiw, 2009; Gates, 2011).

The results of Gotawala and Gates (2009) demonstrated that automated control realized a 29 per cent increase in oil production over constant pressure case and also, the cSOR of the controlled operation is lower, especially early in the operation than that without control. However, the authors pointed out that after 2 years of operation, the cSOR profiles are closer to each other and he concluded that the control algorithm works well in the early stages of the process since the error is based on the subcool temperature difference which only has impact in the near-wellpair region. The authors observed that in the controlled case, the steam chamber is not uniform in height above the well pair after 12 months of controlled operation, as shown in Figure 2-9, and they proposed that since the setpoint is the interval subcool and the control is focused to the near well pair region. Thus, even with an enforced subcool, SAGD beyond early stage would not be effectively controlled by the algorithm and additional data reflecting the behavior of the steam chamber further away from the wellpair is required for effective control. This could potentially be done by using temperature data from observation wells.

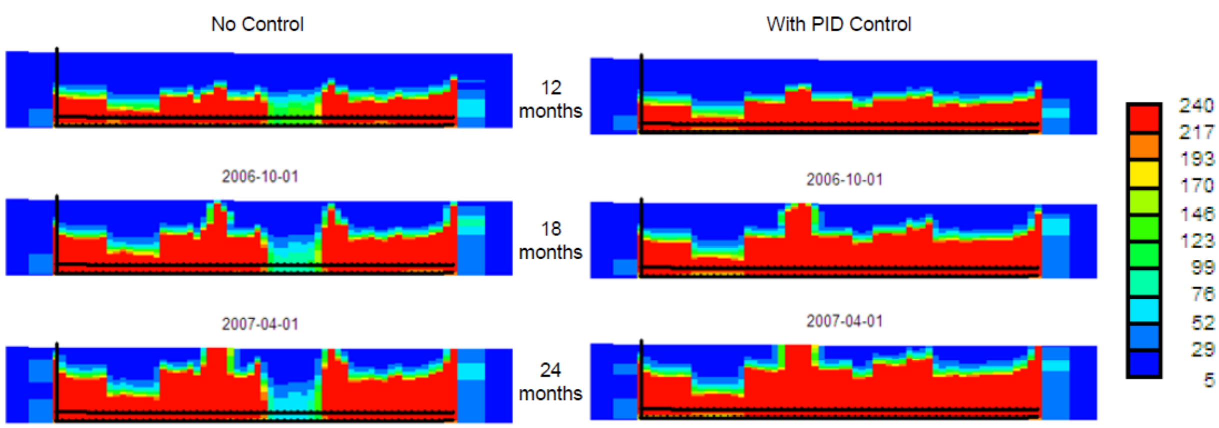

Figure 2-9: Comparison of steam chamber development, expressed in temperature profile between control and no control case after 12, 18 and 24 months operation (used with permission, Gotawala and Gates, 2009).

Gotawala and Gates' work shows an effective control on steam conformance in the early stage of SAGD, through multiple FCVs coupled together to the PID control algorithm. However, control is limited to early stages of SAGD. As soon as the steam chamber grow beyond the near wellbore region, steam trap control loses its effect since temperature difference between the top injection well and bottom production well only reflects steam conformance in the near wellbore areas. Thus, new control algorithms are needed to optimize SAGD beyond its early growth stage. In addition, Gotawala and Gates (2009) only used FCV in the injection well – nothing was done for inflow control in the production well.

Banerjee (2013) studied the passive inflow control devices (PICDs). The author summarized the three key pressure drops critical to controlling injection and production fluid front in horizontal wells:

1. The pressure drop through the horizontal completion. In situation of very long tubing and/or small internal tubing diameter, the fluid flow across the horizontal completion can create considerable pressure drop. For a production well, the inflow fluid at the toe of well is forced to overcome the internal pressure drop that is unseen by the fluid at the heel of well. As a consequence, production through the heel becomes a pathway of least resistance and significantly more fluid is produced at the heel than at the toe. As a result, water-oil and gas-oil contact moves towards the heel production line to fill the vacant pores in reservoir and make water-conning and gas-coning happening. In SAGD, this can lead to live steam production at the heel. Meanwhile, production at the toe end is hindered and much less oil is recovered. For injection well, as steam is injected at the heel, it experiences friction loss as it travels through the horizontal completion. Steam quality and the thermal load decrease as steam flows down the length of the well. As a result, the heel sees the greatest heating and the toe sees the least. This behavior is known as the "heel-toe" effect, and has been observed in most long horizontal wells.
2. The reservoir pressure drawdown that is created by the heterogeneities in the reservoir along the length of the wellbore. In the absence of the heel-toe effect, this heterogeneity along can generate an uneven fluid front.
3. The pressure drop across the completion interface, which involves the pressure drop across inflow control devices, such as the PICD and convergence flow across any sand screen, perforated casing or the slotted liner in this case.

Banerjee also summarized three categories of PICD available today, displayed schematically in Figure 2-10:

1. Orifice/nozzle – based (restrictive). This type of PICD uses constrictions to generate a differential pressure across the device. This device configuration essentially forces the fluid from a larger area down through a small orifice/nozzle, creating flow resistance.

2. Helical-channel/baffled pathway (frictional). This type of PICD depends on surface friction to generate a pressure drop over a relatively long area, as compared to the instantaneous loss through an orifice/nozzle type PICD. When fluid flows through the channel, fluid rheology and channel features interact to create the designed pressure drop.
3. Autonomous PICD. This type of PICD exhibits a changing pressure drop in response to changing features in the producer reservoir fluid. The distinctive feature of this type of PICD is that the flow path way is designed for a particular pressure drop for a desired fluid (oil) and the pressure drop for other undesired fluids (water and/or gas) increasing with encroachment.

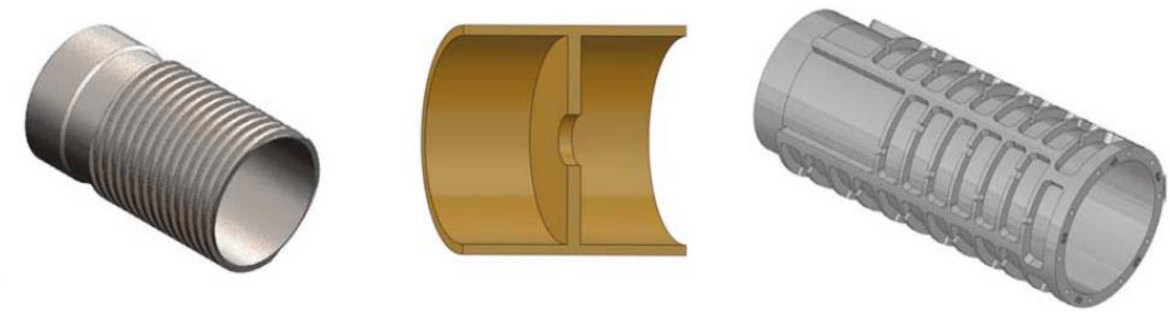

Figure 2-10: The schematic plot of a helical PICD (left), orifice PICD (middle), and autonomous PICD (right) (courtesy of Baker Hughes).

In conclusion, Banerjee pointed out that the deployment of PICDs in injector has an immediate improvement of steam conformance along the length of the horizontal well over that achieved in a slotted liner completion. Furthermore, the deployment of PICDs in the production well creates a synergistic effect by equalizing production along the wellbore length and reinforcing a uniform and flat inflow profile from heel to toe of the well. This uniform fluid profile also helps to maintain a liquid level above the production well and minimizes the risk of live steam production. As a combined result, the cSOR and oil recovery are both improved.

Medina (2013) conducted a study on Passive Outflow Control Devices (POCD, or OCD) for SAGD injection wells. The author proposed a comprehensive design methodology for tubing string deployed POCDs in SAGD. Medina’s design of POCD involves two steps as follows.

Step 1: The interface between horizontal wellbore hydraulics and reservoir injectivity that allows determining the optimum number and location of the steam injection points. The basis of the design integrates the reservoir and field data to establish an injectivity profile along the reservoir. The main objective is to match the profile of steam injection rate into the reservoir with the pay zone thickness along the well. In this manner, the steam chamber will tend to grow proportional to the shape of the reservoir, which would delay heat loss to the top overburden. The field evaluation is done by history matching the injection pressure vs. steam rate data with a model in thermal wellbore simulator. A dynamic pressure gradient (under flowing condition) in the injection string carrying POCD is obtained with a temperature log, taken with fiber optics, where the temperature data is converted to pressure by properties of saturated steam.

Step 2. The design of passive outflow control device itself. The author focuses on the straight-orifice chokes. A schematic plot of this device is shown in Figure 2-12 below. The design of POCD starts with a calculation of chokes with saturated steam. The specification of the devices is provided as a spreadsheet from the equipment supplier. The design inputs data such as steam quality at inlet of OCD, inlet and back pressure and total steam rate at OCD and desired split, then with software calculation, the orifice internal diameter and the amount of chokes required to meet the desired flow conditions is outputted.

A typical POCD design for a SAGD steam injection well arising from Medina's design is displayed in Figure 2-11. In this study, Medina proposed a novel design for ICDs in SAGD. First, temperature data along the well length in field operation is collected by fiber optics. Second, the temperature data is converted to pressure profile along well length, according to saturated steam properties. A pressure gradient with flowing condition is estimated for the field operation. Then a numerical model is built with thermal wellbore simulator and the injection pressure vs. steam rate data is history matched from the model. From there, the history-matched reservoir simulation model is used to design passive OCD locations and the total number of devices as well as the type of devices.

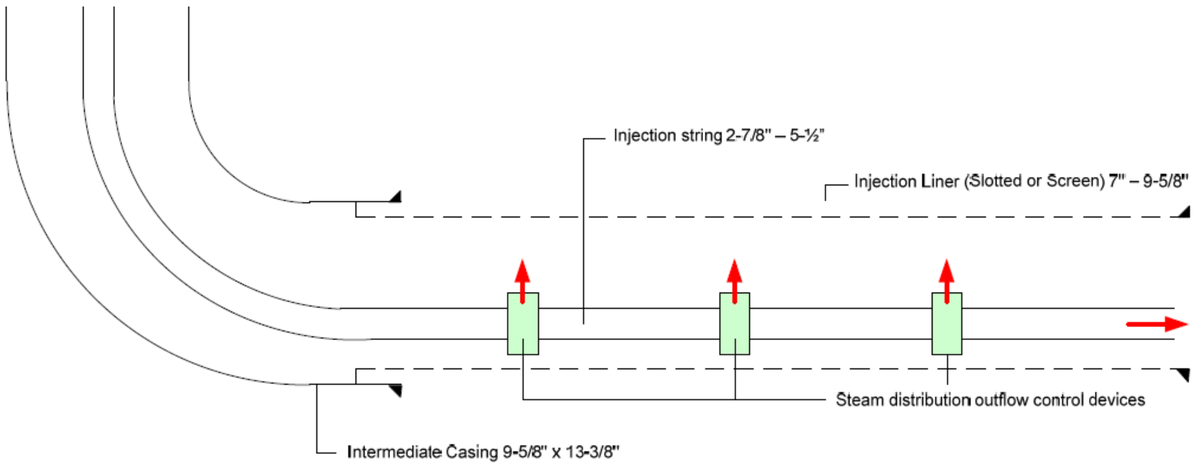

Figure 2-11: A schematic plot of a horizontal injector deployed with multiple POCD along the injection string (courtesy of Baker Hughes). The well is completed with 7 in to 9 5/8 in slotted liner and a single injection tubing of size 2 7/8 in to 5 ½ in run through the length of the wellbore. Three passive outflow control devices are deployed on the injection string along the well length.

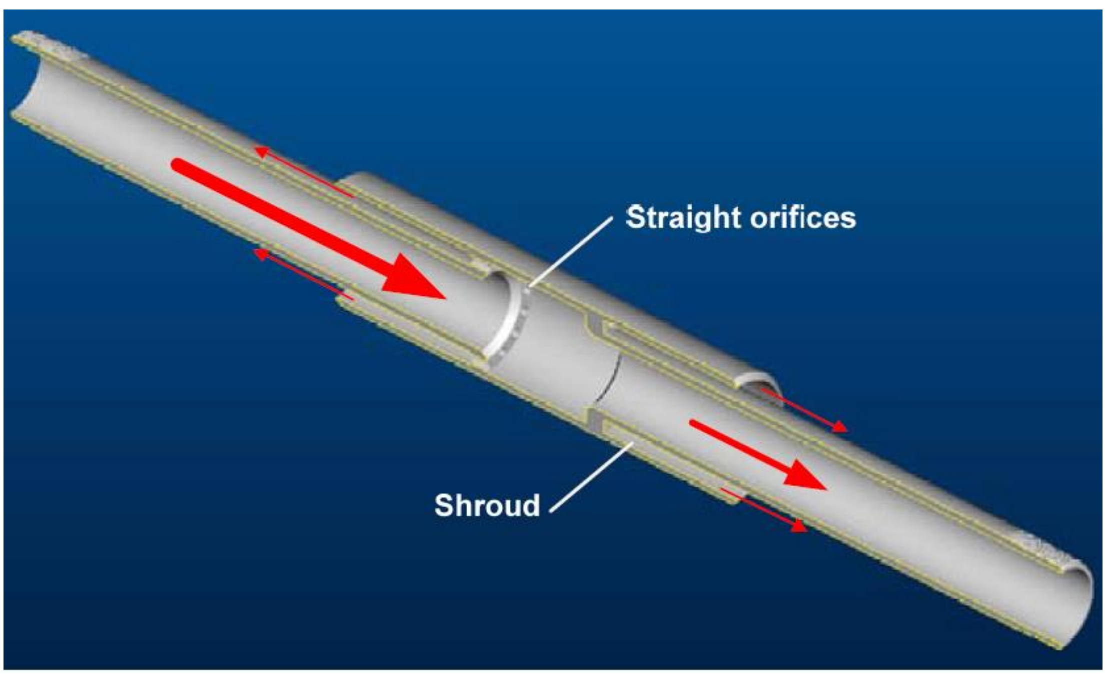

Figure 2-12: A schematic plot of the straight-orifice choke passive outflow control device (courtesy of Baker Hughes). Steam is traveling inside the tubing string, when it hit the straight orifices, a fraction of steam exit through the small orifices and being spread out by the shroud surrounding the device.

The validity of the design can also be seen from the Darcy equation, given by:

$$\frac{Q}{\Delta P} = \frac{k}{u} A \qquad 3$$

where Q is the volumetric flow rate, ΔP is the pressure difference between the upstream and downstream flow, K is the permeability of the reservoir sand, μ is the fluid viscosity, and A is the cross-section area of the flow pathway. In Darcy flow equation above, we can see that flow rate divided by pressure differential is equal to the permeability divided by viscosity. For SAGD steam injection, if we assume the flow cross-section area is constant and the steam viscosity is also constant, then, steam injection divided by pressure differential at the injection point will indicate the local permeability, in other words, the injectivity. However, this design methodology alone would not be able to tell if the reservoir is within a lean zone or a water zone. Since any information regarding oil rate is not involved in the design as it only aims to correlate injection pressure and injection rate.

Hyanpour and Chen (2013) have made similar design on steam splitters and inflow control devices in SAGD. Steam splitters are used to customize steam distribution in the injector. The only physical difference between steam splitters and ICDs is a shroud (as shown in Figure 2-14 below). The shroud is an outer casing on the steam splitter which deflects steam and prevents it from damaging the liner. The author proposed a method to determine the size and position of the steam splitters for injection wells and inflow control devices on production wells. Similar to Medina (2013), they supported their design by flow simulation for the steam splitters and inflow control valve. In the study, the author used the oil production potential (CMG User's Manual, 2012) as a guide for steam splitter and ICD design. The oil production potential is defined by:

$$\mathrm{OPP} = (\mathrm{OFRC}) \times (\mathrm{OA}) \qquad 5$$

$$\mathrm{OFRC} = (\mathrm{K}) \times (\mathrm{b}) \times (\mathrm{NTG}) \times (\mathrm{M_o}) \times (\mathrm{P_{gb}}) \qquad 6$$

$$\mathrm{OA} = (\mathrm{So}) \times (\phi) * (\mathrm{n}) \qquad 7$$

$$\mathrm{K} = \sqrt[2]{K_I^2 + K_J^2} \qquad 8$$

$$M_o = \frac{\mathrm{kro}}{u_o} \qquad 9$$

Where OPP is the Oil Production Potential; OFRC is the Oil Flow Rate Capability; OA is the Oil per unit area; b is the grid thickness; NTG is the Net to Gross Ratio; M_o is the oil phase mobility; $(P)_{gb}$ is the grid block pressure; So is the oil saturation; ϕ is the Input Porosity; n is the net pay; K_I is the permeability in i-direction; K_J is the permeability in j-direction, kro is the oil phase relative permeability, u_o is the oil viscosity.

Hyanpour (2013)'s design methodology uses the oil saturation which would better address lean oil zones along the SAGD wellpair.

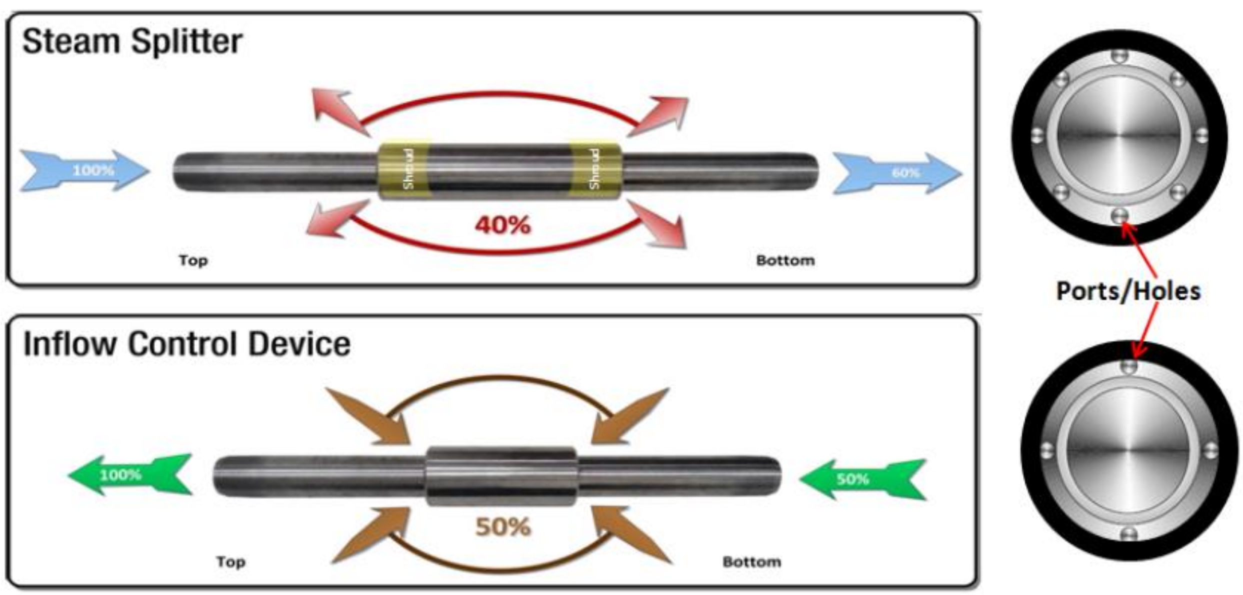

Figure 2-13: A schematic plot of the steam splitters (top) and the inflow control device (bottom) (courtesy of Southern Pacific Resource Corp.).

The design procedure in Hyanpour (2013)'s study follows three steps:

1. By using reservoir simulation, investigate the quantity and impact of steam splitters and ICD on SAGD. In their study for the Senlac heavy oil reservoir, the authors concluded that having one ICD alone increases production by 11.5 per cent; having one steam splitter along increases production by 38 per cent. A

combination of two will increase production by 45 per cent. Also, they concluded that optimum steam distribution can be obtained by setting the steam injection rate (from the ICDs) proportional to the oil production potential.

2. Determining the number of Ports for the steam splitter on the injection well. The ports of an ICD is referred as the orifice or nozzle drilled on the Inflow Control Device, as shown in Figure 2-13 above. In their study for the Senlac site, Hyanpour concluded that the injector ICD performance was optimized by using 14 ports.
3. Determining the number of ports for the ICDs on the production well. In their study on the Senlac reservoir, they concluded that 4 ports is optimum.

In this study, Hyanpour (2013) proposed a novel ICD design methodology which is based on the oil production potential. It is observed that both Medina (2013) and Hyanpour (2013) have proposed similar ICD design methodologies, that is to distribute the steam injection along well length proportional to the pay thickness (in Medina's study) or the oil production potential (which reflects the net pay). While both studies are similar, Medina's design simply focuses on the injectivity, in other words, the steam injection rate versus pressure differential, whereas Hyanpour (2013) put both injectivity and oil saturation into consideration which enables the detection of possible lean zone or water zone within a heterogeneous reservoir.

Stalder (2013) investigated the flow distribution control (FDC) devices (FDC devices are another name for ICDs). Based on the observation of a FDC-deployed SAGD well pair in ConocoPhillips Surmont SAGD operation, Wellpair 102-06, he came to the conclusion that a FDC-deployed single tubing completion achieved similar or better steam conformance as compared to the standard toe/heel tubing injection. In addition, the FDC completion significantly reduced tubing size which in turn reduced the size of slotted liner, intermediate casing, and surface casing. The smaller wellbore size increases directional drilling flexibility and reduces drag making it easier and lower cost to drill the wells. Thus, wells can be drilled much longer than current SAGD wells (tend to be between 500 and 1000 m).

Stone and his colleagues (2010-2013) in a series of studies used advanced well control strategies integrated into a commercial thermal reservoir simulator to evaluate several well completions with flow control devices. Stone and Guyaguler (2010) investigated the use of flow control valves (FCVs) in early stage SAGD (the steam circulation stage and production up to one year when steam chamber is beginning to grow). In the study, actively controlled FCVs in the injection tubing string were used where the FCV device has the capability of multiple valve positions. Also, the injection well was divided into multiple intervals, similar to the well completion in the Shell Orion project (described below). For the production well, passive inflow control devices were deployed to improve the inflow profile. The unique feature of Stone and Guyaguler's completion design is that they proposed the proportional-integral-derivative (PID) feedback controller on steam injection

The study also examined PID controller parameter tuning. For the PID cases, the error between the observed subcool and its setpoint was minimized by the control strategy; the adjusted operating parameters were the steam injection rate. The study serves as a tentative trial of the combination of hardware (the FCV devices) and software (PID and optimization control algorithm) in SAGD. From their results, similar to Gotawala and Gates (2011), the performance of the active multiple-valve-position FCV-deployed tubing string in both injection and production wells, controlled via the PID algorithm, indicates improvement over the uncontrolled cases. As an outcome of the controlled cases, steam conformance was improved by broadening of steam flow path and creation of new flow paths around the wells.

Stone (2011) switched his focus of study to toe-heel dual tubing string completions with PID control. The PID algorithm was applied on both heel and toe tubing strings (and the middle string in case of triple tubing) of both injection and production wells. The purpose of the controller was to achieve uniform along-well steam conformance for injection and production and also to enforce a specified subcool temperature difference. In this study, Stone (2011) investigated the performance of PID-controlled dual and triple tubing strings (shown in Figure 2-14 below) in SAGD and conducted several PID control related sensitivity tests including impact of geological heterogeneity and the loop rate. By loop rate, it means the frequency of changing the manipulated variable in the PID control equation. A higher loop rate would see a more frequent change of steam injection rates in SAGD operation. Stone (2011) used the common PID control equation as follows:

$$IR = IR_{t_s} + K_p \left\{ e(t) + \frac{\int_s^e e(\tau)d\tau}{T_i} - T_d \frac{d}{dt} e(t) \right\} \qquad 10$$

where IR is the manipulated variable, the steam injection rate, IR_{t_s} is the initial steam injection rate when the controller algorithm is started or reset, K_p is the proportional constant, T_i is the integral constant, T_d is the derivative constant, and $e(t)$ is the error term. The process variable in this study is the subcool, in other words, the temperature difference between the injected steam and the fluid in the production well. The $e(t)$ term, in Equation (10), is taken to be the difference between the process variable, the observed subcool and the target subcool setpoint. The PID algorithm set up for dual and triple tubing subcool control in SAGD was an essential part of the study. Stone (2011) has made the following rules for the procedures taking the example of a dual tubing completion:

1. Two separate controllers are used, one for the heel tubing string and one for the toe tubing string, each with an error term.
2. For the heel region, the average pressure in the annulus of the injection well between the heel and middle (the middle and toe) of the well is calculated; the saturation temperature corresponding to this pressure is calculated.
3. The average temperature of in-flowing fluids from the reservoir to the production well, T_p, is calculated and used to calculate the subcool temperature difference.
4. A specified target subcool, T_{offset}, is subtracted to give the errors for both the heel and toe regions. The target subcool, T_{offset}, is the same for both heel and toe regions.

For the PID gains, Stone (2011) explained that:

1. Increasing the proportionality constant, K_p may help the process variable, the observed subcool, to reach its target value more quickly. However, if too high a value is used, oscillations may result. In his study, Stone (2011) chose a value equal to 10.
2. Increasing the integral constant, T_i, helps to reduce the tendency of the process from oscillating but will also slow down the rate at which they reach their target values. In the study, a value of 50 days is chosen.

3. A derivative term T_d slows the rate of change of controller output to kill overshoot in steam rate adjustment. In the study, a value equal to 0.001 is chosen.

The author also mentioned that the values are not optimized, but were chosen after many simulation evaluations.

Stone (2011) concluded that the deployment of PID feedback controller in all cases was able to significantly improve oil production. Also, more frequent updates were necessary to allow the feedback to achieve better conformance and subcool. In addition, Stone found that a higher initial target value, in this study the target subcool, for the time when inflow fluid temperature in producer starts to rise; and a standard target value beyond the early stage would have been more beneficial to the cSOR. For the triple tubing case, the presence of the third tubing string in the middle region allows the SAGD process to achieve improved SOR more quickly than that of the dual tubing case.

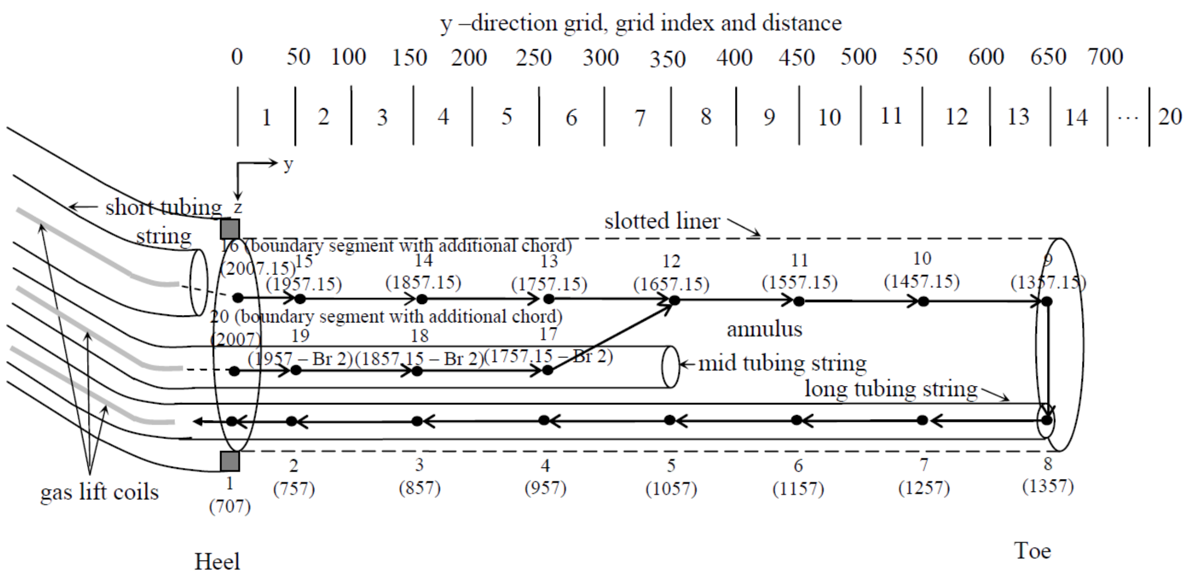

Figure 2-14: A schematic plot of triple tubing string completion (courtesy of Schlumberger).

Stone et al. (2013) continued their previous study of PID controlled dual tubing string completion in SAGD and added in some more elements. For this study, they added passive inflow control devices (ICDs) into the completion designs. A simplified view of the passive ICD is shown in Figure 2-15. The most significant contribution of Stone et al.'s study is that it provided four different well completion scenarios and made side-by-side comparison to choose the best combination. Of course, the 'best' hybrid well completion design is only suitable for the specific reservoir condition and operation constraints under study. However, it still provides guidance for future SAGD completion design. The four well completion designs that were evaluated included:

1. PID-controlled dual-tubing injector and ICD-deployed slotted liner producer.
2. PID-controlled dual-tubing injector and dual-tubing producer.
3. ICD-deployed slotted line injector and ICD-deployed slotted liner producer.
4. Dual-tubing injector and dual-tubing producer.

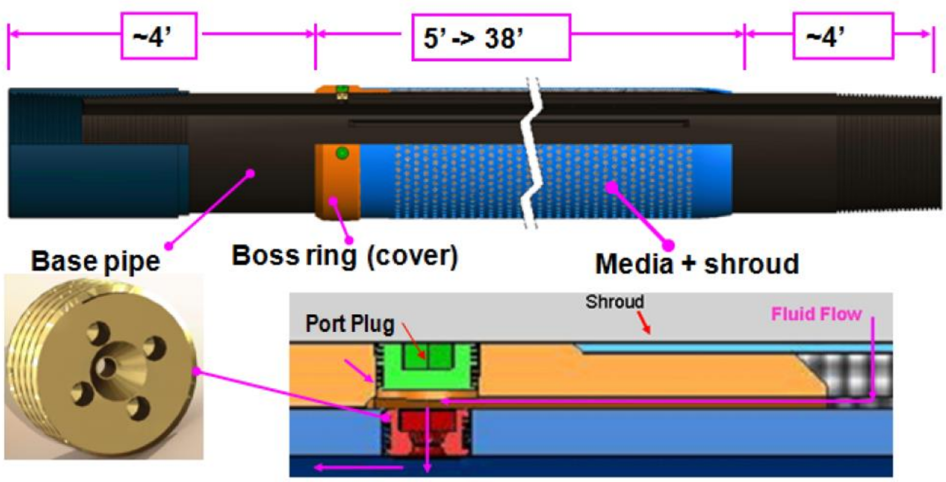

Figure 2-15: A schematic plot of passive inflow control device (courtesy of Schlumberger). Each base pipe is 64 feet long and 7 in in diameter. The screen open flow area per joint is 7.8 per cent for injectors and 15.7 per cent for producers. Each joint is equipped with flow constriction nozzles. The nozzle has an effective throat diameter of 6.4 mm in the injector and 4.2 mm in the producer. Flow across the nozzles obeys the Bernoulli equation.

Among the four hybrid well completion cases, Stone et al. suggested that, based on the synthetic model under study, the method using PID feedback controlled steam injection from dual tubing strings with a producer equipped with ICDs achieved the best performance and its benefits can be seen from the following points:

1. Reduced Capital Expenditure and Operation Expenditure as there is one less tubing string in the producer.
2. The ICD-deployed producer provides a more even inflow which results in better controlled subcool throughout the production cycle, particularly in the early stages after switchover from steam circulation to SAGD mode.

3. Later in the production cycle, the ability of PID controlled injection to force a specified subcool target appears to keep the steam chamber further from the producer and improve the economy of the process.

Also, Stone pointed out there are some areas that remained to be resolved as follows:

1. The ICD modelling with the multiple segments wellbore was compromised due to the coarse lumping of the devices, which combines several devices into one equivalent device.
2. In cases of shale barriers close to the producer that hinders fluid flow, a cooler temperature is observed and the temperature has a much higher resistance to rise, as compared to other regions along the wellbore. Since the subcool control in the PID-controlled dual string injection is based on the average temperature of the heel half and the toe half, a much lower temperature point would effectively lower the average temperature and further affect steam injection.

Stone (2013) continued his previous study of PID-controlled dual tubing string steam injection with inflow control devices deployed in the production well and this time specifically addressed the two issues in the previous study. The author proposed an improved subcool calculation algorithm for better subcool control. Stone (2011) mentioned in earlier study that for the subcool control, the inflow fluid temperature of the production well is simply calculated as the average temperature of the intervals along the production well. In this study, Stone made changes to this algorithm in the following ways:

1. For all intervals along the well, sort the inflowing temperatures from lowest to highest.
2. Starting at the topmost temperature and working downward, calculate a moving average of these temperatures together with the cumulative permeability-completion length (kL) product.
3. When the cumulative kL exceeds 2/3 of the total kL, locate the average temperature at this location.

Stone named the above steps as a “temperature sort” algorithm and it effectively filtered out the coolest temperature in each well, provided that they are significantly lower than the hottest temperature, and provided that their cumulative kL is less than 1/3 of the total kL. Stone evaluated four cases:

1. PID-controlled dual tubing string injection, ICD-deployed producer.

2. Same as 1, but with "temperature sort" algorithm.
3. Same as 1, but with higher target subcool.
4. PID-controlled dual tubing string injection, dual tubing string producer.

The author concluded that the use of the "temperature sort" algorithm in subcool calculation improved the ability of the controller to lock onto and/or progress towards the target subcool, both earlier and more consistently. Also, by using a smaller subcool, rather than a larger value, the algorithm appeared to force the controller to work harder to achieve the target, which in turn benefited the cSOR.

2.5 Field based Studies on Flow Control in SAGD

Stalder described that the standard SAGD well design used at Surmont employs slotted liners with lengths ranging from 800 to 1000 m with toe-heel dual tubing strings. The production well is initially gas lifted through both tubing strings and it is converted to electrical submersible pump (ESP) after approximately 3 years of operation, at which time the toe tubing string is removed from the producer and the well is pumped with the heel string only. For temperature measurement along the wells, thermocouples, and occasionally fiber-optic sensors are used in the horizontal completions. Also, 4D seismic is used to monitor the steam chamber growth. The survey revealed that on average the distribution of the developing steam chamber was less than 50 per cent of the full completion length of the wells. For FDC deployment, the injection liner used 62 joints of 6 5/8 inch base pipe, of which 41 joints had helical restrictor and 21 joints were blank pipe spaced throughout the liner. The size is smaller than the standard 8 5/8 inch injection liners typically used at the Surmont operation. The production well liner consisted of 59 joints of 6 5/8 inch base pipe, each having a helical restrictor and a 17 ft sand exclusion screen. The size is close to the Surmont standard 7 inch liner. The injection and production wells are shown in Figure 2-16. The toe tubing strings in both the injector and producer were removed from the liner after steam circulation, leaving only the heel tubing. It should be noted that the FDC devices are deployed on the liner, instead of the tubing of the completion, which is different from the completion designs described above. The advantages of the liner-deployed FDC include:

1. The entire base pipe is available for fluid flow without the intrusion of a toe tubing string.

2. The liner size can be further reduced, compared to the tubing-deployed completion, since no toe tubing string involved.
3. No requirement of packers or flow restrictors in the annulus between tubing and liner to effectively distribute steam.
4. It eliminates the risk of pulling out a tubing-deployed FDC in producer that would have experience thermal deformation and solids accumulation in the liner.

The key disadvantage of a liner-deployed FDC is that if remediation is required, liner-deployed FDC would not offer the same flexibility of the tubing-deployed ones.

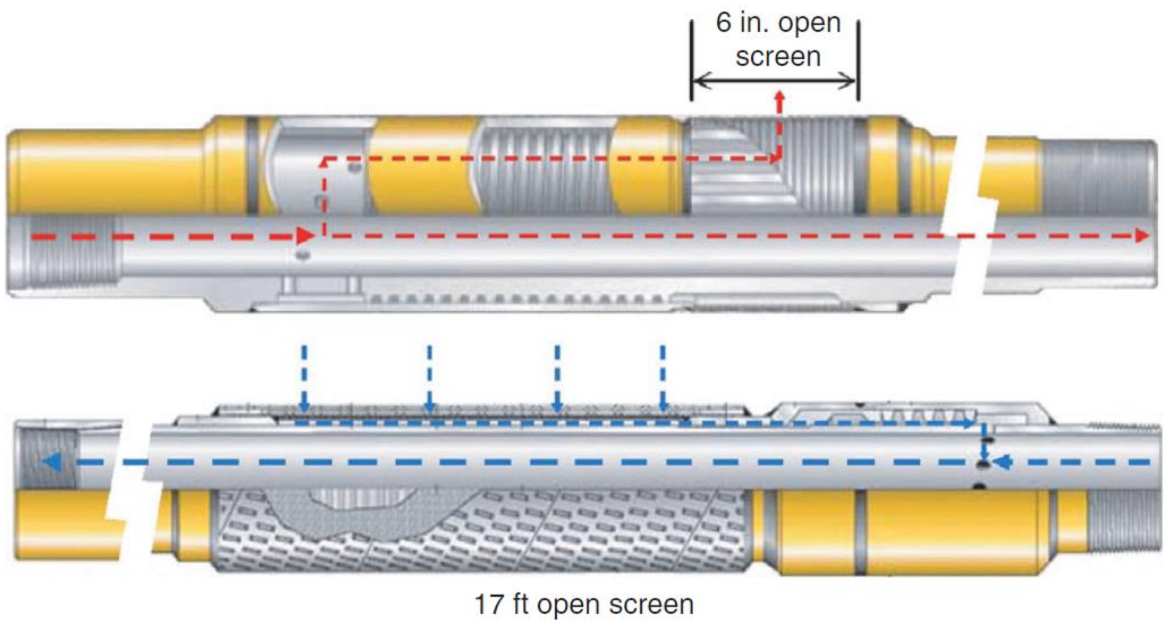

Figure 2-16: The schematic plot of the injector and producer FDC-deployed liners at ConocoPhillips' Surmont Wellpair 102-06 (courtesy of ConocoPhillips Canada).

In ConocoPhillips' completion design, one significant difference is the limited perforation on liner. The typical Surmont liner design as slots cut throughout the surface of every joint of the liner in both the producer and injector; therefore, more than 90 per cent of the liner length is slotted. In contrast, the Surmont 102-06 wellpair has only a fraction of the length of the liners open for fluid flow. In the producer, only 36 per cent of the length is open screen and 64 per cent is blank pipe. In the injector, only 0.7 per cent of its length is open screen and 99.3 per cent is blank pipe. The steam conformance of Surmont 102-06 is shown in Figure 2-17. The, 102-04 and 102-05 wellpairs have similar reservoir qualities as that of 102-06. Well 102-04 and 102-05 were steam circulated in June 2007 and were put on SAGD production in October 2007. Also, all well pairs, except for Wellpair 102-06, were completed with the standard heel-and-toe dual tubing strings in both injection and production wells. Thus, a comparison between the 102-04, 102-05 and 102-06 wellpairs suggests that uniform steam conformance is achieved with FDC-deployed liner without the toe tubing. The 102-06 wellpair also exhibits the highest cumulative oil production and the lowest cSOR, as compared to Wellpairs 102-04 and 102-05, the two most productive well pairs in Surmont 102 North Pad.

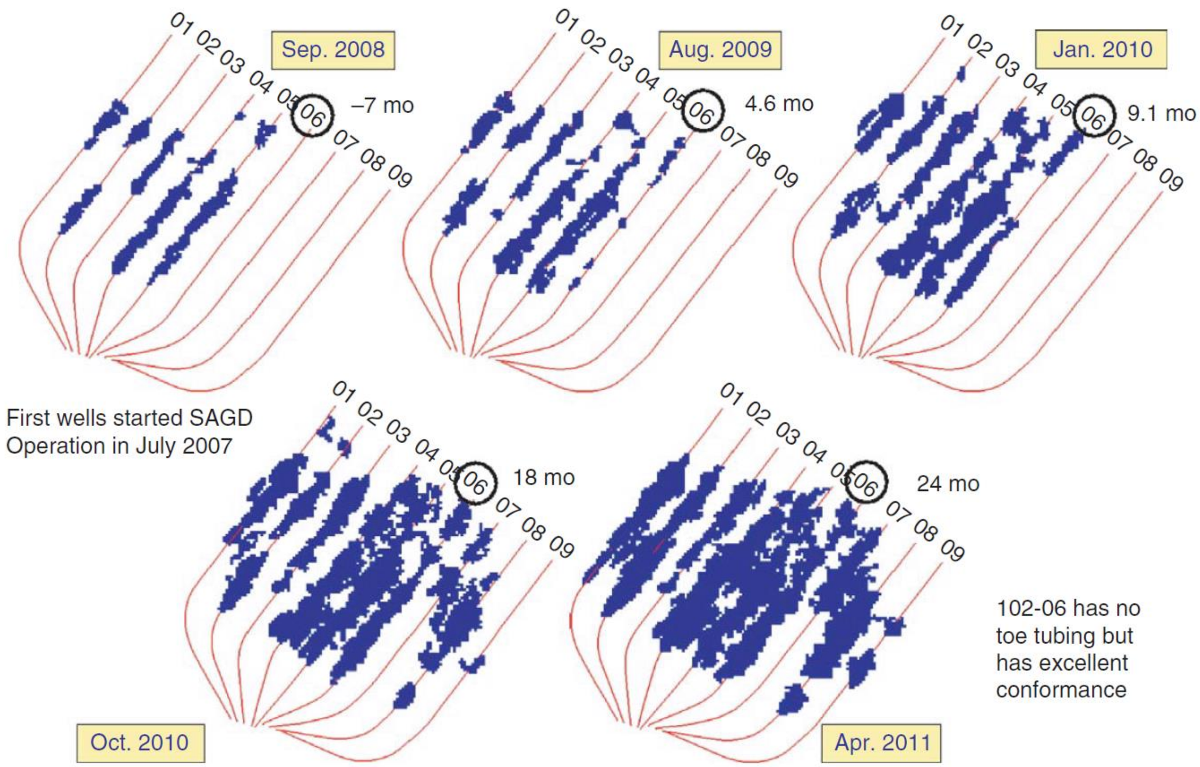

Figure 2-17: The 4D seismic interpretation of steam conformance of Surmont 102 North Pad (courtesy of ConocoPhillips Canada).

In the end of the study, Stalder made several suggestions for future SAGD well design based on the observation of the current flow distribution control device deployed in the Surmont 102-06 well pair:

1. Reduce the liner size.
2. Reduce the density of slots in the injection liners.

3. Use FDC in both injection and production wells to eliminate toe tubing strings.
4. Increase the SAGD completion length beyond the current 800 to 1,000 m range commonly used in industry.

Clark et al. (2013) investigated flow control device for SAGD completion in the Shell Orion SAGD field operation, located in the Cold Lake Oil Sands Area of south-central Alberta. The FCV deployed at the Orion SAGD project is quite different from the devices used in any other SAGD project. It uses active flow control devices with an on-and-off mode. To be more specific, the injector tubing string is deployed with four flow control valve that has the capability of fully opening or closing upon command. The communication to surface is done via hydraulic lines that connect each FCV. There are two hydraulic lines on each FCV, one controlling the opening action and one controlling the closing action. For multiple FCV devices, there is one unique line for the opening control and a common line for the closing control of all devices. Thus, for a tubing string deployed with four FCVs, a total number of 5 hydraulic lines are required. The active FCV-deployed injection tubing string is shown in Figure 2-18. The flow control valve, used at Orion field, is a type of sliding sleeve design capable of withstanding high temperatures and pressure associated with steam injection. The devices have been tested to temperature of 260°C.

Figure 2-18: A photo of steam divert tool used in Shell Orion SAGD project (Courtesy of Halliburton).

What makes the Orion field test even more unique is the use of steam diverter tools. The devices serve to provide segmentation along the injector, so each well interval (zone) will have different steam injection rate/pressure, as compared to other zones. The steam diverter is shown in Figure 2-18. In the Orion SAGD test, three steam diverters were deployed along the injection tubing, each one spaced equidistant between the FCVs. Thus, four isolated well intervals, or zones are created along the well length, with one FCV located at the center of each zone. To evaluate the performance of the active FCV deployed at injection tubing string, Clark et al. first analyzed the injectivity and temperature profile of the four zones. The testing results indicate that Zones C and D towards the toe end of well had higher steam injectivities and higher temperatures along the wellbore as compared to Zones A and B towards the heel end of wellbore. The results of 2D seismic, DTS temperature profile and steam injectivity are shown in Figure 2-19.

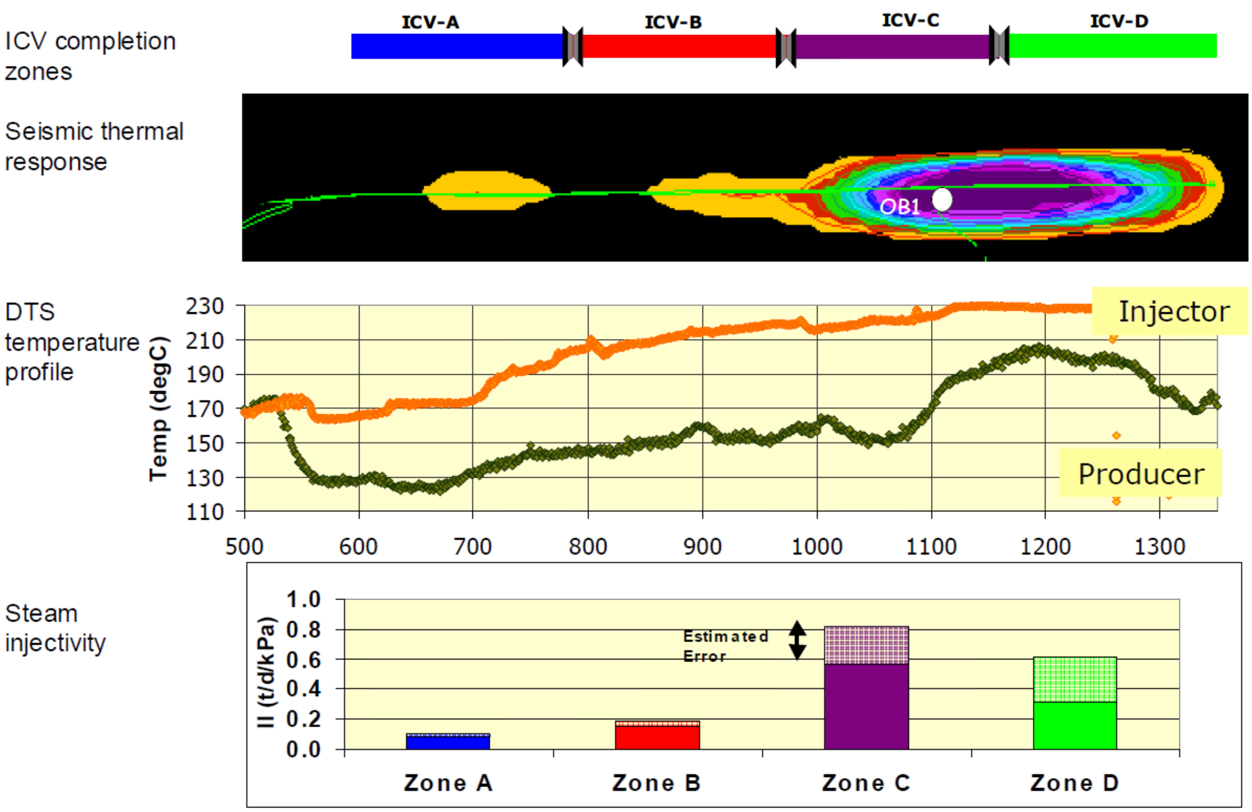

Figure 2-19: The seismic thermal profile, DTS temperature profile and steam injectivity of four isolated zones in Shell Orion SAGD testing (courtesy of Shell Canada).

Based on the analysis of zone performance, a new steam injection strategy was devised. The schedule consisted of cycles of:

1. Three weeks of steam injection into only Zones A and B.

2. One week of steam injection into all Zones A, B, C and D.
3. One day injector and producer shut-in to obtain DTS temperature profiles.

After two cycles, the results indicated that 30 to 70 per cent improvement of injectivity in Zones A and B. Also, a 10 to 20°C increase in temperature was obtained in the heel zones and 20 per cent reduction of the cumulative steam-to-oil-ratio (cSOR) was achieved as compared to those before the new steam strategy was applied. The performance of actively controlled FCV (with on-and-off mode) in Orion SAGD testing confirmed the advantage of multiple, isolated well intervals along injection wellbore. The ability of steam injection in each individual zone significantly improved steam conformance and cSOR over uncontrolled steam injection. To further optimize the performance, Clark et al. suggested in their study:

1. Deploy the active FCVs on both injector and producer, or at least deploy certain type of passive ICDs on the producer to optimize inflow profile.
2. When the technology becomes available, using multiple-position sliding sleeve FCVs to replace the on-and-off mode valve for more accurate control.
3. When the technology becomes available, use FCVs that are capable of resisting higher temperatures i.e. up to 300°C.

2.6 Surmont SAGD Operation

The Surmont lease is located about 63 km southeast of Fort McMurray, Alberta, as shown in Figure 2-20. The project applied SAGD as the recovery method. This study focuses on the 102 North pad (102N) of the Surmont lease. The 102N pad consists of 9 horizontal well pairs, lying parallel to each other, in the direction of NE to SW. The 102N pad started oil production in October 2007 (4 of the 9 well pairs), after 3-month steam circulation. The location of 102N pad is shown in Figure 2-21.

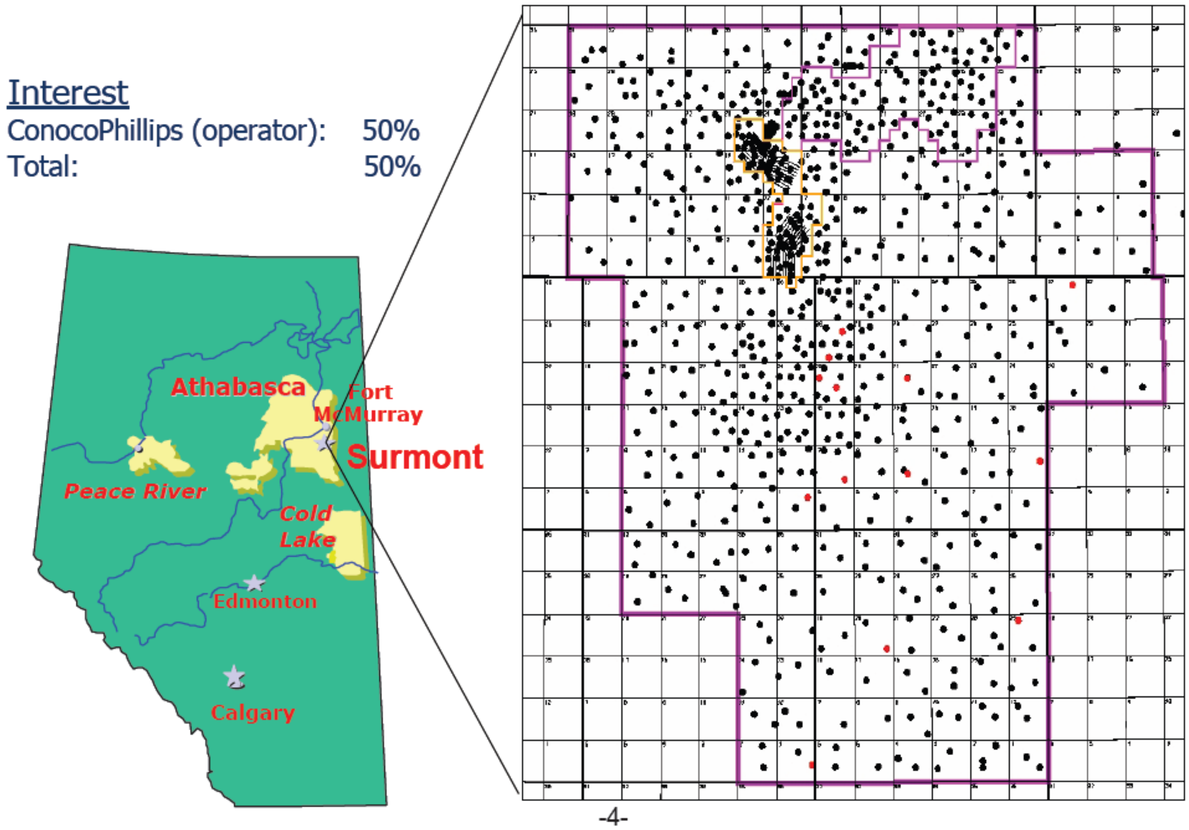

Figure 2-20: Location of the Surmont lease (courtesy of ConocoPhillips Canada, 2013).

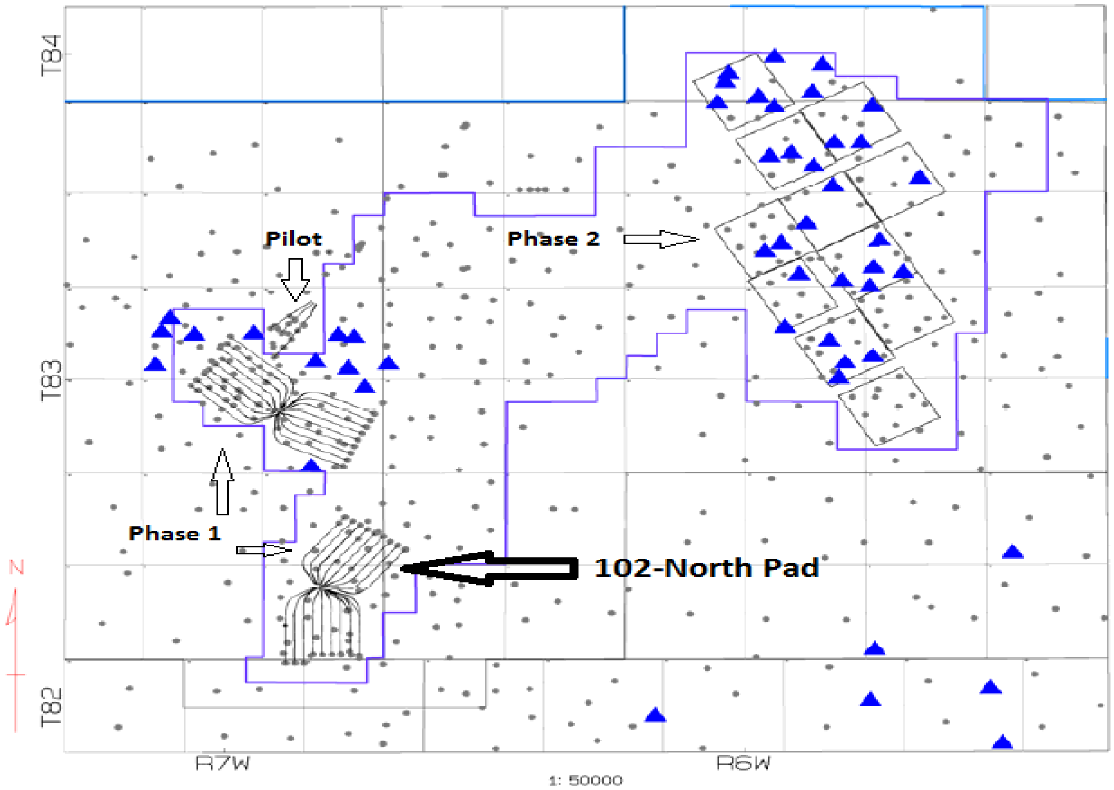

Figure 2-21: the location of 102 North Pad in Surmont lease (courtesy of ConocoPhillips Canada, 2013).

The drainage area for 102N pad has an Original Oil in Place (OOIP) of 7,058 e^3m^3. The average porosity is 0.33 and the average oil saturation is 81.6 per cent. The expected ultimate recovery factor is about 45 per cent. And current cumulative production is 1,321 e^3m^3 and that accounts for a recovery factor of 18.7 per cent (ConocoPhillips 2013).

The 102N pad steam injection follows a declining pressure profile. The initial injection pressure is equal to about 4,500 kPa and over a period of 6 years, the pressure is reduced to about 2,500 kPa. The pressure profile is shown in Figure 2-22 below. The purpose of a declining injection pressure is largely to reduce heat loss from steam to the overburden, which is considered a thief zone in SAGD. The production well was converted to Electrical Submersible Pump (ESP) after 3 years SAGD to help lift fluids to the surface.

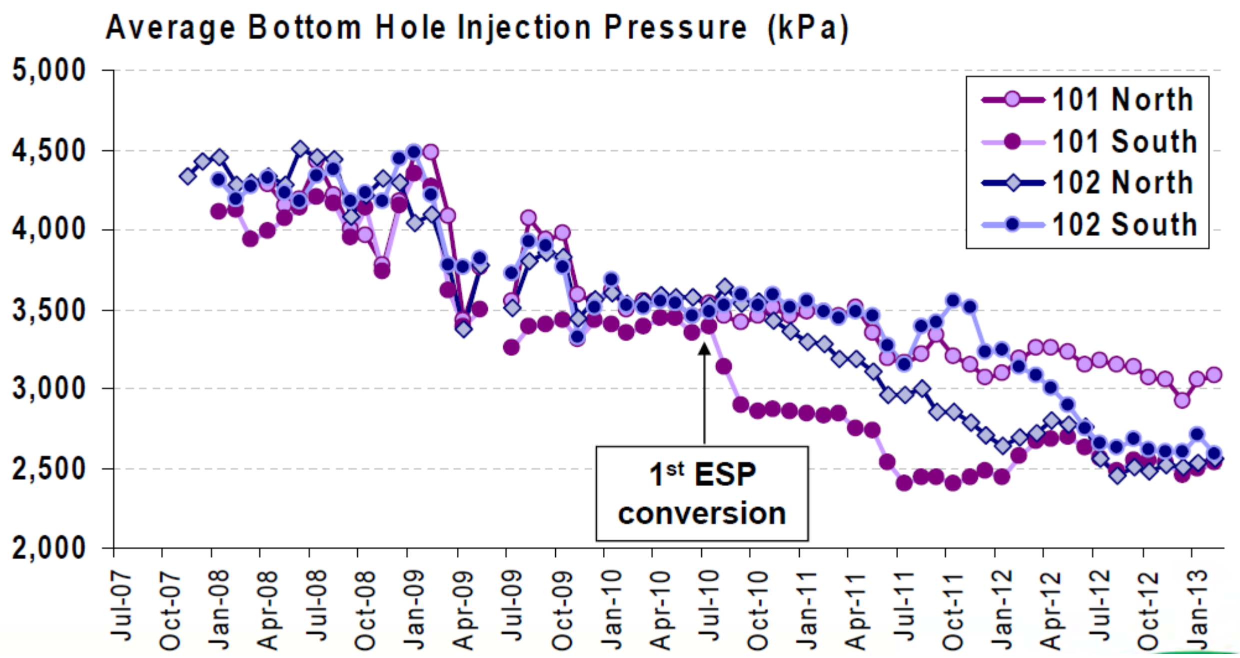

Figure 2-22: Steam injection pressure profile of the 102N pad in Surmont SAGD (courtesy of ConocoPhillips Canada, 2013).

The 102-06 wellpair of Pad 102N was installed with Inflow-Control Devices (ICD). Steam conformance was monitored and analyzed by using 4D seismic surveys every year to create a 60°C temperature contour map. Figures 2-23 to 2-25 illustrate the evolution of steam chamber conformance from 2008 to 2012 for Pad 102N as interpreted from the seismic data.

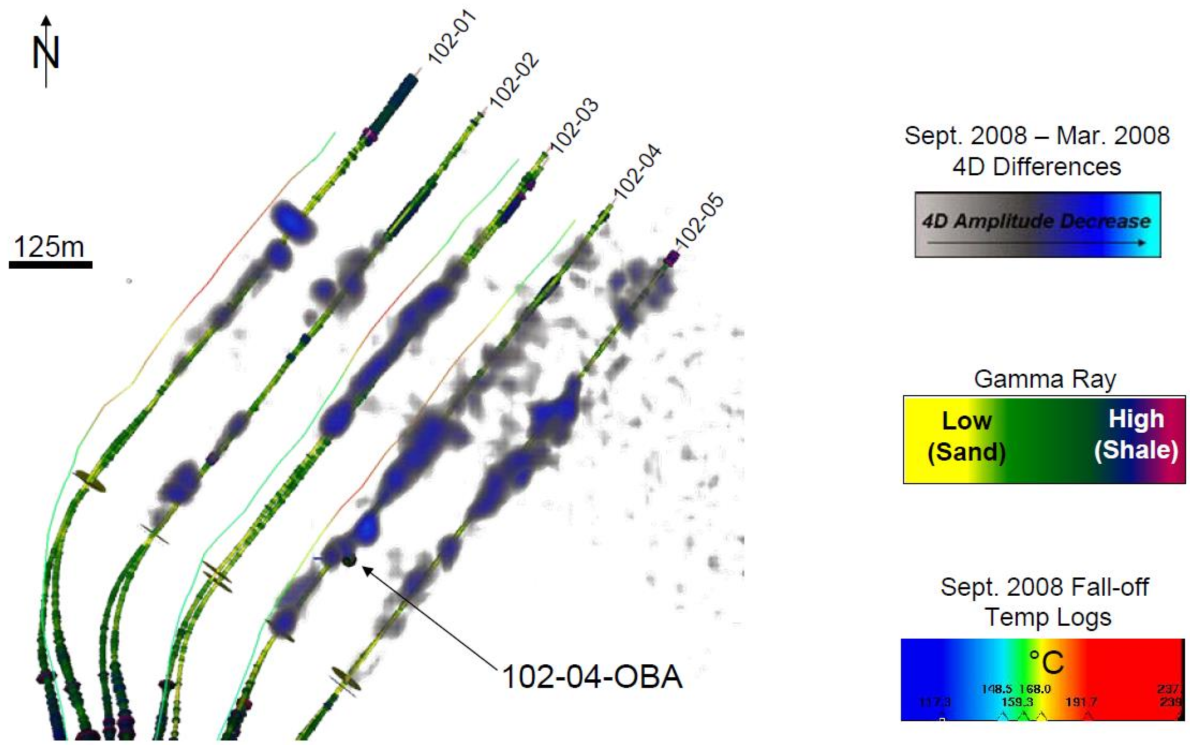

Figure 2-23: 60°C temperature distribution map for Pad 102N in 2008 (courtesy of ConocoPhillips Canada, 2009).

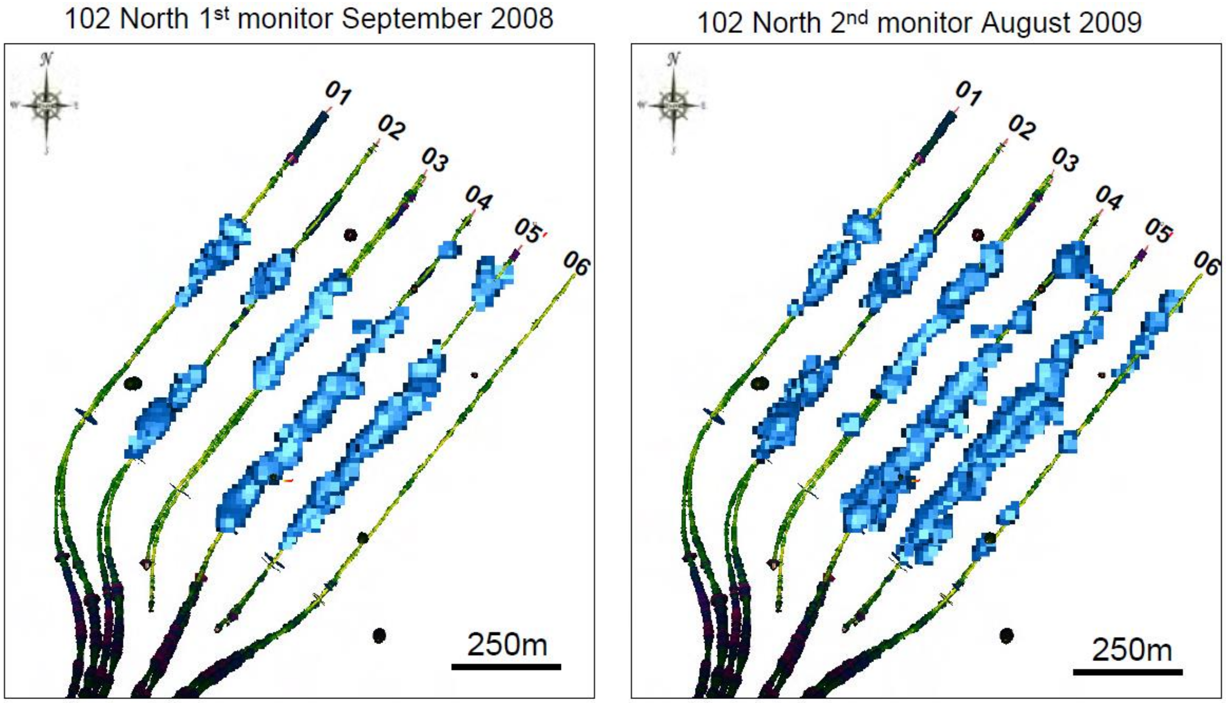

Figure 2-24: 60°C temperature distribution map for Pad 102N in 2009 (courtesy of ConocoPhillips Canada, 2010).

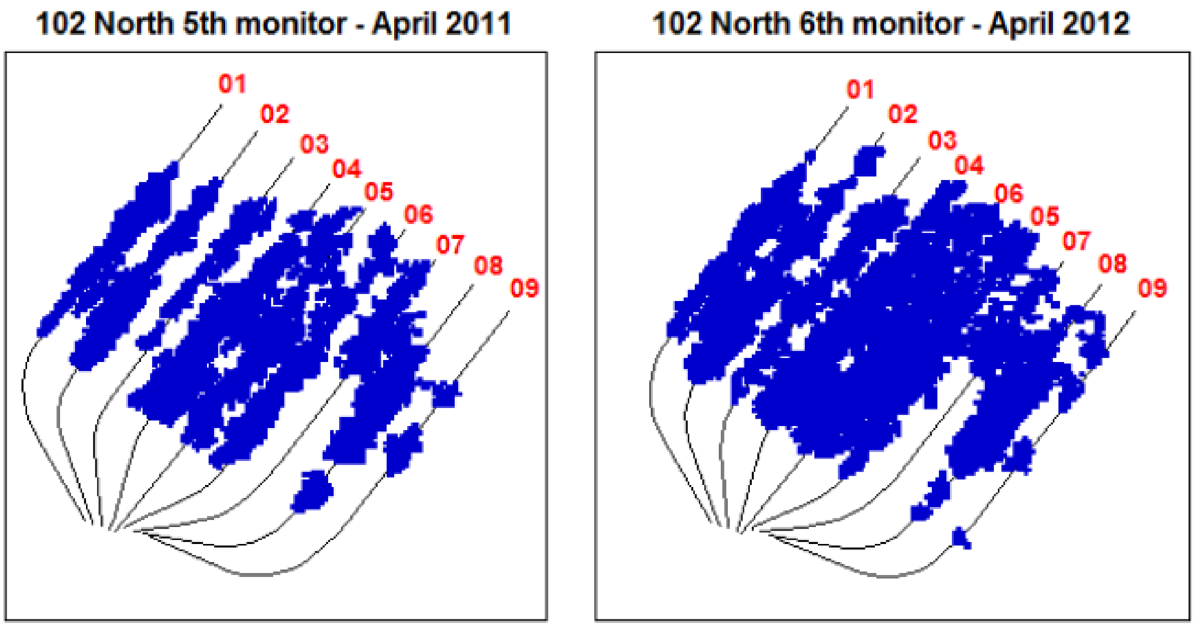

Figure 2-25: 60°C temperature distribution map for Pad 102N in 2012 (courtesy of ConocoPhillips Canada, 2013).

As observed, after 5 years of SAGD operation, in 2012, the steam conformance of Wellpairs 4, 5, and 6 are among the best of the pad. However, Wellpairs 1, 2, 3, and 8 exhibit less than 100% well utilization. Wellpairs 7 and 9 have only about 1/3 of the well length heated to 60°C, which means a good portion of the bitumen is not recovered along those well pairs. Thus, there remain optimization opportunities in the operation, especially in the steam injection strategy. Meanwhile, Surmont 102N pad operation has achieved an industry-leading cumulative steam (expressed as cold water equivalent) to-oil ratio (cSOR) equal to about $2.8m^3/m^3$. Figure 2-26 below shows the instantaneous steam-to-oil ratio (iSOR) profile of Pad 102N.

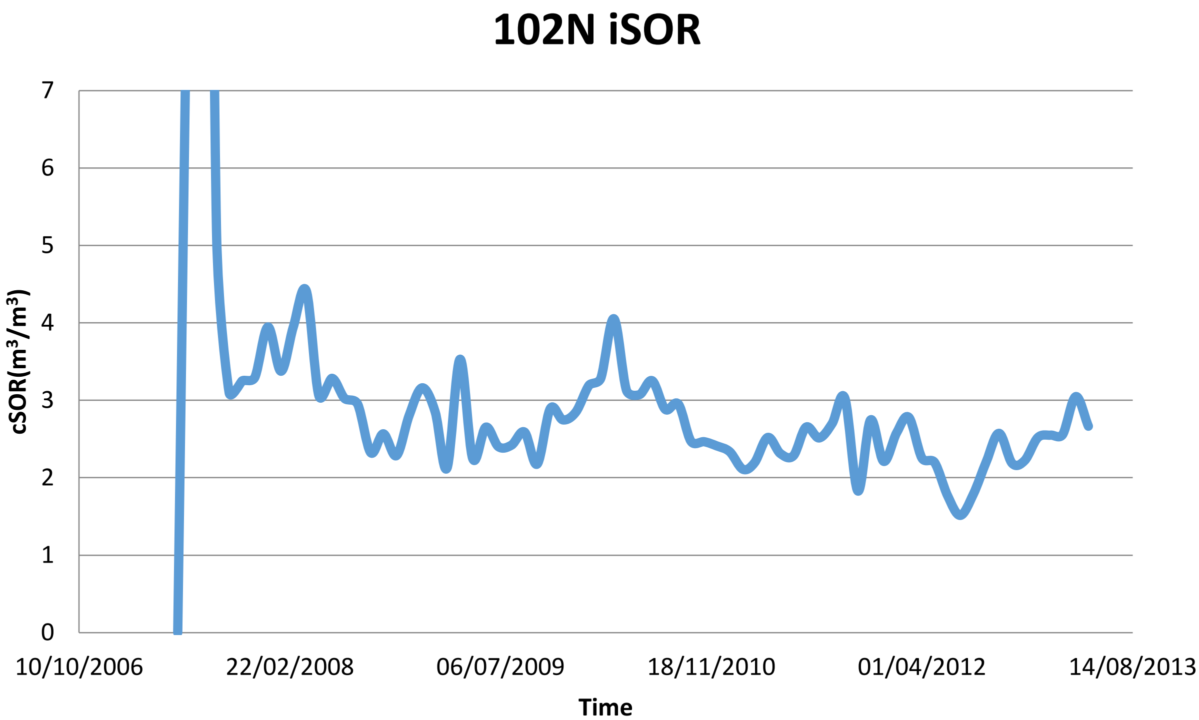

Figure 2-26: The iSOR profile of Pad 102N. The iSOR of Surmont Pad 102N, which contains 9 well pairs, approached an iSOR of 2.8m^3/m^3 in 6 years SAGD.

Many factors have contributed to the low steam-to-oil ratio of Pad 102N: the declining steam injection pressure profile reduces heat losses to the overburden, the conversion to ESP pump increases fluid production, the ICD installation on Wellpair 6 improves the steam conformance on that wellpair. It is not clear how the operator has manipulated steam injection on a routine basis to achieve the low cSOR. However, timely adjustment on steam rate would have been an essential part of the operation. Figure 2-27 displays the steam injection rate profile of each well pair of Pad 102N. The data reveals that the steam rate for each wellpair varies significantly. The performance of each wellpair can be partially explained by the different injectivities.

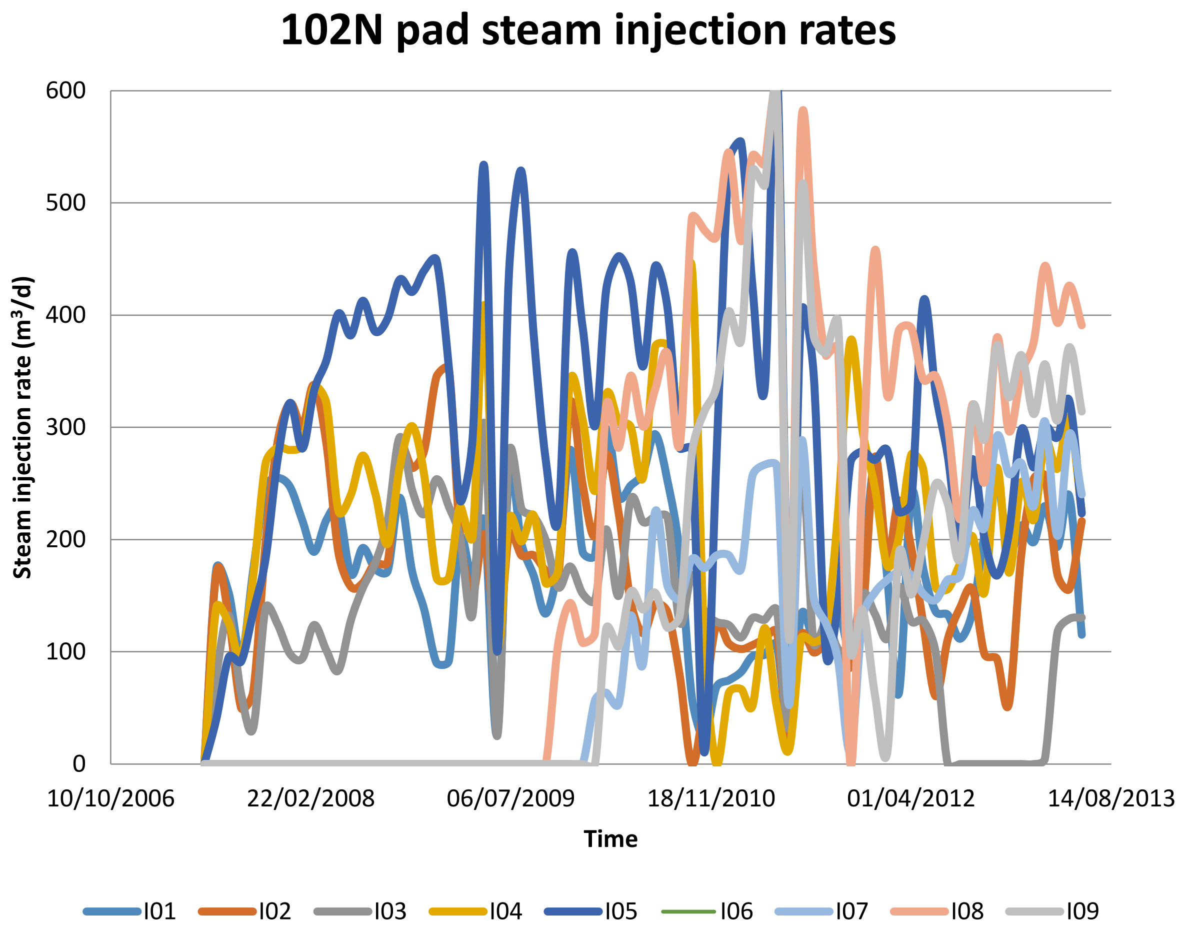

Figure 2-27: Steam injection rate for each well pair of 102N pad.

This thesis presents a study to explore the use of automated control to improve the performance of SAGD at pad scale.

Chapter Three: **Feedback Controlled Steam Injection in SAGD**

3.1 Introduction

SAGD is a complex oil sands recovery process. It involves heat transfer and multi-phase fluid flow in a heterogeneous formation. Recent studies suggest that steam conformance along injector and uniform inflow profiles along producer are the two major issues in SAGD (Gates and Wang, 2011). If most steam injection only happens at the heel and/or toe of the well length, then a portion of the well length (depending on the degree of heterogeneity) will not see heat transfer between steam and bitumen. In other words, the effective well length is reduced. Unfortunately, under the current toe and heel dual-tubing string injection, the steam conformance is doomed to be uneven, due to the reservoir heterogeneity.

In the production well, fluid that flows into the well (referred to as inflow) at the heel and toe experience different friction losses. As a result, heel-based production endures lower resistance when compared to toe-based production, thus creating an uneven inflow profile along the production well. This uneven inflow profile along producer leads to uneven liquid levels above the production, shown schematically in Figure 3-1. Thus, subcool control, used by nearly all SAGD operators to minimize or eliminate live steam production, would not be capable along the entire length of the wellpair.

In Chapter 2, various well completion and control algorithm were introduced to improve steam conformance and inflow profile. Among the techniques, PID-controlled dual tubing steam injection, passive outflow control device, active on-and-off flow control valve with steam diverter tools and PID-controlled active multiple-position flow control valve all show promising results to obtain uniform steam distribution (although the last device is not yet available for commercial use). Meanwhile, limited perforations along the length of the liner/tubing (for example, liners with blank intervals) can operate as a passive inflow control device yielding improvements of the inflow fluid profile, which in turn, can help to enforce subcool along the length of the wellpair.

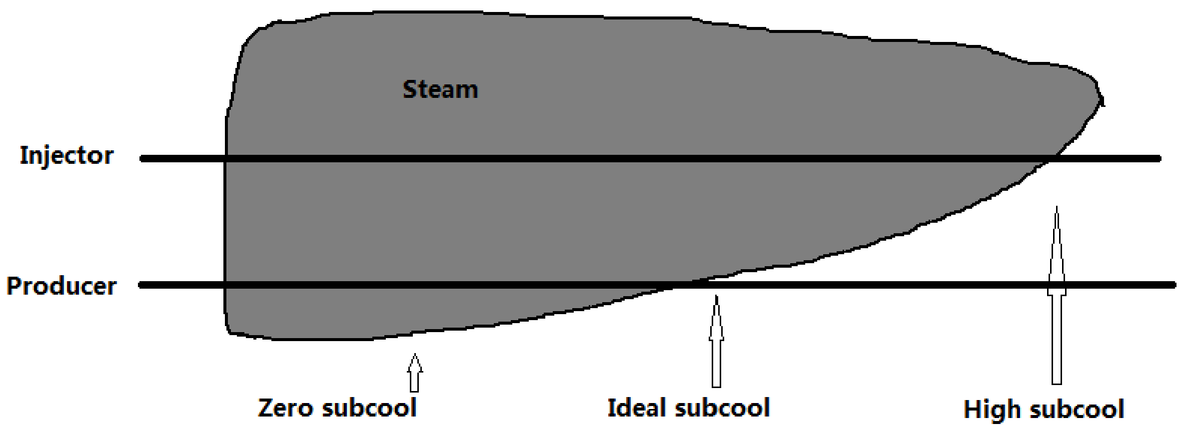

Figure 3-1: A simplified plot of three different subcool scenarios.

In addition, the deployment of FCV/ICDs on the injection and production wells help to eliminate the toe tubing, which in turn reduces the wellbore size. As a consequence, SAGD wells can be drilled much longer than the current range. This directly translates to increased reservoir contact.

The application of fibre optics, multi-phase flow meter, and 4D seismic technologies have provided tremendous data for SAGD with respect to steam conformance and wellpair utilization. These technologies enable the operator to monitor the downhole temperature profile along the wellbores, the multiple phase production rates at the wellhead of each well pair, along with the temperature-affected regions along wellbore (Graham, 2012). SAGD performance optimization has seen a surge of opportunities both in control and monitoring technologies.

This raises the central performance question of SAGD: what can be done to further improve SAGD thermal efficiency? As for now, the majority of SAGD operators focus on the improvement of steam conformance along wellbores, the improvement of inflow, and more effective subcool control. A key cause of these SAGD issues is reservoir heterogeneity which cannot be avoided. Thus, SAGD performance optimization at this point is devising technology to confront reservoir heterogeneity. For example, steam injection by distributing more steam to the less-favorable regions, where steam, by nature, would not choose to flow (steam always follows the path of least resistance).

There are studies that suggest that the steam injection rate should be proportional to the pay zone thickness (Medina, 2013) or the oil production potential (Hyanpour and Chen, 2013). However, as described above, both studies used passive flow control valves on the injection wells, which, although designed for reservoir conditions and desired steam rates, have no flexibility for adjustment or real time control capability; there is no adaptive control mechanism in their approaches. In other words, their success still exclusively depends on the pre-drilling geology survey. Even though those surveys are in general reliable, any incorrect interpretation of reservoir heterogeneity, for example, the proximity of extended shale barriers to the wellpair or unexpected lean (water-rich) zone, significantly reduces the benefits of such pre-designed passive flow devices.

Here we consider an adaptive control technology to make the process less sensitive to reservoir heterogeneity. In other words, an automated control strategy that adaptively controls steam injection to manage steam conformance within heterogeneous reservoirs. Here, we use injection wells, each with a multiple-position flow control valve, controlled by the proportional-integral-derivative (PID) algorithm, along with production wells each with a passive inflow control device. The design does not prioritize steam conformance within the reservoir but rather delivers steam proportional to the relative reservoir qualities.

In practice, the approach requires a multiple-position flow control valve at the steam injection wellhead. With such completion, the operator would have full control of steam injection pattern. As a consequence, the accuracy of geological survey before positioning the wells becomes less critical. In other words, SAGD well placement will depend less on the geological conditions.

The algorithm used here is based on PID feedback controller. While the majority of related studies use subcool to calculate the errors of the PID function to guide steam injection rates, here, the PID controller use the instantaneous steam-to-oil ratio (iSOR) as the target variable so as to guide steam injection rates.

3.2 Proportional-integral-derivative control to achieve a target iSOR

In past studies, PID feedback control has been used to improve steam injection uniformity along SAGD wellpairs by targeting a subcool temperature difference between the injection well (steam temperature) and the production well (produced fluids temperature). The error used in the PID algorithm is then the difference between the achieved subcool temperature difference and a sub cool set point. The principle for this design is to enforce a specific subcool so as to effectively prevent live steam production from the system. As pointed out by Gotawala and Gates (2009), the key issue faced by using the subcool as the target value is that the subcool temperature difference measures a performance measure that is in the near well region. In other words, after the steam chamber has grown beyond the wellpair and is extending into the reservoir, the subcool no longer provides a good representation of a measure of steam conformance. Thus, its ability to provide uniform steam conformance along a SAGD wellpair is seen only over the first few years of operation. Gotawala and Gates (2009), by using subcool as the target variable, showed that the impact of PID-based control in intervals along the wellpair on steam conformance started to vanish after about 2 years of operation.

Here, to have a variable that provides a better measure of the steam conformance for the entire life of the wellpair, the instantaneous steam-to-oil ratio (iSOR) is used. On a daily basis, the iSOR is the ratio of the total steam injected into the steam injection well, expressed as cold water equivalent, to the total oil produced from the production well in that day.

The control mechanism is straightforward; for an interval of the wellpair (isolated by steam diverter tools) or the entire well, the iSOR is a measure of the steam injected per unit volume created due to drained oil in the reservoir. The lower the iSOR, in that day, the greater the oil drained per unit steam injected. That the oil is draining for relatively small steam injection implies that steam conformance is being achieved (steam replaces the oil in the pore space) and that in that interval, conformance is relatively good. On the other hand, if the iSOR is relatively high, then this implies that a relatively small amount of oil is draining and thus the steam conformance is poorer than other intervals where the iSOR is lower. From the perspective of subcool control, if the liquid level above the production well (the steam trap) decreases until it is at the level of the production well and the segment starts to produce live steam, then the iSOR for that segment will rise quickly since the steam, being diverted to the production well is not contacting oil-bearing zones of the reservoir leading to drainage. On the other hand, if the liquid level rises too high above the producer and oil at the bottom of the steam trap becomes too viscous, the oil flow rate into the production well is hindered and as a consequence, the iSOR rises. Thus, a rising iSOR becomes an indicator of an undesired subcool state.

The major advantage of the iSOR as the target value is that it measures both steam injectivity and flow into the reservoir, oil volume in place (the greater the oil saturation, the larger the mobilized volume of oil that drains), effectiveness of oil drainage, and inflow of oil into the production well. On steam injectivity, as it is injected into the formation and rises to contact the oil sand, under ideal conditions, it loses its latent heat to the oil sands and condenses to water. The mixture of condensate and mobilized oil drains under gravity to the production well. In such case, a steady iSOR is expected. However, if there is a shale barrier above the injection well, regardless of the distance between the well and the shale layer, when steam rises to touch the shale barrier, its flow path is blocked which prevents access to oil above the shale layer and despite heat transfer through the shale layer, the mobilized oil there does not drain past the shale layer. In this case, the iSOR would suffer.

The iSOR data is also a good indicator of when steam chambers touch the overburden. When this happens, steam loses its latent heat to the overburden but this heating of non-productive rock returns no oil. Thus, the iSOR also suffers.

3.3 Two-Dimensional (2D) Reservoir Model

A 2D reservoir model with typical Surmont reservoir properties, listed in Table 3-1, was made for this study. The average porosity and oil saturation of the oil column within the reservoir are equal to 0.34 and 0.86, respectively. In the horizontal directions, the average permeability is equal to about 3,866 mD. In the vertical direction, the average permeability in clean sand is equal to 3,635 mD. Ultra low permeability layers are interbedded within the sandy intervals of the model and in some cases exist just above the injection wells which cause issues for steam chamber growth.

Table 3-1: Reservoir Properties for numerical simulation.

Item	Value
Formation temperature, ^{O}C	10
Initial Reservoir Pressure at 280 m, kPa	1,400
Average Oil Zone Horizontal Permeability, mD	3,866
Average Oil Zone Vertical Permeability, mD	3,635
Average Porosity	0.34
Average Water Saturation	0.14
Steam Injection Pressure, kPa	3,500
Steam Quality	0.9
Formation dilation pressure, kPa	4,800
Oil Viscosity @ reservoir temperature, cP	1,700,000
Oil Viscosity @ steam temperature, cP	5
Rock heat capacity, J/m^3-C	2.39E+6
Thermal conductivity of Rock, J/m^3-day-C	6.6E+5
Thermal conductivity of Water, J/m^3-day-C	5.35E+4
Thermal conductivity of Oil, J/m^3-day-C	1.25E+4
Thermal conductivity of Gas, J/m^3-day/C	2,000

The model contains three major layers: the top water zone, the middle oil zone and a thin bottom water zone. The formation ranges from 40 to 60 m thick and consists of mostly sandstones, interbedded with shale layers. The top layer is mainly composed of silty sands and is saturated with water – it is considered a thief zone (ConocoPhillips, 2006-2010). For rock types, the model consists of five distinctive sets, which are displayed in Figure 3-2. The porosity-permeability transforms for each rock type were generated from core data obtained from wells in the vicinity of the Surmont pad.

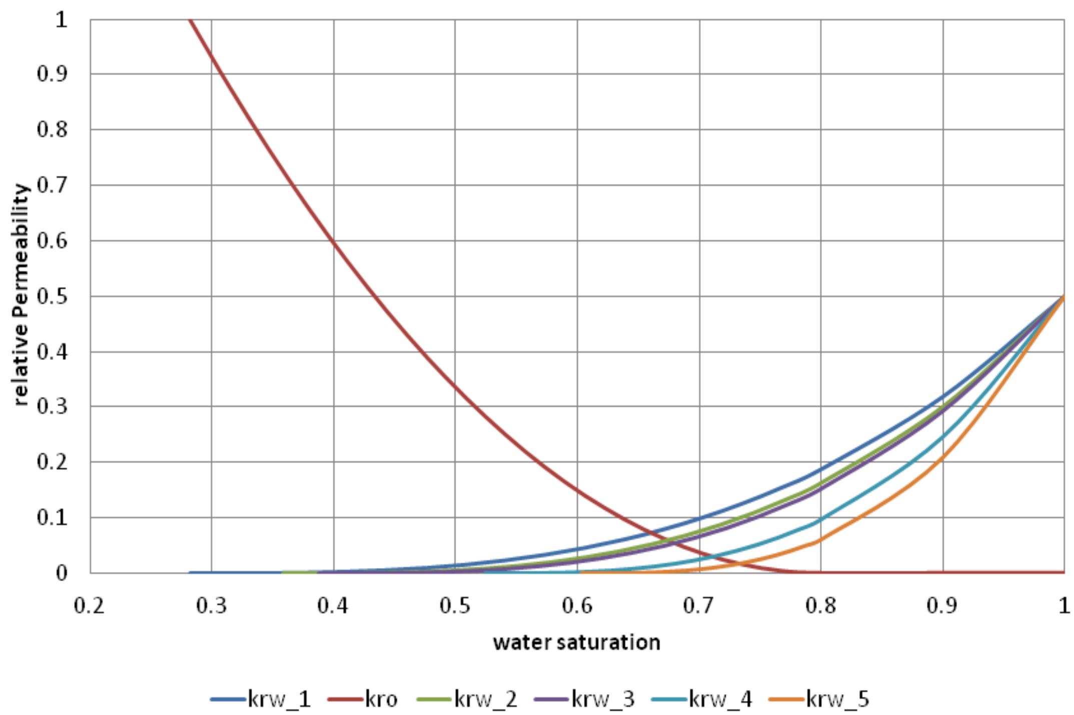

Figure 3-2: Relative permeability curves for different rock types in the reservoir simulation model.

The 2D model was extracted from a three dimensional model by cutting a slide in the across-well direction, so instead of 9 full-length well pairs, the 2D model contains 9 pairs of 25-m long well sections. Since the model is using the sink-and-source wellbore, it can be considered to be 9 pairs of injection/production points across the length of the model. The reason for using a smaller 2D model, instead of a full-scale 3D model is that for the initial stage of the research, we are more focused to explore the control work flow of using PID function with iSOR as the target value. A 2D model would have only one reservoir heterogeneity realization, so it is simpler to apply the control algorithm and it is also more obvious to see the effect of the novel algorithm, if there is any. However, if we directly use the 3D model, then the heterogeneity along the wellbore would dampen the effect of control. In other words, we would need to place ICD on the producer and deploy the multiple-position FCV on the injector with steam diverter tools for a complete set up of the novel control idea. That would be too much uncertainty involved. Thus, the plan would be to set up the work flow first by using a 2D model, with the convenience of sink-and-source wellbore and single heterogeneity. Thus, the purpose of the 2D model is not to make side-by-side comparison with other well completion designs, it only serves to set up the control work flow for later to use. Also, the 3D model is quite large, with more than 5 million active grids in total. Thus it takes much longer to run, compared to the 2D model, which contains around 90,000 grids. The grid dimension of both models is the same: 25 m in the along well direction (i direction), 1 m in the cross-well direction (j direction) and 1 m in the vertical direction (k direction). Top view and 3D view of the 3D model is shown in Figure 3-3 and Figure 3-4 below. The 3D model was generated geostatistically by using Sequential Gaussian Simulation conditioned to available log and core data in a commercial geomodeling software package (Schlumberger, 2012). The 3D geological model was directly converted into a numerical model and the nine well pairs, listed in Table 3-2, were placed within the reservoir model, according to well trajectories.

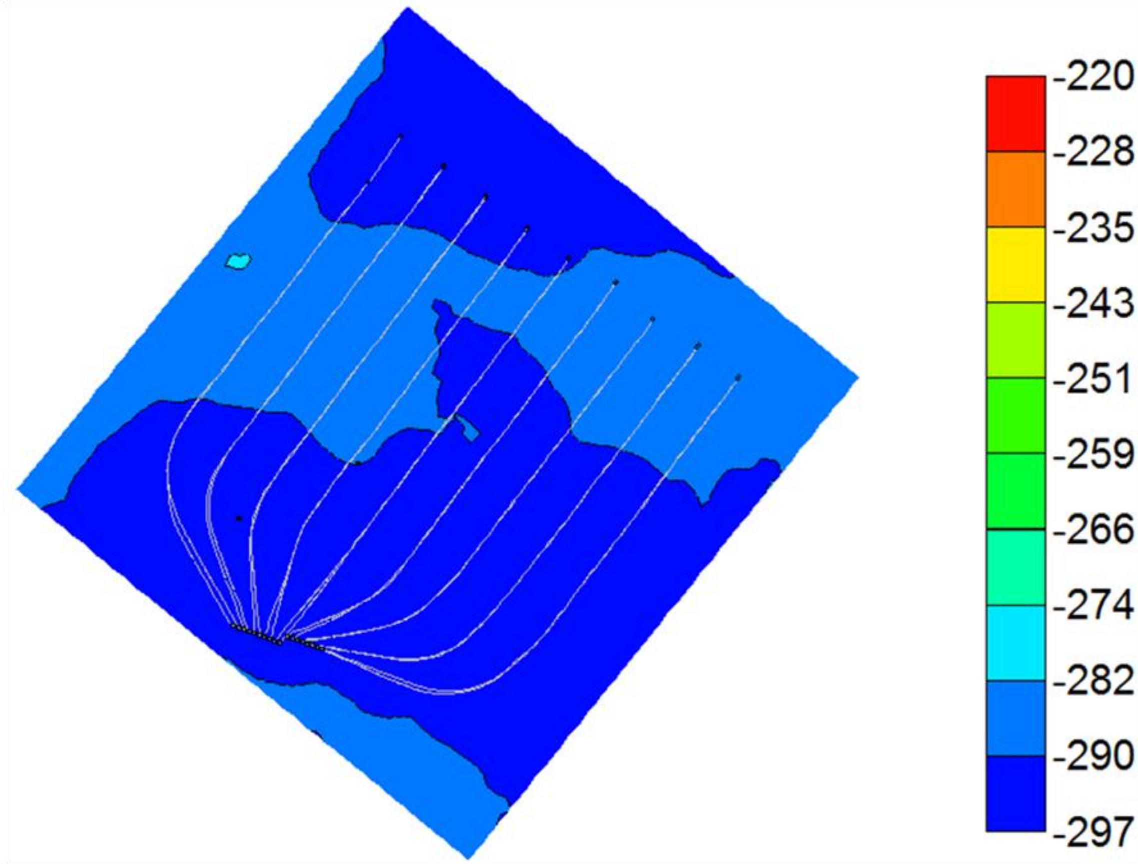

Figure 3-3: Top view of the reservoir model including well pair placements.

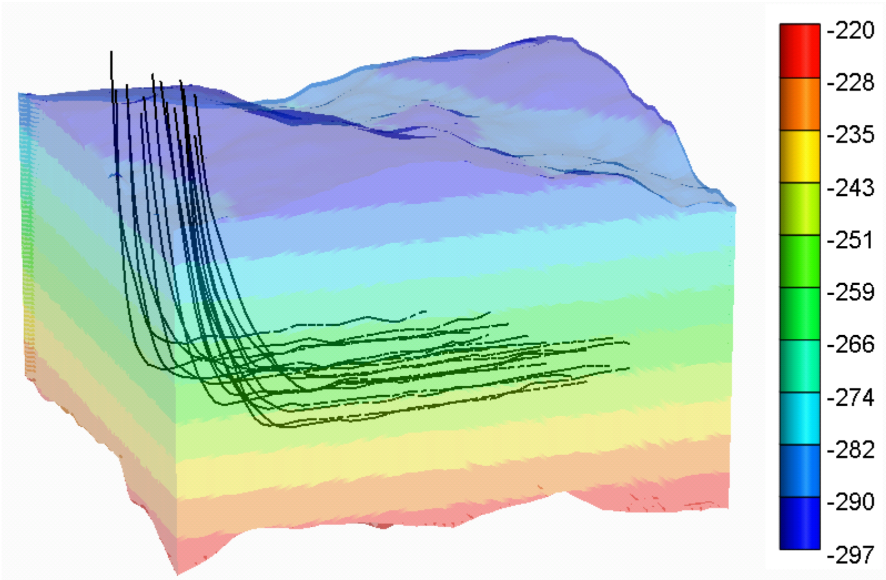

Figure 3-4: Three-dimensional view of the reservoir model including well pair trajectories. The domain has been exaggerated in the vertical direction.

Table 3-2: Well names, identifiers, and horizontal well length.

Well Name	Well ID	Horizontal Length (m)
102-I01	103/07-12-083-07W4/0	768
102-I02	102/07-12-083-07W4/0	853
102-I03	108/08-12-083-07W4/0	867
102-I04	105/08-12-083-07W4/0	878
102-I05	104/08-12-083-07W4/0	852
102-I06	110/08-12-083-07W4/0	878
102-I07	102/05-07-083-06W4/0	870
102-I08	104/04-07-083-06W4/0	849
102-I09	106/04-07-083-06W4/0	880
102-P01	100/10-12-083-07W4/0	929
102-P02	100/07-12-083-07W4/0	876
102-P03	100/08-12-083-07W4/0	856
102-P04	102/08-12-083-07W4/0	855
102-P05	103/08-12-083-07W4/0	885
102-P06	109/08-12-083-07W4/0	876
102-P07	100/05-07-083-06W4/0	885
102-P08	103/04-07-083-06W4/0	906

102-P09	105/04-07-083-06W4/0	938

A major concern of using extracted 2D model from the full-scale 3D model is that whether the extracted model is able to represent the original reservoir properties. Of course, with only one heterogeneity realization in the original model (one slide compared to 59 slides in the cross-well direction, although active slides are only about 40), the situation is much simpler. However, our priority is to test the functionality of the control algorithm, thus as long as the performance of two models have a similar trend, then the work flow built from the 2D model would be able to use in the 3D one. The reservoir properties of the 2D model are shown in Figure 3-5 and 3-6 below, which is equal to the average reservoir properties of the 3D model.

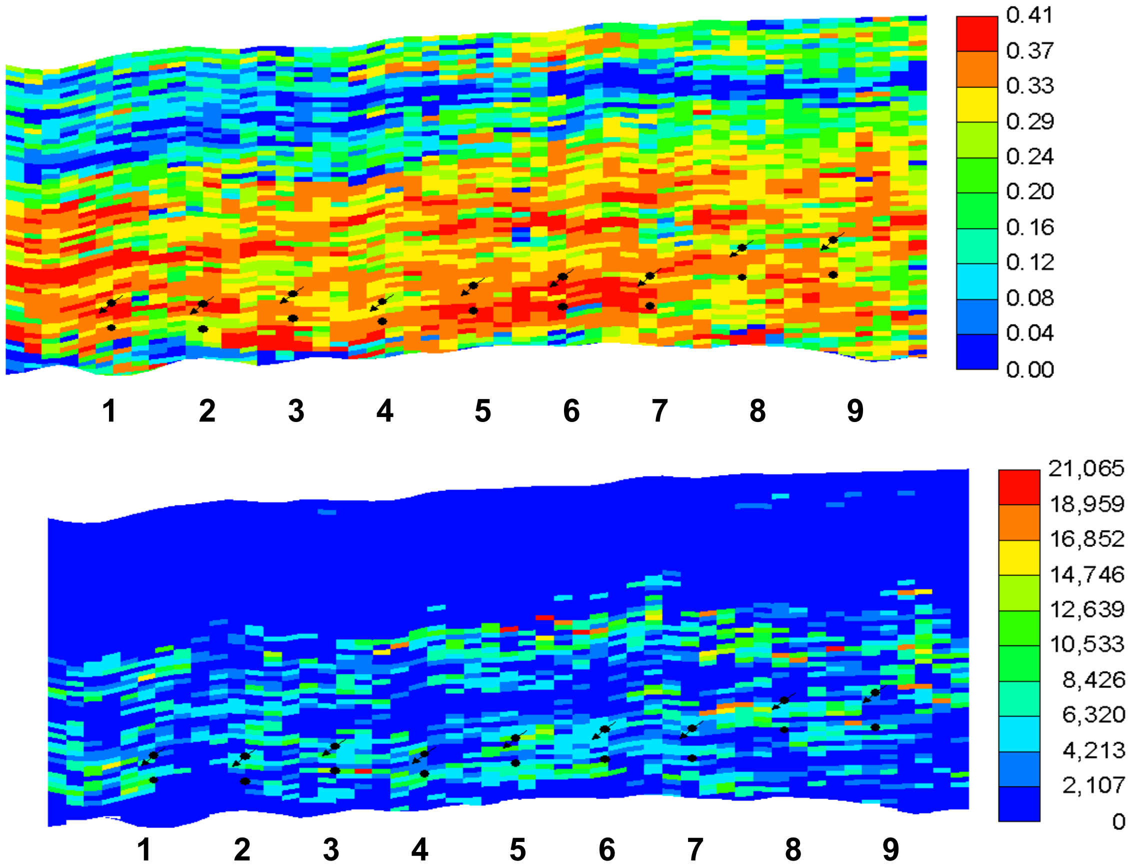

Figure 3-5: Reservoir properties of the 2D slice proxy model. Top: Porosity and locations of SAGD well pairs; Bottom: Horizontal permeability. The thickness of the reservoir is equal to about 40 m whereas the width, in the cross-well direction, is equal to 1,200 m. In the down-well direction, viewed as into the page, the dimension is equal to 25 m. The average porosity is equal to 0.34, the average horizontal permeability is equal to 3,866 mD, and average water and oil saturations are equal to 0.14 and 0.86, respectively.

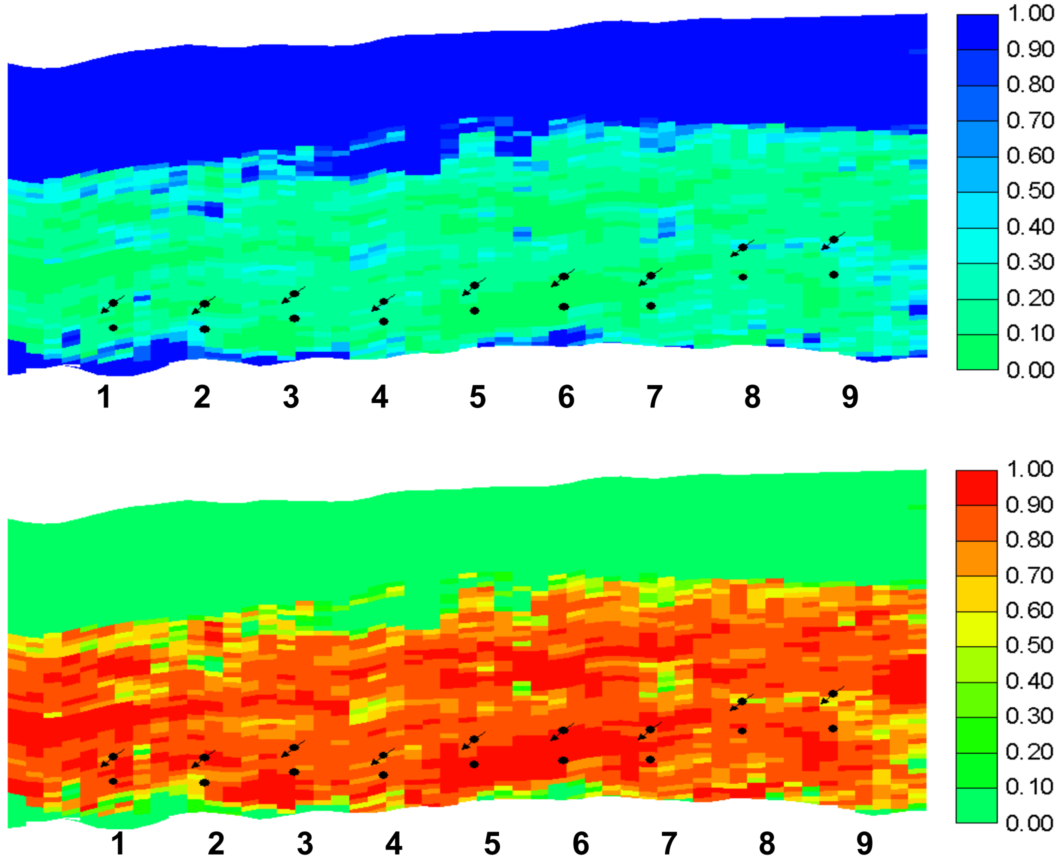

Figure 3-6(continued): Reservoir properties of the 2D slice proxy model. Top: water saturation; Bottom: oil saturation.

Also, we compared the performance of the 2D and the 3D model, with the same control constraints. The results are shown in Figure 3-7 below. It shows that the water cut for the 2D and 3D model are nearly identical. While the cumulative Steam Oil Ratio have similar trends, with local fluctuation within small ranges. The cumulative steam injection and cumulative oil production of the 3D model appears to be a roughly constant factor over that of the 2D model. Thus, it is confident to say that the two models behave similar in terms of SAGD.

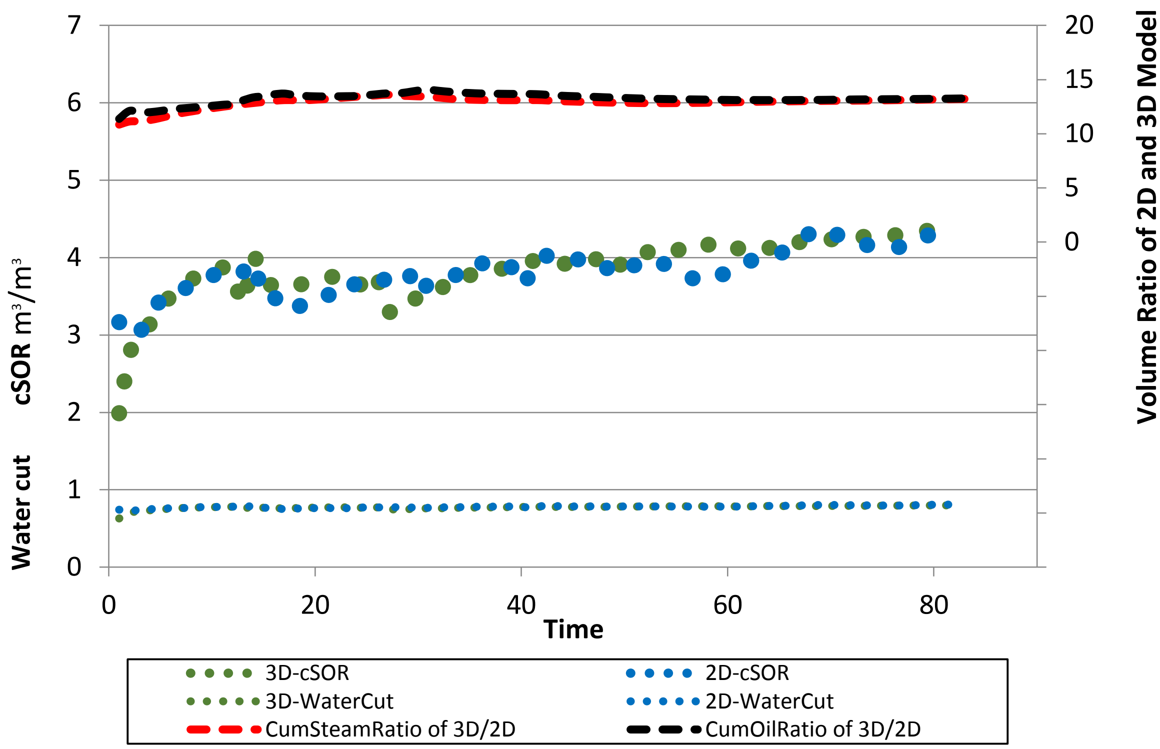

Figure 3-7: Comparison of 2D and 3D model results. The top dash lines represent the volume ratio of 3D model over 2D model; black for cumulative oil production and red for steam injection. The middle dash lines show cSOR; blue dots for 2D model and orange dots for 3D model. The bottom dash lines show water cut; blue dots for 2D model and orange dots for 3D model.

3.4 Customized Proportional-integral-derivative (PID) control

3.4.1 Customized PID control function

PID control was introduced in Chapter 2. Here, we customize the feedback controller for SAGD. In this algorithm, the process variable is the iSOR, and the manipulated variable is the steam injection rate and the set point is a specified iSOR. Thus, the error term in the control equation will be the difference between the observed iSOR and the target iSOR. The iSOR reflects the instantaneous ratio of steam injection rate over oil production rate. Thus, in general, iSOR would exhibit more fluctuations. In terms of PID control, targeting iSOR would provide quicker response on steam rate adjustment, since iSOR is more related to short-time change in operation. For example, when steam rises to a shale barrier, the iSOR rises due to the short of oil production at the moment. In this manner, the error term is as follows:

$$e(t) = iSOR_{observed} - iSOR_{target} \qquad 11$$

And the PID control equation is given by:

$$Q_{i,new} = Q_{i,old} + K_P \left[e_i(t) + \frac{1}{T_I} \int_0^{t_i} e_i(t)dt + T_D \frac{de_i(t)}{dt} \right] \qquad 12$$

Where $Q_{i,new}$ is the new steam injection rate for the next control cycle, m^3/d, $Q_{i,old}$ is the steam injection rate from the start of reset of the process, m^3/d, and $e_i(t)$ is the error term, m^3/m^3. In the case of steam injection pressure control, Equation (12) becomes:

$$P_{i,new} = P_{i,old} + K_P \left[e_i(t) + \frac{1}{T_I} \int_0^{t_i} e_i(t)dt + T_D \frac{de_i(t)}{dt} \right] \qquad 13$$

Where $P_{i,new}$ is the new steam injection pressure for the next control cycle, kPa, $P_{i,old}$ is the observed steam injection pressure from the start of reset of the process, kPa, $e_i(t)$ is the error term, m^3/m^3.

In the control algorithm, the error, its integral, and derivative are evaluated every three months. This time interval was chosen since it represents sufficient time to observe response of a SAGD wellpair to operational changes. Although this may be considered to be a low updating frequency, however, in the field, the operation of down-hole flow control valve, or even the wellhead steam injection choke involves risk of damaging the equipment which requires plant shut-in to repair. It is especially concerning for FCV control via hydraulic lines. Although proven to be reliable in high temperature environments, a more frequent operation would definitely raise the risk of malfunction (Clark, 2013). In the control strategy used here, every three months, the iSOR is updated and the steam injection rate (or steam injection pressure) is changed. The complete control loop is presented in Figure 3-8.

The control algorithm starts with an initial steam injection rate which is set after conversion from steam circulation to SAGD mode. After three months of steam injection at constant steam rate, a series of iSORs is obtained for the past 3 months (three iSOR data points are collected, one at the beginning of each month). The reason that three data points are used is to obtain the overall trend of the error versus time. Given the heterogeneity of the reservoir, iSOR data can be very rough. The error is then calculated by subtracting the target iSOR from the collected data. The errors are then used to calculate the integral and derivative contributions to the control equation. Thereafter, a new steam injection rate is calculated for the next controlling cycle.

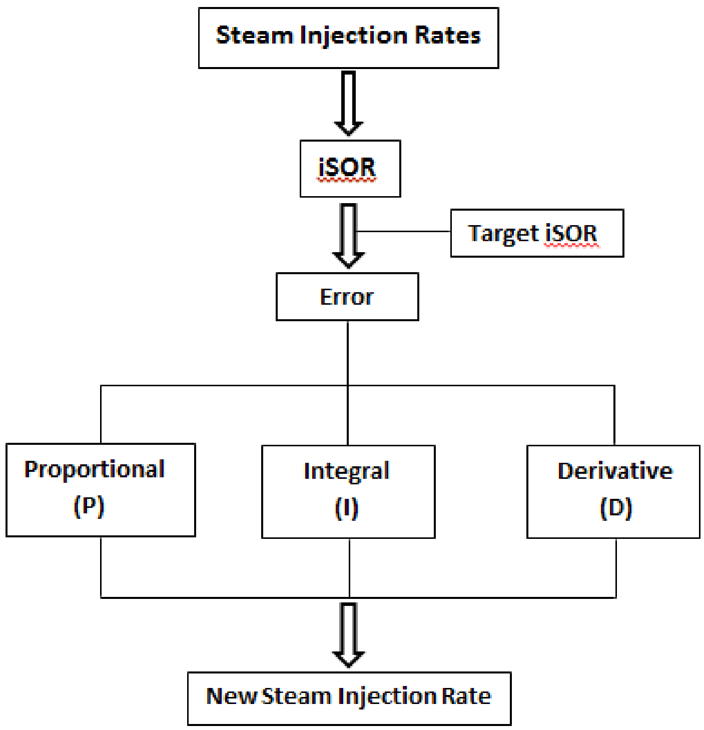

Figure 3-8: A simple description of the PID feedback control loop.

3.4.2 Customized PID control work flow

For this study, a commercial thermal reservoir simulator, the CMG STARS^{TM} is used to numerically simulate the SAGD process. CMG STARS^{TM} is a commercial simulator that specializes in thermal simulation. The simulator solves mass transfer equation and heat transfer equation within finite volume model (CMG STARS^{TM} User Manual, 2012). The simulator does not support built-in PID control function and so the simulation is stopped every three months and the data is extracted from the simulation results and processed to determine the new values of the steam injection rates (or pressure). The work flow is listed here step by step.

a. Load the simulation output file into the post-processor to plot the iSOR curve (shown in Figure 3-9).

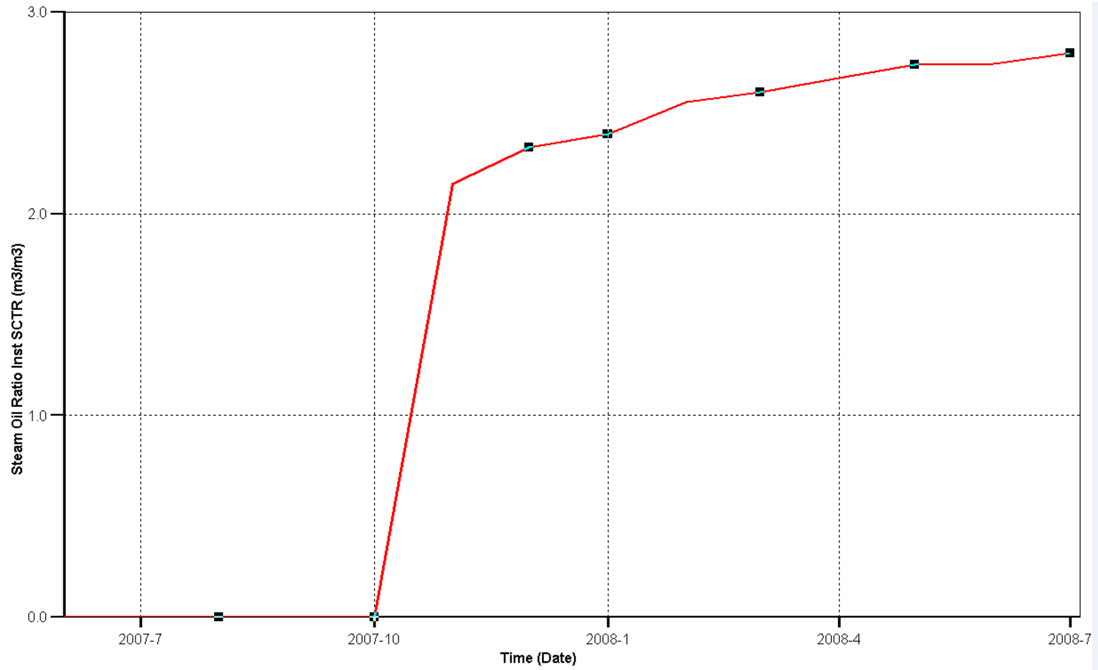

Figure 3-9: The iSOR curve plotted with CMG Results_Graph for iSOR data exportation.

b. Export the iSOR curve directly to MSExcel (listed in Table 3-3).

Table 3-3: The iSOR data extracted from simulator. The first two columns show the time and date, and the third column shows the iSOR data. The iSORs over the first four months of the operation are equal to zero because this is when the steam circulation period is done.

Time, day	Date	iSOR, m^3/m^3
0	6/1/2007	0
30	7/1/2007	0
61	8/1/2007	0
92	9/1/2007	0
122	10/1/2007	0
153	11/1/2007	2.149052
183	12/1/2007	2.330564
214	1/1/2008	2.39678
245	2/1/2008	2.555887
274	3/1/2008	2.604568
305	4/1/2008	2.674866
335	5/1/2008	2.741778
366	6/1/2008	2.74617
396	7/1/2008	2.797274

a. The error at each date is calculated (listed in Table 3-4). In this case, the target iSOR is equal to 2.7m^3/m^3 (the choice of target iSOR selection will be discussed below).

Table 3-4: The PID Error Table

Time Step	iSOR, m^3/m^3	Error
1	2.741778	0.042
2	2.74617	0.046
3	2.797274	0.097

The error data versus time step is regressed by using a quadratic function. The fit obtained for the data listed in Table 3-4 is displayed in Figure 3-10.

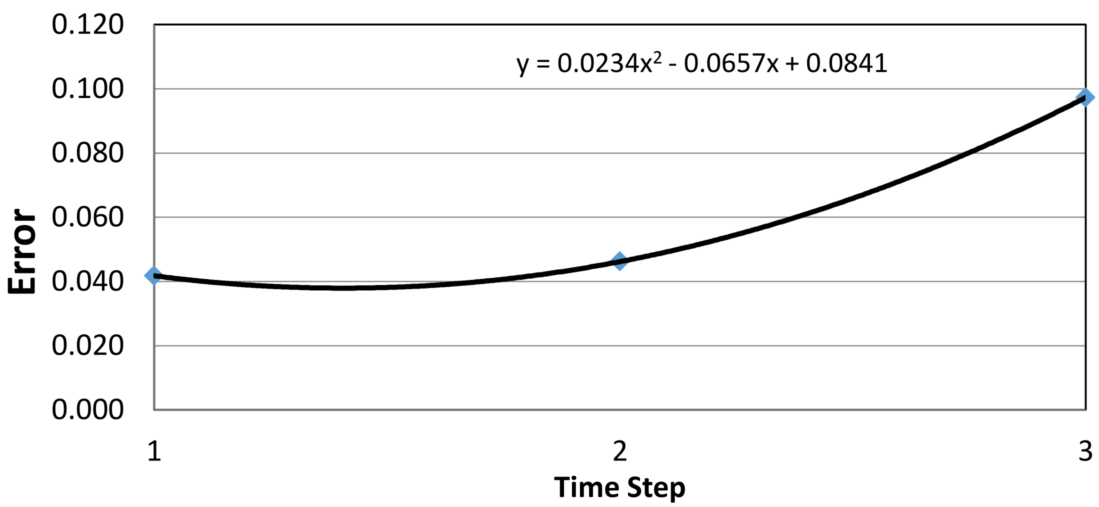

Figure 3-10: Fit of error data to a quadratic function.

b. The integral and derivative terms are calculated by using the fitted quadratic function. The results are listed in Table 3-5. The new steam injection pressure is calculated from the PID control equation.

Table 3-5: Calculation of the new steam injection pressure (a, b, and c are the coefficients of the fitted quadratic function).

P_i	3,500 kPa	Set point iSOR, m^3/m^3	2.7
a	2.34E-02	K_p	-20
b	-6.57E-02	T_D	1
c	0.0841	T_I	-50
t	3	e_i	0.10
2t	6	$\frac{de_i(t)}{dt} = 2at + b$	7.47E-02
$\frac{t^2}{2}$	4.5	$\int_0^t e_i(t)dt = a\frac{t^3}{3} + b\frac{t^2}{2} + ct$	1.08E-01
$\frac{t^3}{3}$	9	P_{i+1}	3,416 kPa

To ensure that the injection pressure remains practical, additional constraints on the feedback control algorithm are imposed as follows:

- If P_{i+1} is negative, then the value will only be reduced by a fraction of 0.1
- If $|P_{i+1} - P_i| > 500$ kPa, then the pressure will be changed by 500 kPa for the next control cycle
- If $P_{i+1} > 4800$ kPa, the fracture pressure, then the new injection pressure will stay at 4,800 kPa, the maximum operating pressure. In the field, the injection pressure of SAGD operations is constrained to be below the fracture pressure of the reservoir.

If the operating pressure goes over the fracture pressure, then the integrity of the formation will be damaged and the steam chamber may penetrate to shallow water aquifers leading to oil invasion into these zones. If the change in injection pressure is too high, then it is difficult to do this in the field. The steam injection pressure is directly related to the iSOR. In other words, an increase in injection pressure will increase the iSOR.

3.4.3 PID parameters tuning

The first objective of PID control is to establish proper controller parameters, that is, the gains K_P, T_I, T_D and set point value. Here, to speed up the calculations, the PID controller was tuned by using a single 2D SAGD wellpair model (same model as used for the study, but with only one pair of well sections left) for its simplicity.

3.4.3.1 Selection of the set point value

The selection of the set point value for PID control has a direct impact on its performance as a controller. For example, Stone (2013) described in his study that using a smaller subcool temperature difference as the set point value improves SAGD performance over that of a larger subcool. To estimate the set point value for the SAGD cases done here, a single case was run with the following features:

1. The original 2D reservoir model was modified to have more homogeneous properties in the oil column. By using this model, the performance of the SAGD wellpair, as measured by the iSOR, is expected to be better than that achieved in the original model. Thus, this provides a meaningful target iSOR to try to achieve in the original model.
2. The injection well constraint was set equal to constant steam injection pressure of 3,500 kPa and the production well constraint was set to mimic steam trap control with a maximum steam production rate equal to 0.04m^3/day/m well length.
3. Only proportional control (integral and derivative were disabled) was used.

By running the case for 7 years, a stable cumulative steam-to-oil ratio (cSOR), defined by the ratio of the total steam injected (expressed as cold water equivalent) and total produced oil, was obtained equal to 2.7m^3/m^3. The cSOR provides an "integrated" version of the iSOR providing an overall value for the steam-to-oil ratio. Given the improved quality of the reservoir and constant operating pressure, the cSOR obtained provides an estimate of the "best" case cSOR that can be achieved. In other words, this value serves as a target value for the original model to achieve. Field data demonstrates that a cSOR equal to 2.7m^3/m^3 is an excellent steam-to-oil ratio (Gates and Larter, 2013). Furthermore, ConocoPhillips' field operation data reveals that among the nine well pairs in the Surmont 102N pad, the best cSOR achieved by a single well-pair is also roughly equal to 2.7m^3/m^3.

The cSOR and iSOR profiles, along with a cross-sectional view of the steam chamber, are displayed in Figure 3-11. The results reveal that the iSOR stays relatively steady until after ~25 months of steam injection when the steam chamber reaches the top of the oil column (the top water zone). For the early stage, or the period where no heat loss is concerned, the cSOR remains at about 2.7 m^3/m^3. This value is used as the set point in the PID cases evaluated in this research.

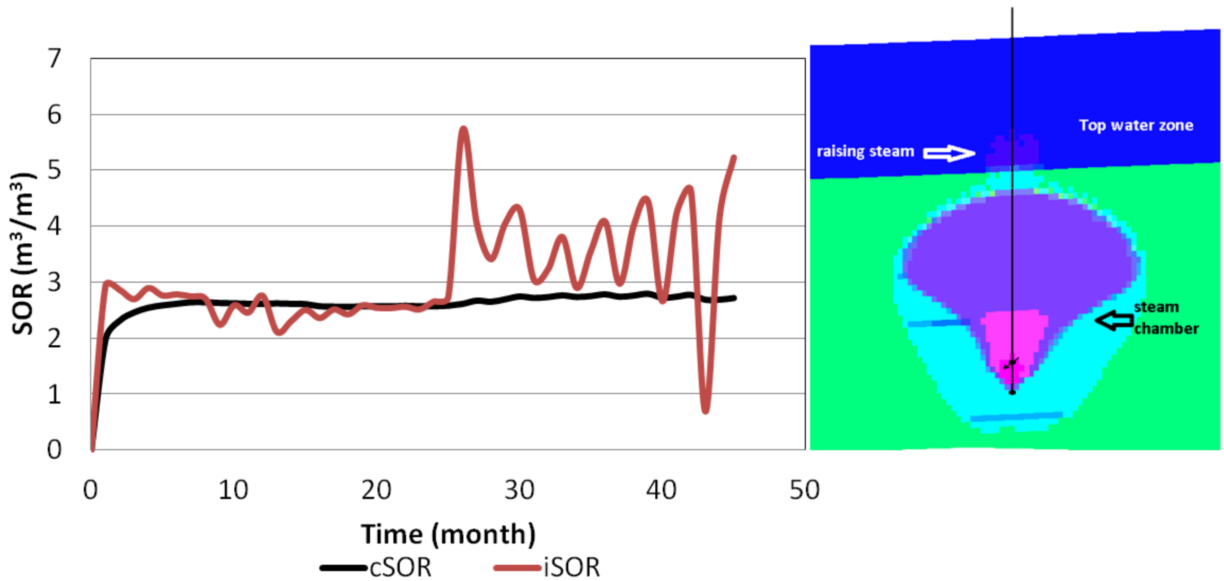

Figure 3-11: The iSOR and cSOR profiles and steam chamber shape from 2D ideal run to determine target value for the PID control.

3.4.3.2 Tuning of K_p, T_I and T_D

To tune the gains, the Ziegler-Nichols tuning method was partially used (Stephanopoulos, 1984). First, T_I and T_D were disabled so that a proportional controller was used. Different values of K_p were then evaluated. The results, shown in Figure 3-12, reveal that proportional control yields oscillations of the iSOR. In Figure 3-12, the orange curve represents the response when K_p = -50 m^3/day and the blue curve represents the response when K_p = -100 m^3/day. The gray line represents the set point iSOR equal to 2.7m^3/m^3. It is observed that when K_p = -100 m^3/day, the process approaches the set point more rapidly than when K_p = -50 m^3/day. However, at K_p = -100 m^3/day, the process starts to oscillate at quite large amplitude around the set point and appears to become unstable with growing fluctuations of the iSOR (and consequently the steam injection rates). In SAGD operations, in practice, it is not desired to oscillate the steam injection rate excessively due to equipment limitations. On the other hand, the K_p = -50 m^3/day curve is relatively slow to respond to reach the set-point, which is also not desired in SAGD operations.

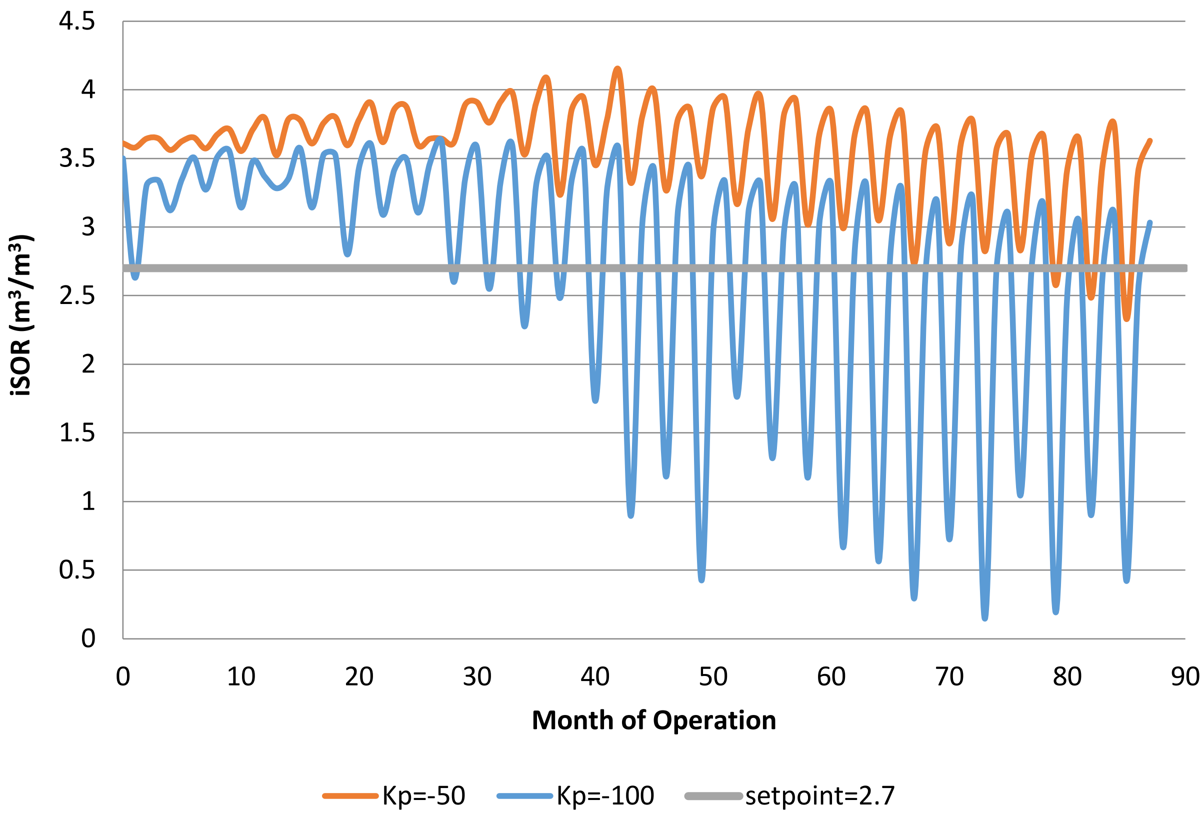

Figure 3-12: Effect of proportional gain: K_p = -100 m^3/day yielded larger oscillations than that with K_p = -50 m^3/day.

Thus, a dynamic proportional gain is proposed, in which K_p = -100 m^3/day is used in the early stage of the SAGD process due to its ability to lower the iSOR in the early stage, and a K_p = -50 m^3/day in the late stage is used because of its ability to confine the oscillation more so than that achieved by the larger value of the proportional gain. The results of the two-step proportional gain are shown in Figure 3-13.

Once the proportional gain was found, the T_I and T_D were tuned to accelerate the process to the target iSOR and kill the overshoot in adjustment. The values obtained after several trials were equal to T_I = 12 and T_D = 1.5. The effect of adding integral and derivative control is shown in Figure 3-14. These values of T_I and T_D are not likely optimal; this needs to be explored in future work.

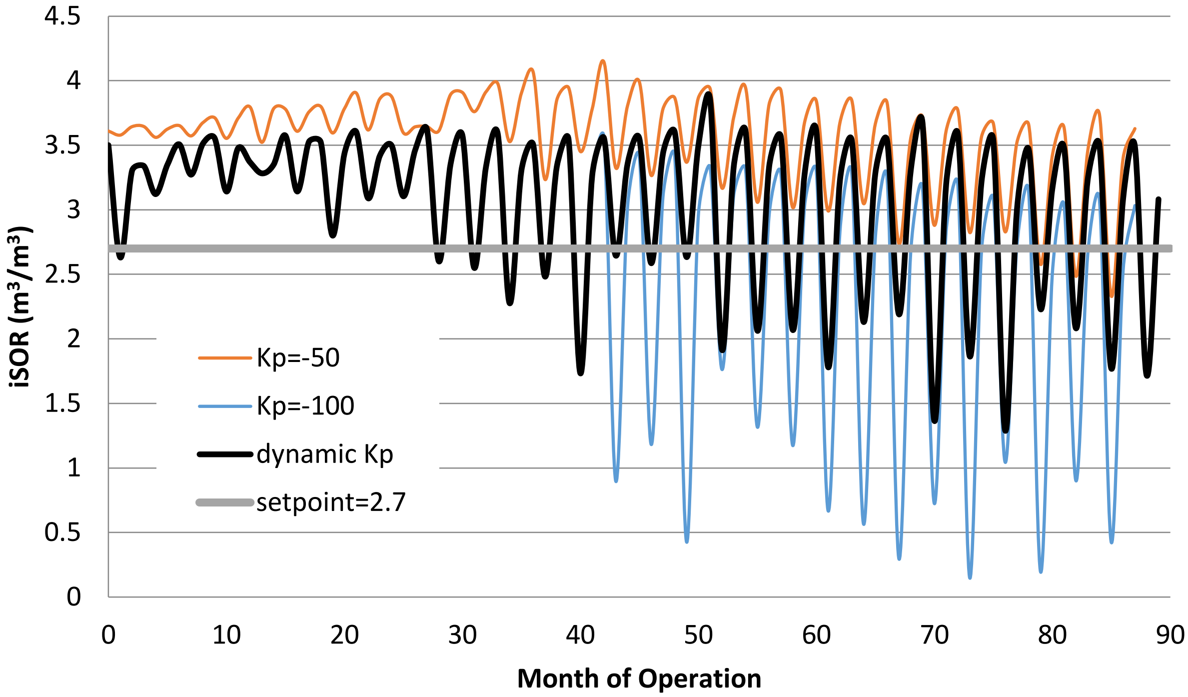

Figure 3-13: Effect of dynamic proportional gain: a relatively large Kp at start and a relatively small Kp at end stabilized the oscillation.

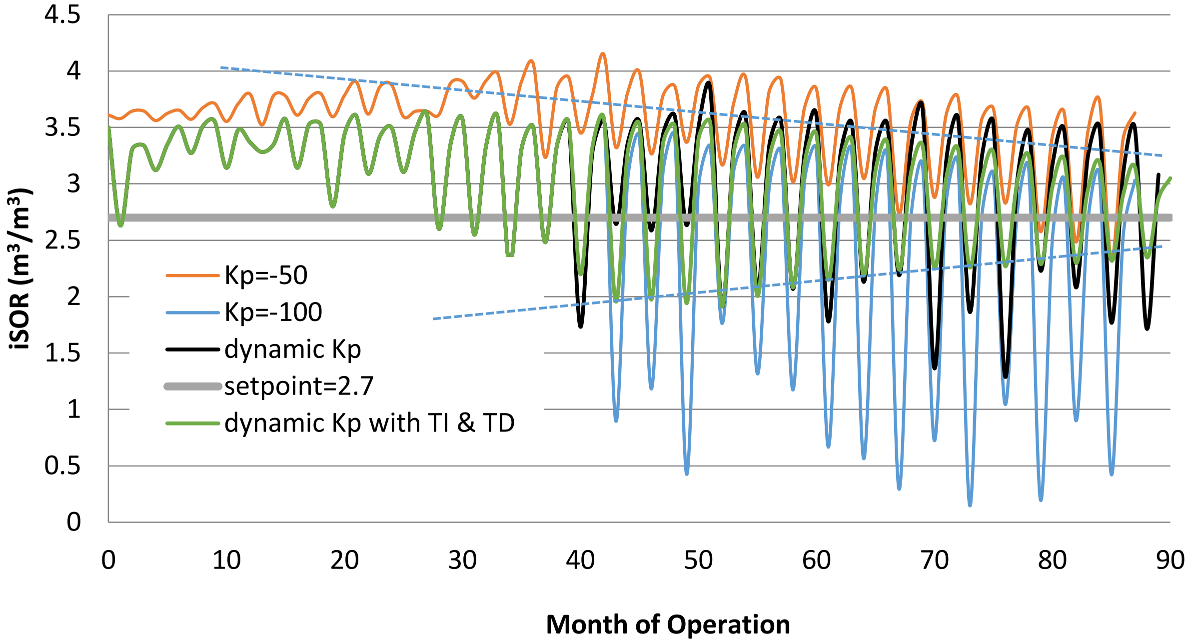

Figure 3-14: Effect of integral and derivative gains in approaching target value and in supressing overshoot. The Kp, TI and TD values are by no means optimized. They are selected from many simulation runs.

3.5 Case Studies

Two cases, Cases I and II, were created to evaluate PID control, along with a base case, which is not PID controlled. The base case and Case I will be introduced here whereas Case II will be introduced in Chapter Four. For evaluation of case performance, focus is made on four factors:

1. The total amount of steam injection. It represents the total energy input which is important in SAGD operations since it is the single biggest expense in SAGD.
2. The cumulative steam-to-oil ratio (cSOR). The cSOR represents the overall cost-to-revenue ratio and is a good indicator of operational profitability (it does not include the capital required to build the plant and thus is not a replacement for the net present value or rate of return). Although the target value of the process is the iSOR, the overall measure of the performance of the process is the cSOR since it provides a

overall measure of the steam-to-oil ratio. The iSOR provides a measure of the steam-to-oil ratio on a daily basis only.

3. The oil rate. The oil rate is the revenue stream in the process and accounts for the positive contributions to the cash flow.
4. The temperature distribution. The temperature distribution within the reservoir during SAGD operation indicates steam conformance. The temperature distribution provides the relationship between steam injection and reservoir heterogeneity and this will be a main focus in Chapter Four.

3.5.1 Base Case

A base case was created by using simple well operating constraints that would be typically assumed for designing a SAGD operation. In the base case, a constant injection pressure equal to 3,500 kPa is applied in each injection well in the 2D reservoir model. The choice of 3,500 kPa injection pressure was based on the Surmont field injection strategy which has a similar early stage injection pressure. To mimic steam trap control, the steam rate into the production well is constrained to 0.04 m^3/day per meter length.

In the 2D model, all 9 wellpairs start steam circulation on June 1 2007. Steam circulation is modelled by using line heaters placed in the same locations as the injection and production wells. The temperature of the line heaters are set equal to 200 ℃. After 4 months of circulation, the temperatures of the region between the wells have reached the target temperature of about 80 ℃ (due to conductive heating from the wells) and on October 1 2007, all well pairs were converted to SAGD mode where steam is injected into the top wells and fluids are produced through the lower wells. In SAGD mode, the line heaters are disabled. SAGD operation lasted for 7 years, ending on October 1 2014. The results of base case are shown in a series of Figures below.

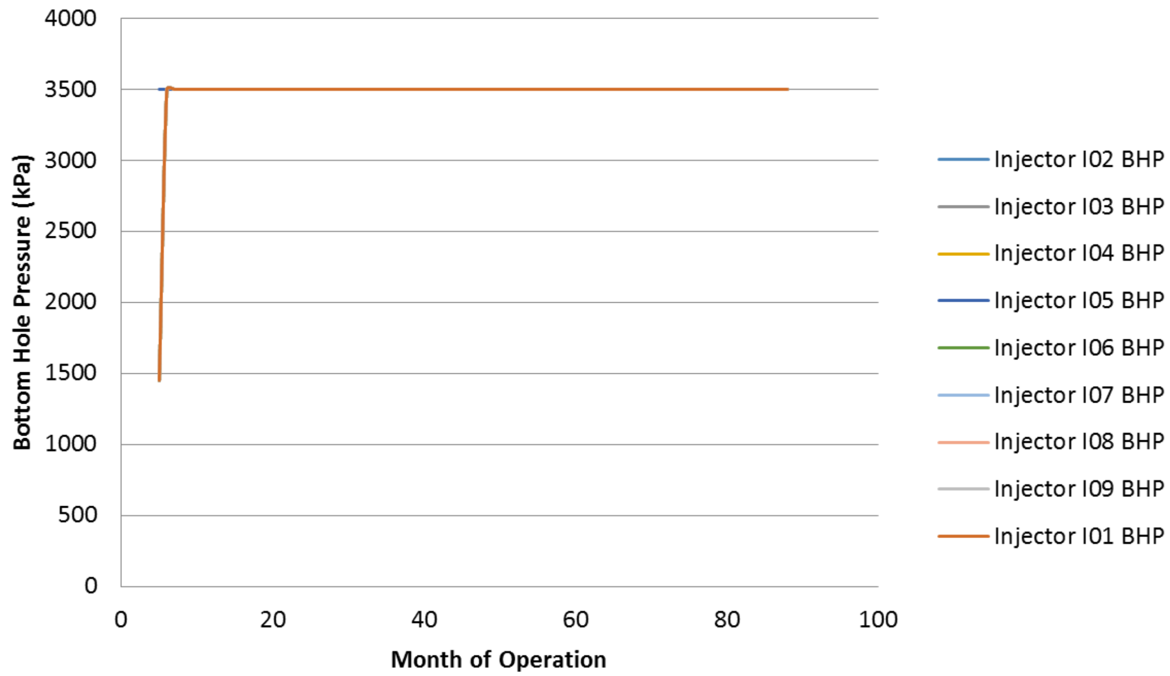

Figure 3-15: Base Case, injection well bottom hole pressure. All of the profiles are on the same line.

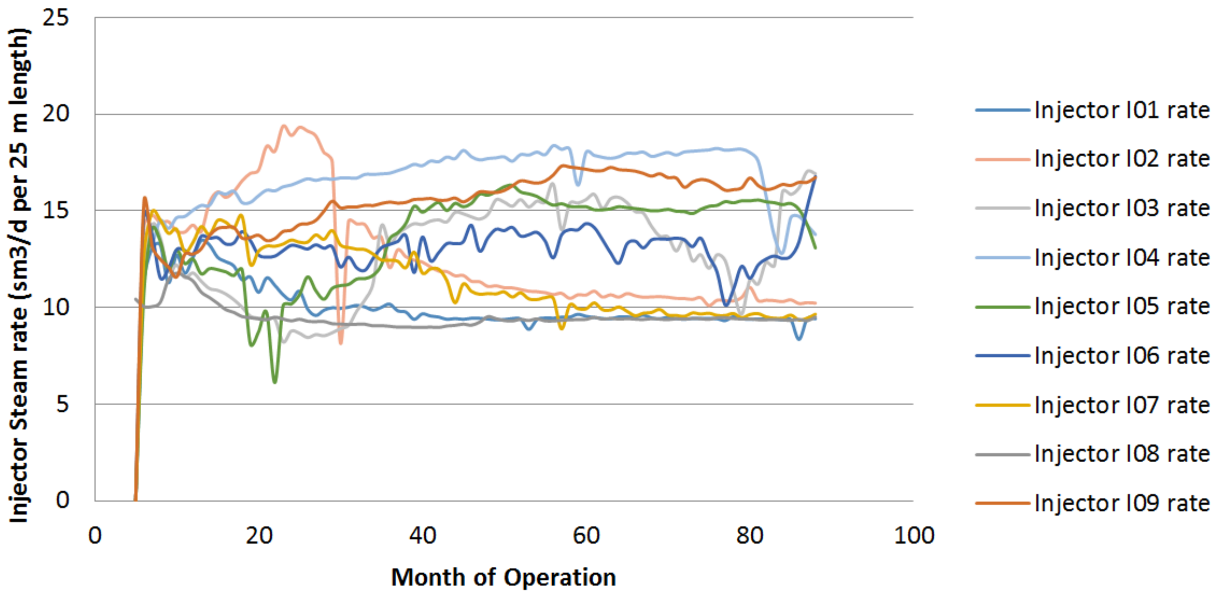

Figure 3-16: Base Case, injection well steam rates

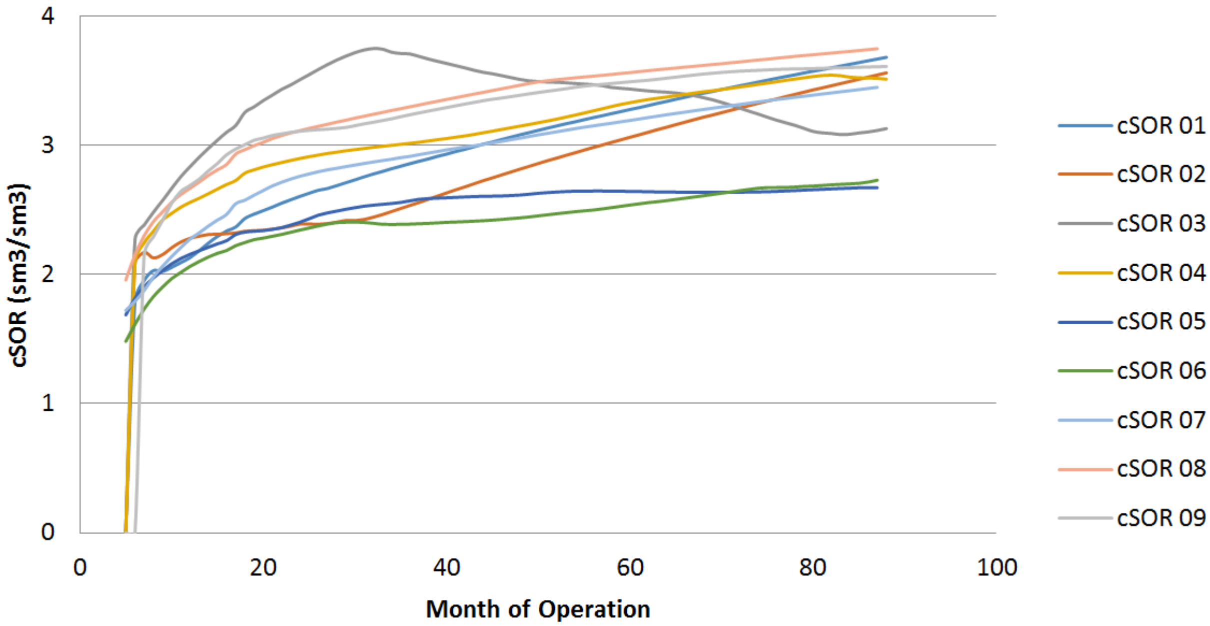

Figure 3-17: Base case, cumulative steam-to-oil ratio, cSOR.

The results of the base case reveals that under constant steam injection pressures, different steam rates and cSOR profiles are obtained. This is a direct reflection of the heterogeneity of the reservoir – the cSOR profiles provide a basic understanding of the heterogeneity of the reservoir. Since each well pair is under the same injection pressure of 3,500 kPa, then the injector with more shale barriers on top has smaller steam injection rate, for the reason that path of the rising steam chamber is blocked by the low permeability layers. In other words, the steam injection rate at constant steam injection pressure is a direct reflection of injectivity. In Table 3-6, the steam injection rate of each well pair is averaged over the operating life of the process and sorted in order of steam rate from the largest (the best injectivity) to the smallest (the worst injectivity). The cSOR (at the end of the operation) of the nine wellpairs are also ranked from the lowest to the highest in Table 3-6. The cSOR rank reflects the thermal efficiency of the well pairs which is not reflected by injectivity alone. For instance, the existence of lean zones and thief zones with high permeability would have exhibited good injectivity (in other words, high steam injection rates under constant injection pressure). However, the corresponding cSOR would be higher because per unit steam injection, there is a smaller volume of oil mobilized and drained. Also, the heterogeneity in oil saturation is reflected in the cSOR data. Thus, to rank the local reservoir quality, a production index can be generated which combines the steam injection rate under constant injection pressure and the cSOR. The production index is as follows:

$$\mathrm{PI} = \frac{Avg_{q_{steam}}}{cSOR} \qquad 14$$

Where PI is the Production Index; $Avg_{q_{steam}}$ is the average steam injection rate under constant injection pressure; cSOR is the end point steam-oil-ratio. The production index of each well pair is also listed in Table 3-6. A higher production index suggests relatively better reservoir quality.

From the results listed in Table 3-6, Wellpairs 5 and 6 achieved the lowest cSOR of 2.7 m^3/m^3 and also has the highest production index, suggesting that reservoir in those areas have the best potential for oil recovery. Also interesting is Wellpair 4, which has the largest injectivity, but a relatively low cSOR. Thus, the production index is only ranked third after Wellpairs 5 and 6. Wellpairs 4, 5, and 6 are ranked the best three well pairs whereas Wellpairs 7, 1, and 8 are the worst ones. A cSOR range of 2.67 to 3.75m^3/m^3 is obtained for the base case. The cumulative fluid and overall cSOR are listed in Table 3-7.

Table 3-6: The ranking of steam injection rate under constant injection pressure, cSOR and production index for 9 well pairs.

Well pair	Average steam rate, m^3/day/25 m	**Well pair**	cSOR, m^3/m^3	**Well pair**	Production Index
4	16.8	**5**	2.67	**5**	6.3
9	15.5	**6**	2.73	**6**	5.7
5	13.8	**3**	3.13	**4**	4.4
6	13.1	**7**	3.45	**9**	3.8
3	12.9	**4**	3.51	**3**	3.7
2	12.7	**2**	3.56	**2**	3.6
7	11.4	**9**	3.61	**7**	3.2
1	10.1	**1**	3.68	**1**	2.7
8	9.5	**8**	3.75	**8**	2.5

Table 3-7: Base case, cumulative fluids and steam-to-oil ratio.

Cumulative steam injection (m^3)	12,094
Cumulative oil production (m^3)	3,621
Cumulative steam oil ratio (m^3/m^3)	3.33

3.5.2 ***PID Case I***

In this case, the maintenance of target steam-to-oil ratio is the objective. As observed in the base case, a cSOR of $2.7m^3/m^3$ is only obtained from two of the best wellpairs, Wellpairs 5 and 6. The worst cSOR is as high as $3.7m^3/m^3$. To conduct the simulation, a PID controller is applied to each SAGD well pair. Thus, a total of nine controllers are used. Equation (12) is used to control the steam injection rate and a constant iSOR set point equal to 2.7 m^3/m^3 is applied to each controller. The same work flow described in Section 3.4.2 above is followed (except using steam rate as manipulated variable, instead of pressure). As for the production constraints, a maximum steam production rate of $0.04m^3/d$ per m length is applied to mimic steam trap control. The results obtained from PID Case I are displayed in Figures 3-18 to 3-20.

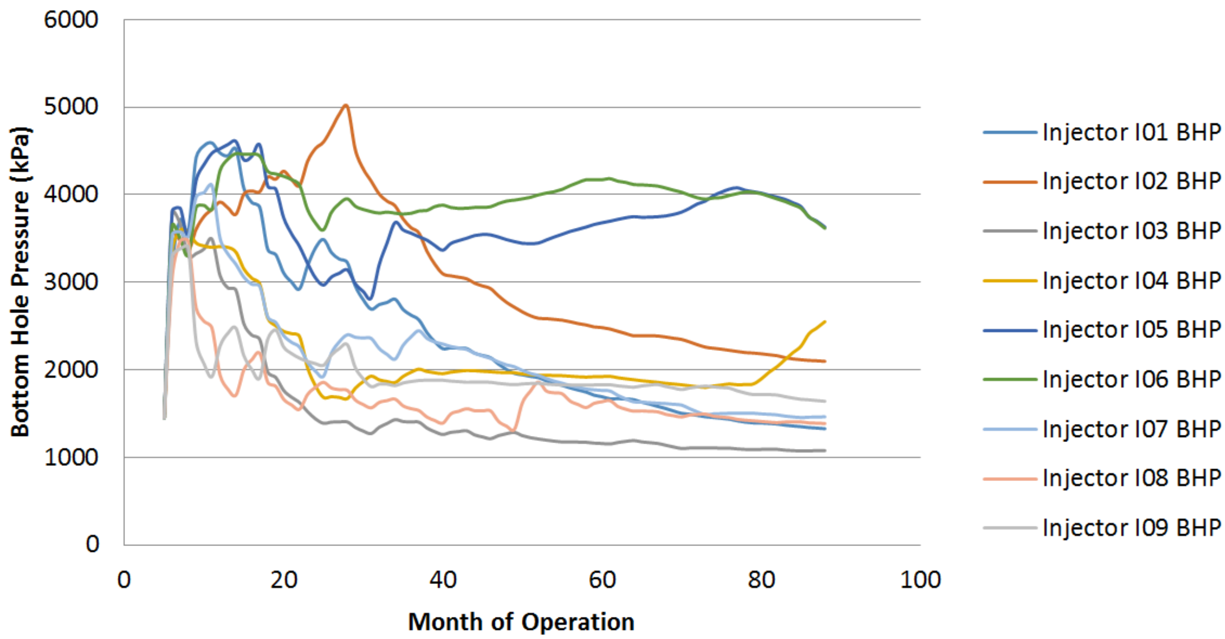

Figure 3-18: PID Case I, injection well bottom hole pressures.

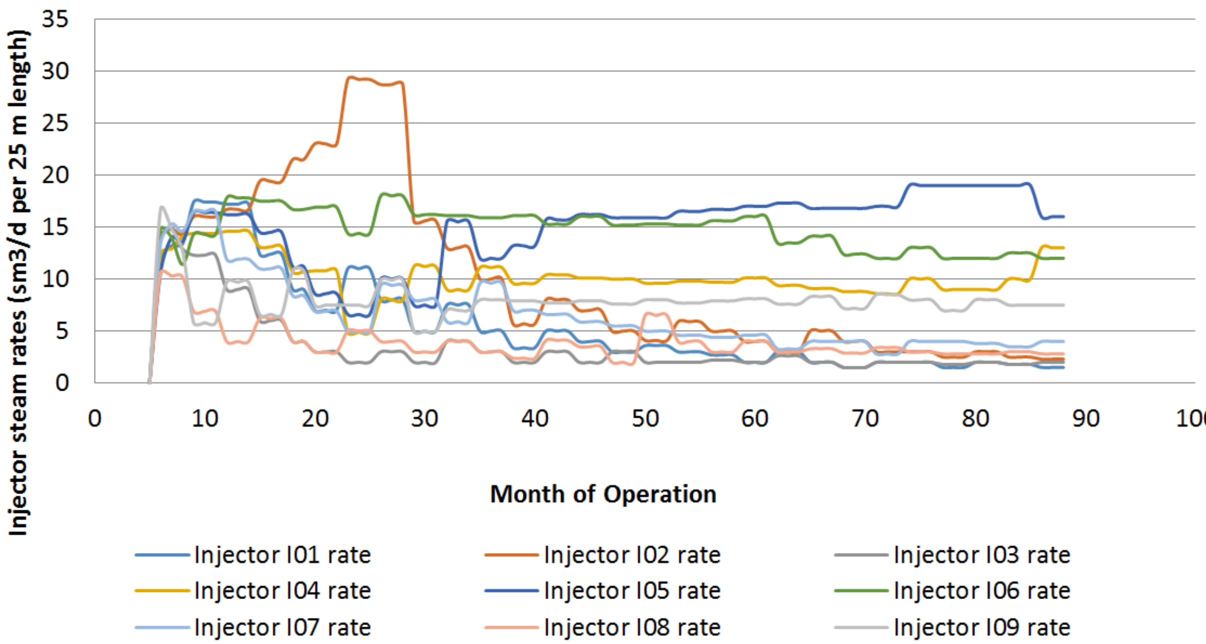

Figure 3-19: PID Case I, injection well steam rates.

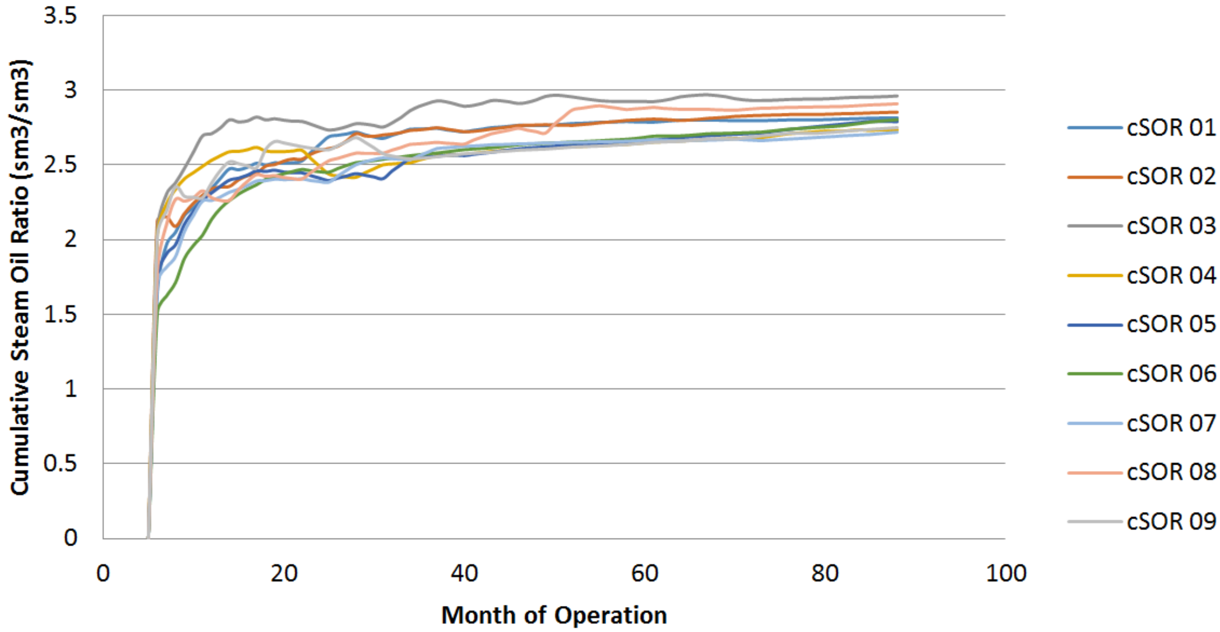

Figure 3-20: PID Case I, cumulative steam-to-oil ratios.

Figure 3-18 demonstrates that the automated control strategy yields injection pressure profiles that in general start at elevated pressure and decline to lower pressures later in the process. This is consistent with the optimized strategy determined through genetic algorithm optimization by Gates and Chakrabarty (2006). Furthermore, the declining trend of the steam injection pressure from the early stage to the late stage for the majority of wellpairs is similar to what the Surmont operator applied to their 102N Pad shown in Figure 3-21. Typically, as shown by Gates and Chakrabarty (2006), the reduction in injection pressure after 3-4 years operation corresponds to the time when steam chamber touches the overburden. A reduction in injection pressure would effectively lower heat loss to the water zone on top. With PID control, shown in PID Case I, the frequency of steam rate (or steam pressure, fundamentally will be the same thing for SAGD control) adjustment is much higher than the Surmont field strategy and we would expect better performance as a result.

Figure 3-19 shows the steam injection rate profiles obtained from the controller using PID control. For most of the wellpairs, the injection rates decline as the operation proceeds. The base case revealed variable steam injection rates under constant steam injection pressure which are attributed to the local injectivity which in turn arises due to reservoir heterogeneity around the wellpairs. In PID Case I, the variation of steam rates from well pair to well pair is even larger, as a result of PID control, to better serve the control objective: a constant and same cSOR for each well pair.

From Figure 3-20, it is observed that the cSOR of the wellpairs all approach the same target value with range at the end of the operation from 2.72 to 2.96 m^3/m^3. Compared to the cSOR range of 2.67 to 3.75m^3/m^3 from the base case, it is clear that the PID controller is narrowing the window of cSOR achieved by the wellpairs. The reduction in the deviation between the observed and target cSOR is shown in Figure 3-22. The results demonstrate that the deviation of wellpair cSOR and the target cSOR is relatively large in the base case whereas it is significantly reduced in the PID controlled case. A summary of the cSORs at the end of the operation for the base case and PID Case I is listed in Table 3-8.

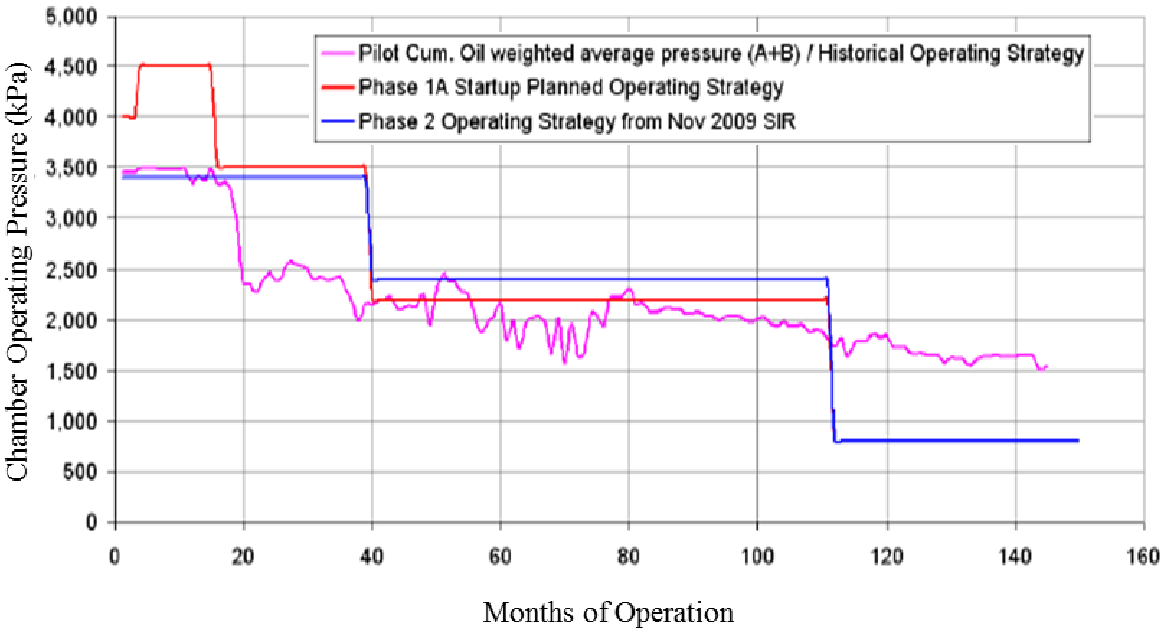

Figure 3-21: ConocoPhillips' Surmont SAGD steam injection strategy: the operation started with 3,500 kPa high pressure injection; after 3-4 years operation, the injection pressure was reduced to 2,500 kPa; after 9 years operation, the pressure is planned to maintain at 900 kPa (courtesy of ConocoPhillips Canada, 2013).

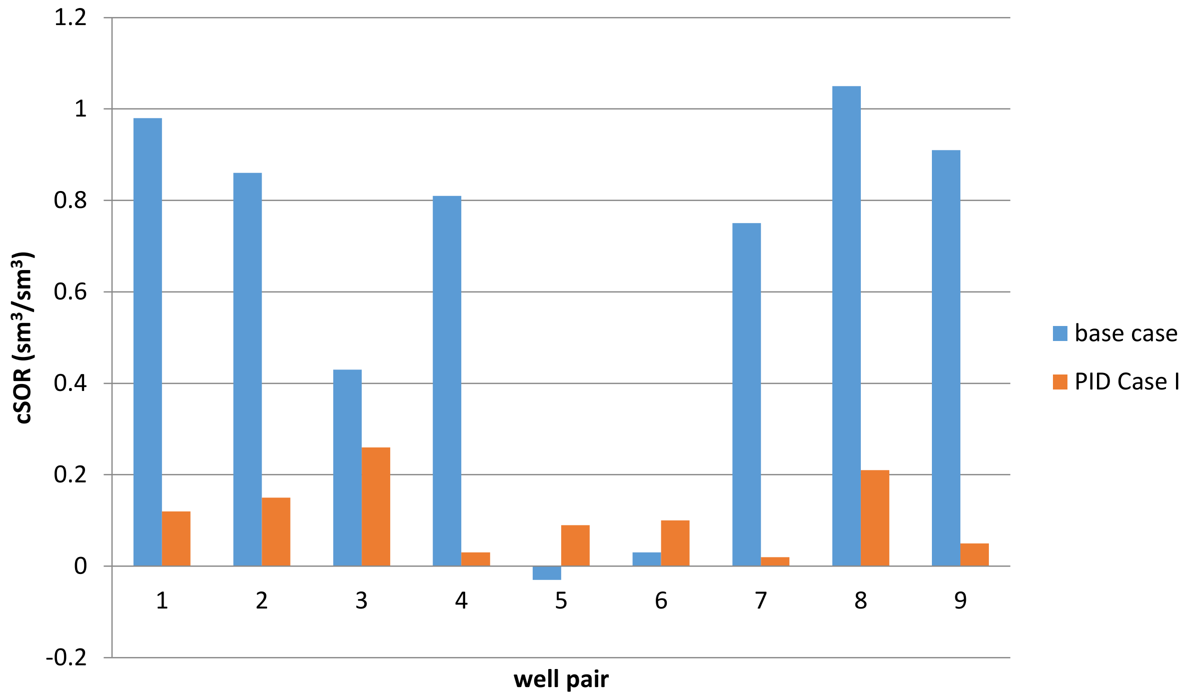

Figure 3-22: Comparison of base case and PID Case I cSOR deviation from target value of 2.7m^3/m^3.
Table 3-8: The end-point cSORs for the base case and PID Case I.

	cSOR, m^3/m^3			
Well pair	Base case	PID Case I	Deviation, base case - 2.7	Deviation, PID Case I-2.7
1	3.68	2.82	0.98	0.12
2	3.56	2.85	0.86	0.15
3	3.13	2.96	0.43	0.26
4	3.51	2.73	0.81	0.03
5	2.67	2.79	-0.03	0.09
6	2.73	2.8	0.03	0.1
7	3.45	2.72	0.75	0.02
8	3.75	2.91	1.05	0.21
9	3.61	2.75	0.91	0.05

The key benefit of a PID-deployed SAGD operation is that the process is adaptively controlled to shift the steam-to-oil ratio to the target value with no input from humans. The iSOR signal provides a measure of the steam injectivity, oil storage and drainage through steam conformance, and thus the reservoir heterogeneity and thus provides a good method to control the process. The PID controller considers the error in current operation, the cumulative error in production history, and the change of error through time, so that it is able to provide more accurate adjustment on the steam injection, either steam rate or steam injection pressure, and can do so most likely better than a human could. Human decisions often only depend on personnel experience and knowledge, which varies from person to person.

The injectivity of each well pair is different as shown in the base case injection rates (all done at constant injection pressure). Also, the oil saturation and the distance from injector to the overburden vary from well pair to well pair; the distance of injector to overburden of the nine well pairs is summarized in Table 3-9. Thus, in the SAGD process, the resulting cSOR of each well pair arises from complex, interacting features of the system. These features include the number and extent of shale barriers above the injectors, the time it takes the steam chamber to reach the overburden (after which heat loss increase), and the heterogeneity of the oil saturation (a lean zone would yield a higher cSOR for the same steam volume).

Table 3-9: Distance between injection well and overburden of nine well pairs.

Injector	Distance to overburden (m)
I01	27
I02	28
I03	24
I04	26
I05	31
I06	31
I07	26
I08	25
I09	22

For example, the performance of Wellpair 8, which according to the production index in Table 3-8 has the lowest injectivity and production index, is caused by extended shale barriers above the injector (see Figure 4-11). This barrier blocks steam within the formation. The time it takes for the steam to rise to the barrier depends on the separation between the shale barrier and the injection well. The rising steam will not able to by-pass the shale barriers until it has grown beyond the extent of the barrier. As a result, for the given amount of steam injected, the oil recovery suffers because: 1. the shale layer contains no oil and thus there is no drainage from it, 2. steam cannot contact the oil beyond the shale layers however there will be heat transfer through the shale layer to the oil zone above, and 3. there is oil drainage path. Thus, the iSOR rises for that well pair. As a consequence, the controller attempts to lower the iSOR back to the target value and the manipulated variable, the steam injection rate, is reduced. The cumulative fluid and cSOR of PID Case I is listed in Table 3-10. At pad-scale, PID Case I has definitely lower total steam injection and lower total oil production than that of the base case. However, the overall cSOR reaches the target cSOR better than that of the base case; it is almost 16% lower than that of the non-controlled case.

Table 3-10: Cumulative fluid and steam-to-oil ratio for PID Case I.

Cumulative steam injection (m^3)	7,982
Cumulative oil production (m^3)	2,897
Cumulative steam oil ratio (m^3/m^3)	2.78

3.5.3 ***Discussion: Application to Three-Dimensions***

PID Case I is a 2D reservoir model. The reality is that reservoirs are three-dimensional (3D) and that the control strategy must work in a 3D system. The 2D results demonstrate that the control algorithm effectively detects reservoir heterogeneity in the 2D vertical plane perpendicular to the wellpairs. In a 3D system, if control is done along intervals of the wellpairs, then in each interval, the system approaches that of multiple 2D systems. Thus, the PID algorithm should be able to handle control of steam injection rates into each interval to improve the cSOR. However, if control is done in the entire wellpair, then the result of the iSOR is an integrated result spanning the entire length of the wellpair. Thus, given the length of the wellpair (typically between 500 and 1,000 m), local heterogeneities with length scales of order of tens to a few hundred meters will not be well represented by the wellpair iSOR signal. Thus, this suggests that interval control is required to ensure that the algorithm can deal with heterogeneities that have smaller length scale than that of the wellpair length. Gotawala and Gates (2010) suggested that the intervals should be of order of 100-200 m in length. However, that result may be incorrect in the context of point bar deposits as shown by Su et al. (2013).

3.6 Conclusions

The results of the study reveal that PID control can be used to shift the steam-to-oil ratio to a set point and that the iSOR provides a signal that measures the injectivity of the steam, the storage and mobilization of oil, the heterogeneity of the reservoir, and the oil drainage rate. The results also reveal that the controlled case exhibits a decreasing injection pressure trend which is consistent with previous research and ongoing SAGD field operations.

This chapter provides a detailed work flow of PID controlled SAGD operation, in which the iSOR is used to guide steam injection rate, so as to achieve target cSOR in the long run. The workflow includes how iSOR data is extracted to MSExcel for process and how the error function is constructed and how the PID function is executed. Thus, any SAGD operator, with access to computer and MSExcel would be able to perform the automated control process to provide easy tool for reservoir and well management in field.

Chapter Four: **Dynamic Steam Distribution via PID control in SAGD pad operation**

In this Chapter, PID Case II is introduced. PID Case II is nearly the same as PID Case I except that the total steam injection rate into all of the nine wellpairs, the pad, remains constant as would be the case in a field operation where the steam generator operates with constant steam rate. In PID Case I, the steam injection rates is adjusted to move the iSOR towards the iSOR set point. This means that the total steam rate into the pad declined as the process evolved. Since less steam was injected into the reservoir, less heating of the formation occurred and thus the overall oil rate from the pad declined. In PID Case II, the daily steam injection rate at the pad scale is fixed to a constant value. In this case, the control algorithm decides how much steam (of the pad amount) to allocate to each wellpair. This case more closely represents the situation in the field where the steam generation plant, typically a once-through steam generator, is constrained to a constant steam rate – in general, it is not possible to provide variable steam rates from a once-through steam generator.

In PID Case I, the PID controller on each well pair is considered an independent device and the nine controllers work independently to adjust its own steam rates. However, in PID Case II, on daily basis, the fixed amount of steam has to be injected among the nine well pairs. Thus, the control algorithm ranks and allocates the steam to each of the wellpairs based on the iSOR signals from each of the wellpairs.

4.1 Control Workflow

The control workflow in PID Case II has an additional step more than that of PID Case I where the steam rate is normalized and allocated among the wellpairs. The nine PID controllers associated with the nine well pairs work as usual to calculate steam rates from previous iSOR data. However, the new steam rates from the controllers are summed and then the fractions of the sum are determined for each wellpair. Then, the new steam rate applied is determined from the fixed steam plant capacity multiplied by the fraction. In this study, the fixed steam plant capacity for the 2D model was determined from the base case (described in Chapter Three) average total steam rate which was equal to 117m^3/day (per 25 m length of the 2D model). Figure 4-1 illustrates the calculation from the raw controller specified injection rates to the normalized ones.

PID suggested Q_{i+1} (m^3/d)										
	Injector									
cycle	1	2	3	4	5	6	7	8	9	sum
0	13.4	14.3	12.9	14.1	13.6	11.4	14.6	10.2	12.7	**117.1**
1	17.4	16.3	14.1	16.1	16.0	13.8	16.7	10.4	11.7	**132.5**
2	16.7	18	10.9	16.2	16.2	15.3	16.2	9.6	10.7	**129.8**
3	15.4	19.4	7.5	15.8	17.2	16.5	15.3	8.4	10.5	**126.0**
4	13.0	21.0	3.1	15.7	17.0	17.4	12.5	7.1	10.2	**117.0**
5	10.6	22.6	2.7	15.6	16.8	18.3	9.7	5.8	9.9	**112.0**
6	9.1	23.1	3.8	15.3	17.7	17.9	9.8	6.2	10.1	**113.0**
7	7.7	20.1	3.4	15.1	18.0	17.5	8.9	5.2	10.7	**106.6**
8	6.3	17.1	3.2	14.9	18.3	17.1	8.0	4.2	11.3	**100.4**
9	4.9	14.1	3.0	14.7	18.6	16.7	7.1	3.2	11.9	**94.2**
10	4.5	9.8	2.7	14.3	19.1	16.9	7.0	5.3	10.4	**90.0**
11	3.3	8.6	2.4	14.1	19.0	17.4	6.3	4.5	10.1	**85.7**
12	4.8	6.7	2.0	13.6	18.8	17.7	5.3	3.2	10.1	**82.2**

Normalized Q_{i+1} (m^3/d)										
	Injector									
cycle	1	2	3	4	5	6	7	8	9	sum
0										**0**
1	15.4	14.4	12.5	14.2	14.1	12.2	14.7	9.2	10.3	**117**
2	15.1	16.2	9.8	14.6	14.6	13.8	14.6	8.7	9.6	**117**
3	14.3	18.0	7.0	14.7	16.0	15.3	14.2	7.8	9.8	**117**
4	13.0	21.0	3.1	15.7	17.0	17.4	12.5	7.1	10.2	**117**
5	11.1	23.6	2.8	16.3	17.6	19.1	10.1	6.1	10.3	**117**
6	9.4	23.9	3.9	15.8	18.3	18.5	10.1	6.4	10.5	**117**
7	8.5	22.1	3.7	16.6	19.8	19.2	9.8	5.7	11.7	**117**
8	7.3	19.9	3.7	17.4	21.3	19.9	9.3	4.9	13.2	**117**
9	6.1	17.5	3.7	18.3	23.1	20.7	8.8	4.0	14.8	**117**
10	5.9	12.7	3.5	18.6	24.8	22.0	9.1	6.9	13.5	**117**
11	4.5	11.7	3.3	19.2	25.9	23.8	8.6	6.1	13.8	**117**
12	6.8	9.5	2.8	19.4	26.8	25.2	7.5	4.6	14.4	**117**

Figure 4-1: the normalization of steam injection rates for each well pair in PID Case II. Cycle refers to the control time interval index.

For example, consider Cycle 1 and Injector 1. The PID-calculated new steam rate is 17.4 m^3/d (per 25 m length of the 2D model), and the sum of all the controller steam rates is equal to 132.5 m^3/d for that cycle. Thus, the fraction of steam rate for Injector 1 is obtained as

$$\text{Steam Rate Fraction Injector 1} = \frac{17.4 \text{ m3/d}}{132.5 \text{ m3/d}} = 0.13132$$

This fraction is multiplied with the fixed pad steam rate of 117m^3/d to obtain the normalized steam rate for Injector 1:

$$\text{Normalized Steam Rate Injector 1} = 0.13132 * 117\frac{\text{m}^3}{\text{day}} = 15.4\frac{\text{m}^3}{\text{day}}$$

4.2 PID Case II Results and Discussion

To recall, the conditions of the base case, PID Case I, and PID Case II are summarized in the Table 4-1.

Table 4-1: Summary of base case, PID Case I and PID Case II.

Cases	Target	Injection Constraints	Features
Base Case (No PID Control)	-	Constant steam injection pressure of 3,500 kPa	-
PID Case I	Maintain constant cSOR of 2.7	PID feedback control sets steam rates with NO fixed pad rate	Declining injection pressure profile
PID Case II	Maintain constant 117 m^3/25m/d pad steam rate	PID feedback control sets steam rates with fixed pad rate	Dynamic steam distribution among well pairs

4.2.1 Pad scale steam injection rate

The pad scale steam injection rates of the base case, PID Case I, and PID Case II are compared in Figure 4-2. Consistent with the steam plant capacity, PID Case II has a constant steam injection rate equal to 117m^3/day. The base case has a steam rate that hovers around 117m^3/day. PID Case I exhibits a declining steam rate from about 120m^3/day to about 60 m^3/day. The cumulative steam injection volume of the three cases, shown in Figure 4-3, shows that base case and PID Case II have the same volume of steam injected whereas the volume injected in the PID Case I is smaller.

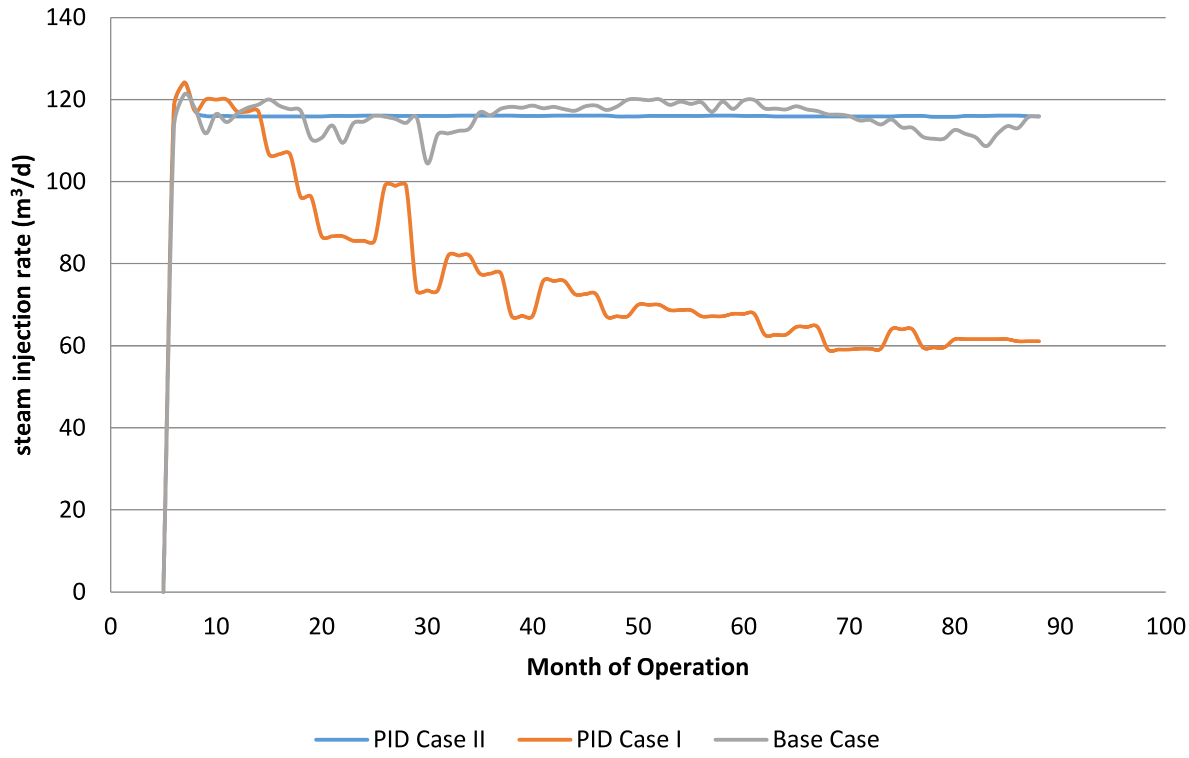

Figure 4-2: The pad scale steam injection for base case, PID Case I, and PID Case II.

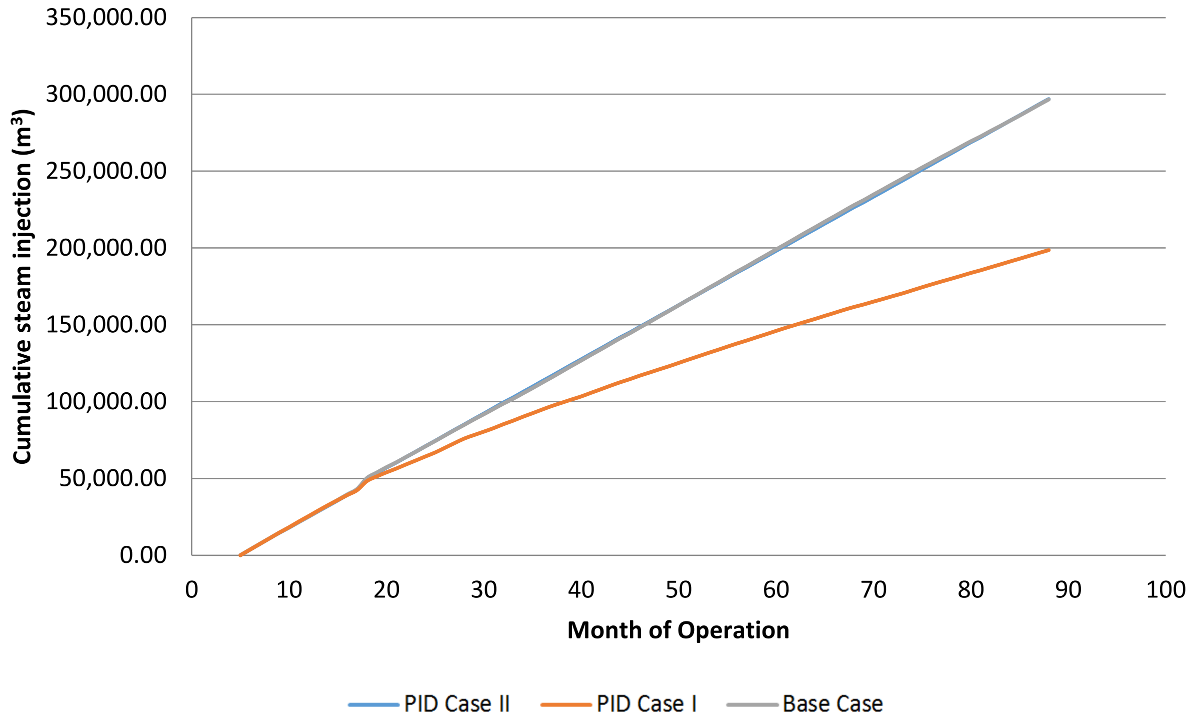

Figure 4-3: The cumulative steam injection for base case, PID Case I, and PID Case II.

4.2.2 Injection pressure profile

The steam injection pressure profiles of PID Case II are shown in Figure 4-4. The injection pressure profiles of the wellpairs in PID Case II, in general, show a declining trend with the exception of Wellpairs 3, 5, and 6. Injectors 5 and 6 have quite high pressure throughout the process whereas Injector 3 has a gentle inclining trend. Injector 4 follows a gentle declining trend, but by the end of 70 months of operation, the injection pressure increases and merges with that of Injectors 5 and 6. The results, displayed below, reveal that the steam chambers of Wellpairs 4, 5, and 6 merge causing the pressure surge seen in Injector 4.

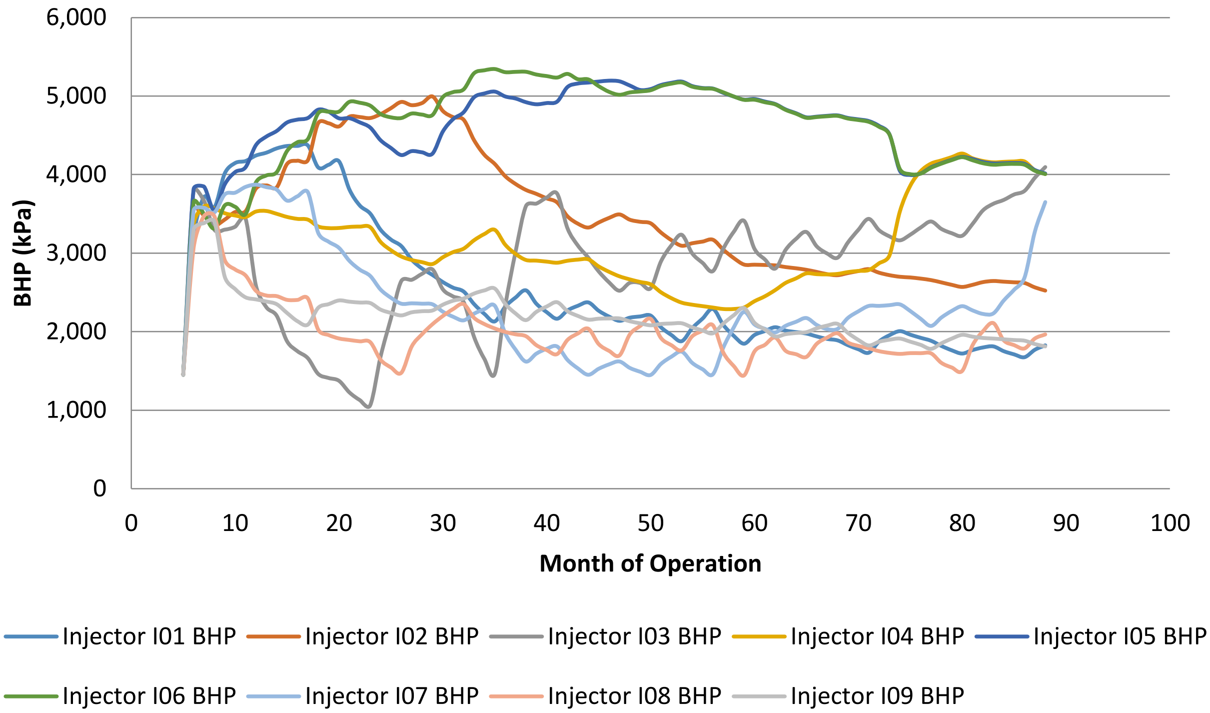

Figure 4-4: Injection pressure profiles in PID Case II.

The production indices calculated in Chapter Three for the wellpairs of PID Case II are plotted in Figure 4-5. Wellpairs 5 and 6 have the highest production indices among the nine wellpairs and their injection pressures, in PID Case II, are also the highest among the wellpairs. On the other hand, Wellpairs 1 and 8 are ranked the lowest in terms of production index; their injection pressure also declined to be the lowest among the wellpairs. As expected, the results suggest a direct relationship between the well production index and injection pressure.

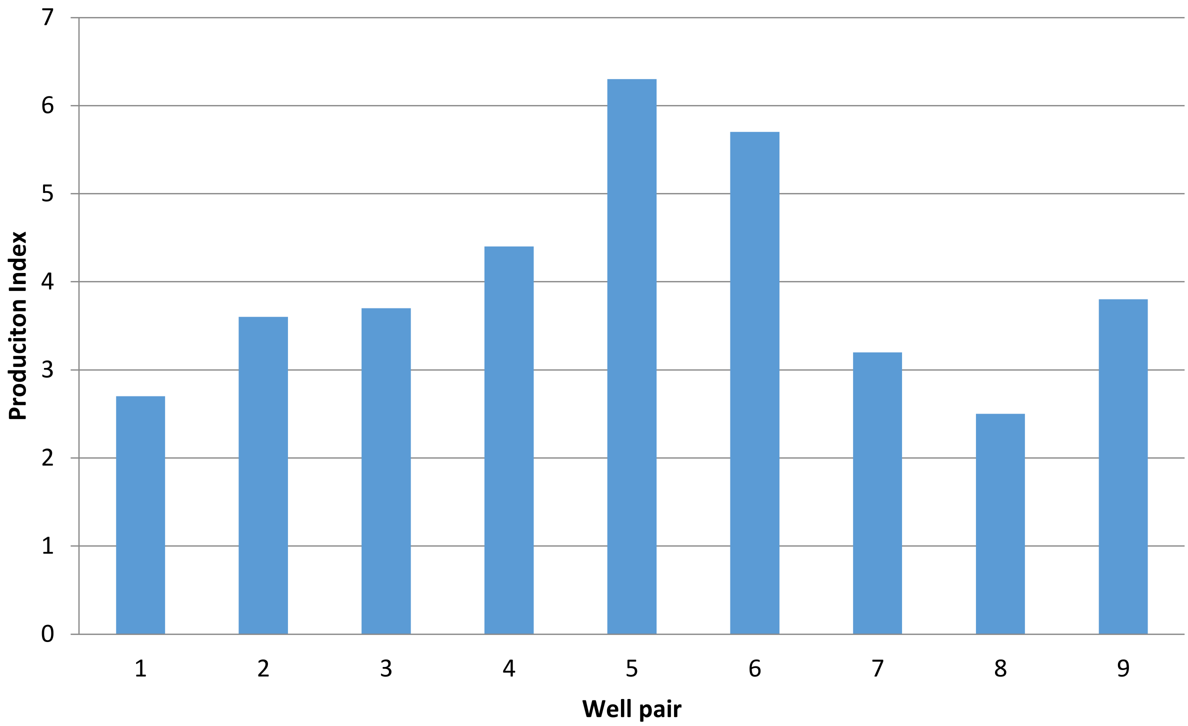

Figure 4-5: The production index of nine well pairs. The production index is calculated by dividing the average steam injection rate by the end-point of cumulative steam oil ratio in a constant injection pressure operation. The production index reflects local injectivity and oil saturation. A larger production index indicates a relatively better reservoir quality.

4.2.3 Steam injection rates from 9 well pairs

The steam injection rates of the well pairs are shown in Figure 4-6. The steam rates of PID Case II, in general, correlate well with the injection pressures (shown in Figure 4-4). Injectors 5 and 6 have the highest rates (and also the highest injection pressure) among the wellpairs. Also, Injectors 1 and 8 are among the lowest steam rates (and also the lowest injection pressure) among the well pairs. Injector 4 also shows gentle declining in the early to middle stages and a surge by the end of 70 month of operation, corresponding to the injection pressure profile.

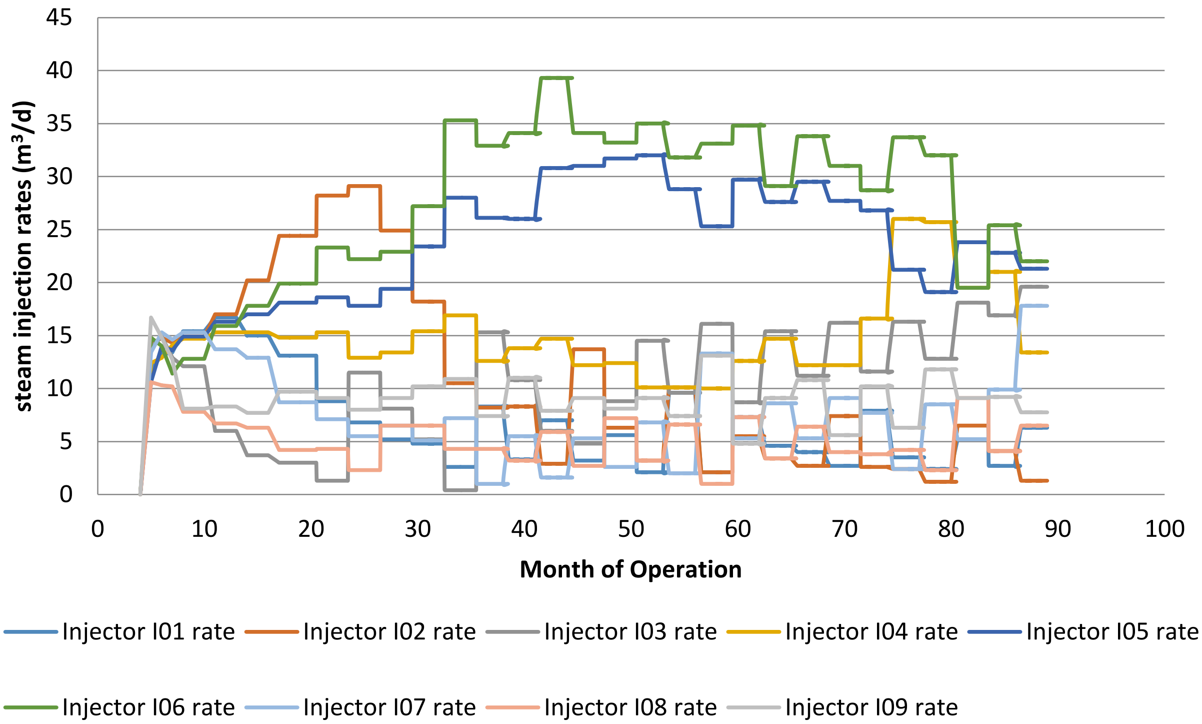

Figure 4-6: The well pair steam injection rate in PID Case II

In PID Case I, towards the end of operation, the steam injection rate profiles of the wellpairs become more flat. However, in PID Case II, steam rates adjustments are more dramatic. This reflects that the controller in PID case II has more difficulty approaching the target value. In PID Case I, if a reduction in steam rates is needed to reduce the cSOR, then the controller will reduce the rate for each well pair. However, in Case II, if, for instance, eight of the well pairs require a reduction of the steam rate, then it would not be completely satisfied because the pad steam rate is fixed. Thus, steam will be distributed in such a way that more steam is distributed to wellpairs that are less likely to surge iSOR with more steam injection and less steam is distributed to wellpairs that, even with a small increase in steam rates, would see an increase of iSOR. The sensitivity of iSOR to steam rates arises from the heterogeneity of the reservoir. Thus, in PID Case II, the target cSOR of $2.7m^3/m^3$ is rarely met simply due to the constant amount of steam injection that must be used.

In PID Case II, since the steam rates cannot be reduced as suggested by PID algorithm due to the steam plant constraint, the algorithm allocates steam to preferred wellpairs, as measured by the iSOR, which receive more steam whereas non-preferred wellpairs receive less steam. In other words, the algorithm is constantly looking for better spots, or sweet spots, by which we refer to those regions within formation, that have a better iSOR which reflects a relatively higher steam injectivity (a relatively higher permeability, lower amount or less extensive shale barriers, and higher oil saturation and drainage capability. If one well pair contains relatively homogeneous clean sands with high oil saturation, then according the PID control strategy done here, the majority of steam would be distributed to this zone.

4.2.4 cSOR Comparisons

Figure 4-7 displays the cSOR profiles for PID Case II wellpairs. A comparison of the pad-scale cSOR profiles of the base case, PID Case I, and PID Case II is shown in Figure 4-8. For PID Case II, the cSOR of well pairs ranges from 2.85 to 3.30 m^3/m^3. The window is wider compared to the cSOR ranges of PID Case I (2.72 to 2.96 m^3/m^3) but it is narrower compared to the non-controlled base case (2.67 to 3.68 m^3/m^3). Thus, PID control still improved the cSOR in the case with fixed steam plant capacity. At the end of the operation, at pad scale, PID Case II results in a cSOR equal to 3.09 m^3/m^3 whereas PID Case I results in a cSOR of 2.78 m^3/m^3 and the base case results in a cSOR equal to 3.30 m^3/m^3. PID Case II made a 7.2% cSOR improvement over that of the base case for exactly the same amount of steam injection. This reflects improved oil production from the reservoir.

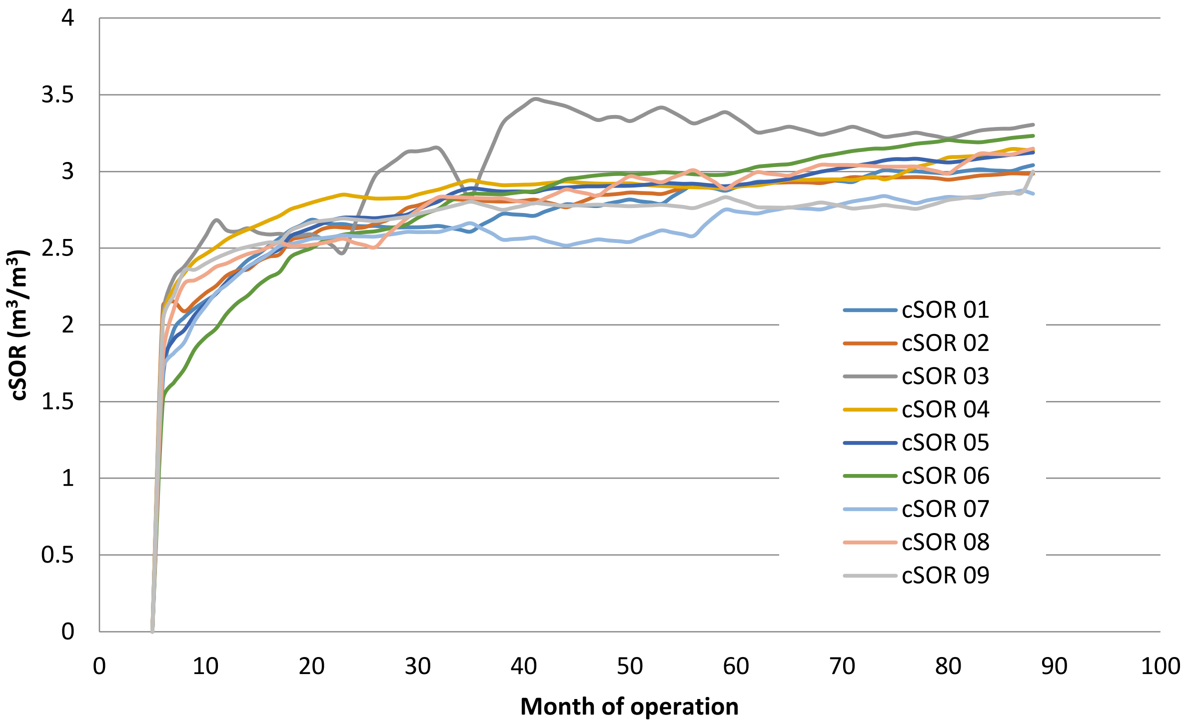

Figure 4-7: The cumulative steam to oil ratio of well pairs in PID Case II.

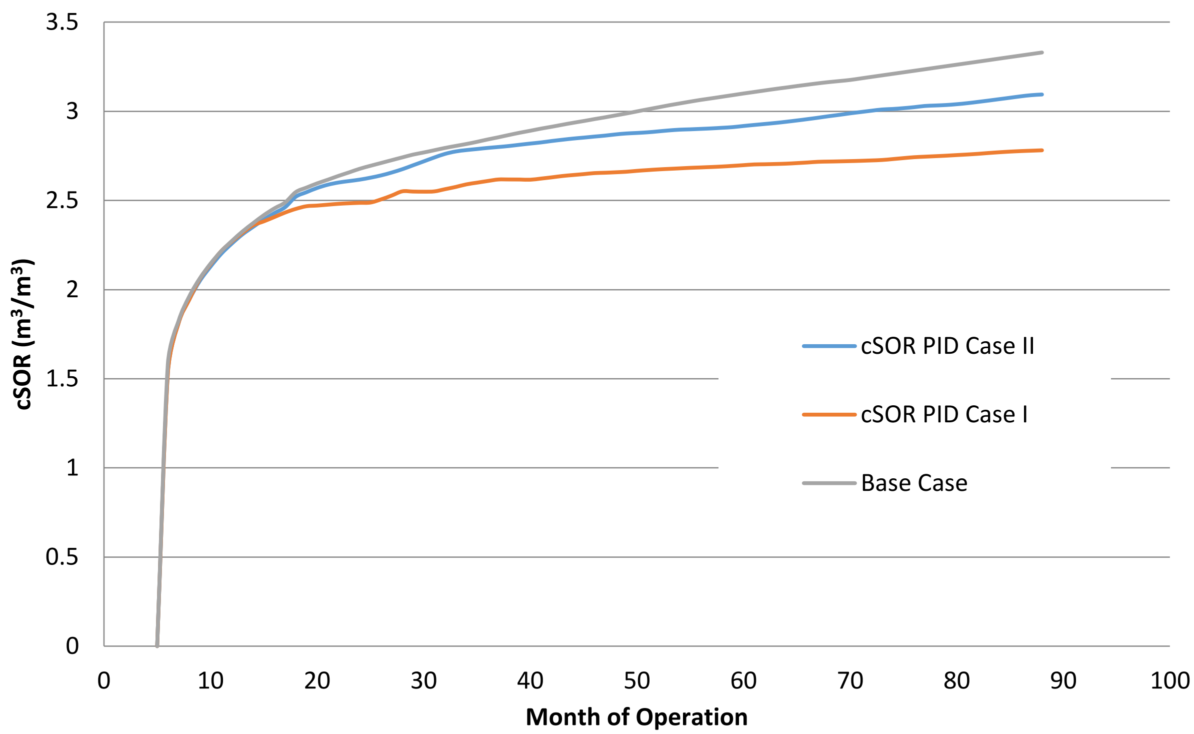

Figure 4-8: Comparison of overall cSOR profiles for base case, PID Case I, and PID Case II.

4.2.5 Cumulative Oil Production

The cumulative oil produced in the base case, PID Case I and PID Case II are compared in Figure 4-9. The results show that the cumulative oil recovery for PID Case II is 5.6% higher than that of the base case. The results confirmed the effectiveness of novel PID control algorithm in SAGD, since both the cSOR and oil recovery have seen improvement over base case, for the same steam rates. In other words, for the same energy input, PID control managed to output more oil recovery. The results of all three cases are summarized in Table 4-2 below for reference.

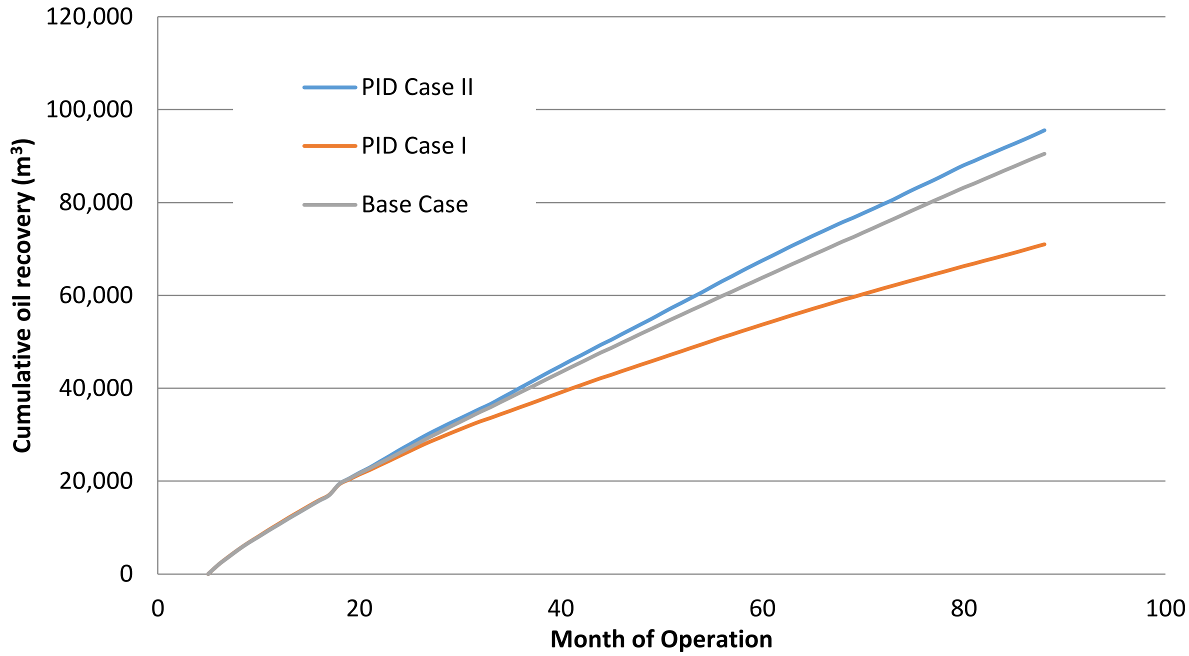

Figure 4-9: Cumulative oil recovery of base case, PID Case I, and PID Case II.

Table 4-2: Summary of results for base case, PID Case I, and PID Case II.

	cSOR, m^3/m^3	Cum. Steam Injection, m^3 per m length of well pair	Cum. Oil Production, m^3 per m length of well pair
Base Case	3.33	12,094	3,621
PID Case I	2.78	7,982	2,897
PID Case II	3.10	12,021	3,838

4.3 Mechanisms and Discussion

The steam chambers surrounding the wellpairs are displayed in Figure 4-10 after 7 years of SAGD operation. The top image shows the steam chamber for the base case, the middle one is PID Case I, and the bottom one shows the chambers for PID Case II. The ternary diagram illustrates the phases present in the system: the red color represents 100 per cent gas phase, the green color represents 100 per cent oil phase, and the blue color represents

100 per cent water (aqueous) phase. Thus, any color close to purple represents largely steam with various amounts of oil and water.

To compare the base case and PID Case II, the steam chambers surrounding Wellpairs 5 and 6 exhibit a large difference in steam conformance among the cases. In PID Case II, the steam chambers have merged and a significantly larger region in between the wellpairs has been recovered. The production indices indicated that Wellpairs 5 and 6 are among the best and the results in Figure 4-10 reveals that in PID Case II, the control algorithm injects more steam to those regions. In contrast, the steam chamber of Wellpair 8 in PID Case II is smaller than that in the base case. Again, referring to the production index, Wellpair 8 obtained the lowest score among all nine wellpairs due to the extended shale barriers above the injector, shown in Figure 4-11. Wellpair 8 has the smallest steam chamber among all of the wellpairs. Thus, it is fair to say that the control algorithm again, dynamically distributed much less steam to the relatively less productive regions of the reservoir as indicated by the iSOR.

Steam chooses the least resistant path to flow within the reservoir. As a consequence, less productive regions (with lower permeability, less oil content) will have less steam flow whereas more productive regions (with higher permeability and greater oil content which when produced leads to enhanced relative permeability of the gas phase leading to greater steam flow) attract steam flow. The PID controllers, by using the iSOR as the measure of the productivity of oil and injectivity of steam are emphasizing this tendency to produce the better quality parts of the reservoir over that of the poorer quality parts. The merging of the steam chambers associated with Wellpairs 5 and 6, as discussed previously, reflects that the PID algorithm purposely directs more steam to the more productive regions more so than if you had constant pressure injection as is the case in the base case. For Wellpair 8, the steam chamber under PID control is relatively small. This reflects that the PID algorithm directed less steam to this wellpair to direct the process to the iSOR set point.

The base case and PID Case I show quite similar phase distributions at the end of the operation. However, wells with lower production index, that is, Wellpairs 1, 7, and 8 all show smaller sizes in the PID Case I, indicating that PID control reduced steam injection in those regions to achieve the overall iSOR target. The results also show that steam losses to the top water zone occur above Wellpair 9.

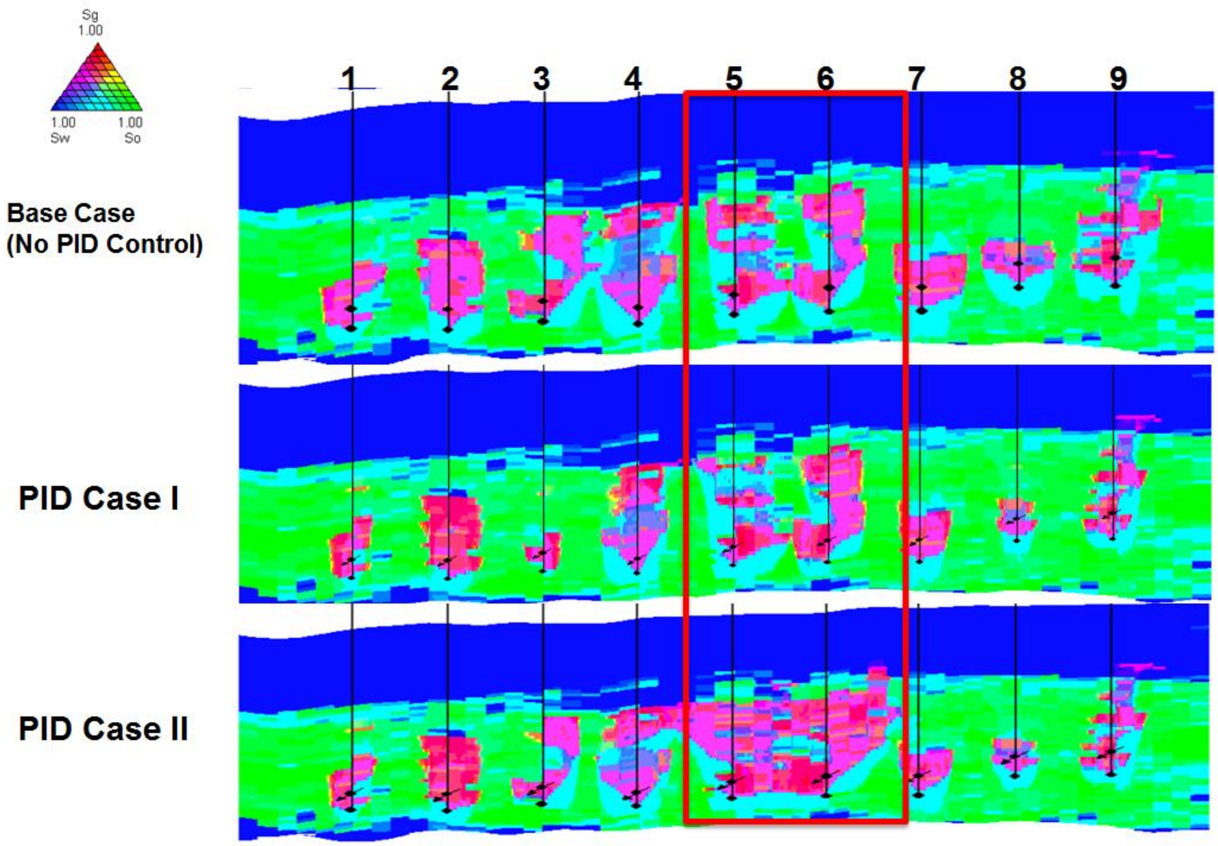

Figure 4-10: The steam chambers after 7 years SAGD for base case, PID Case I and PID Case II.

The vertical permeability, shown in the Figure 4-11, reveals that a significant control on the steam chamber growth is shale barriers. In the vertical permeability plot, the scale is set to a maximum of 100 mD. The overburden, consists of mostly silts, has relatively low permeability. For the oil column, the location and extension of shale barriers vary from wellpair to wellpair, and this is one of the fundamental factors that determines Wellpair performance (or more specifically, the steam injectivity and oil productivity). The relationship between shale barriers and injectivity is straightforward. Take for example Wellpair 8 which has the poorest performance. Several extensive low permeability layers exist above the injection well. On the other hand, the highest injectivity wellpair, 4, is located in a relatively clean area, where no major low permeability layer exists.

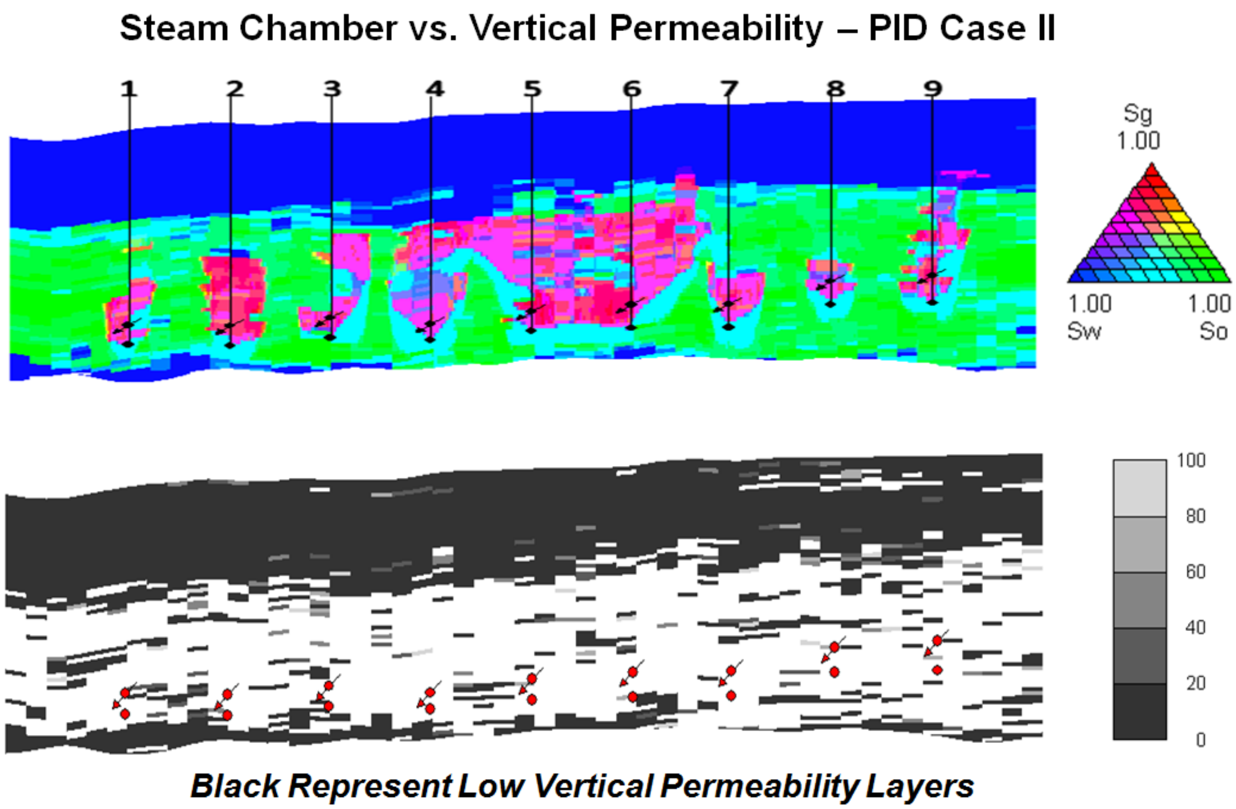

Figure 4-11: The steam chamber of PID Case II and the vertical permeability distribution (in mD, the white regions of the model have vertical permeability greater than 100 mD).

A comparison between the steam chamber of PID Case II and the vertical permeability, again confirms that the PID control algorithm is distributing the majority of the steam to more productive parts of the reservoir. For wellpairs with extensive low permeability nearby, for example, Wellpair 8, a limited steam rate is assigned, which is sufficient to keep the wellpair warm enough so that the steam chamber does not cool down; however, the chamber does not grow significantly as the process evolves. For well pairs with relatively few low permeability layers, for example, Wellpair 4, a greater amount of steam is allocated to enhance the oil rate from this well. As for the rest of wells, location and size of low permeability layers show different patterns. Wellpair 1 has thick shale barriers above but not as close as the layers in Wellpair 8; the steam chamber has an initial growth potential and steam flow to the oil-bearing zone above the shale layers is easier than is the case for Wellpair 8. Wellpair 3 has several short layers just above the injection well and a short thin layer between the wells. Wellpair 9 has short layers randomly imbedded in the formation but none provide a complete barrier to flow.

Although insights can be determined from log, core, and seismic data, the location and lateral extents of shale barriers are unpredictable within the reservoir. This probably is the most difficult thing to deal with in SAGD operation, but meanwhile, this also allows PID control with iSOR as target value to show its value in steam distribution since the iSOR is sensitive to both the existence of shale barriers (steam injectivity and oil drainage) and the oil saturation (production index).

Figure 4-12 shows the individual steam injection rates for the wellpairs of PID Case II in the context of the vertical permeability distribution with focus on the Wellpair 1 and 8 rates. Something Wellpairs 1 and 8 shares in common are their low rates and the extended shale barriers on top of injectors. However, the distance between the barrier and injection wells is larger in Wellpair 1 than is the case for Wellpair 8. Thus, the Wellpair 1 rate rises in the early stage, indicating a degree of steam chamber growth, until the barriers are reached. Thereafter, because the iSOR suffers, the PID controller reduced the steam injection rate (after about 10 months of operation) to lower the iSOR. The Wellpair 8 injection rate starts to drop earlier due to the closer proximity of the barrier to the injection well. Figure 4-13 focuses on the Wellpair 2 and 3 rates. The Wellpair 2 rate is among the highest in the early stage. This makes sense according to the vertical permeability distribution since no shale barriers exist. High steam injection rates and oil drainage rates accelerate steam chamber growth and after 24 months of operation, the chamber reaches the top of the oil column. After the chamber reached the top of the oil column, the PID controller sensed the high iSOR signal and reduced the steam injection rate. The Wellpair 3 injection rate, in contrast, dropped quickly in the early stage, since it is relatively close to a shale barrier which sits to the left of the injection well. As steam injection continues, the steam chamber grows towards the more productive direction and steam by-passes the barrier, and since the iSOR indicates good performance, the PID controller directs more steam to that region.

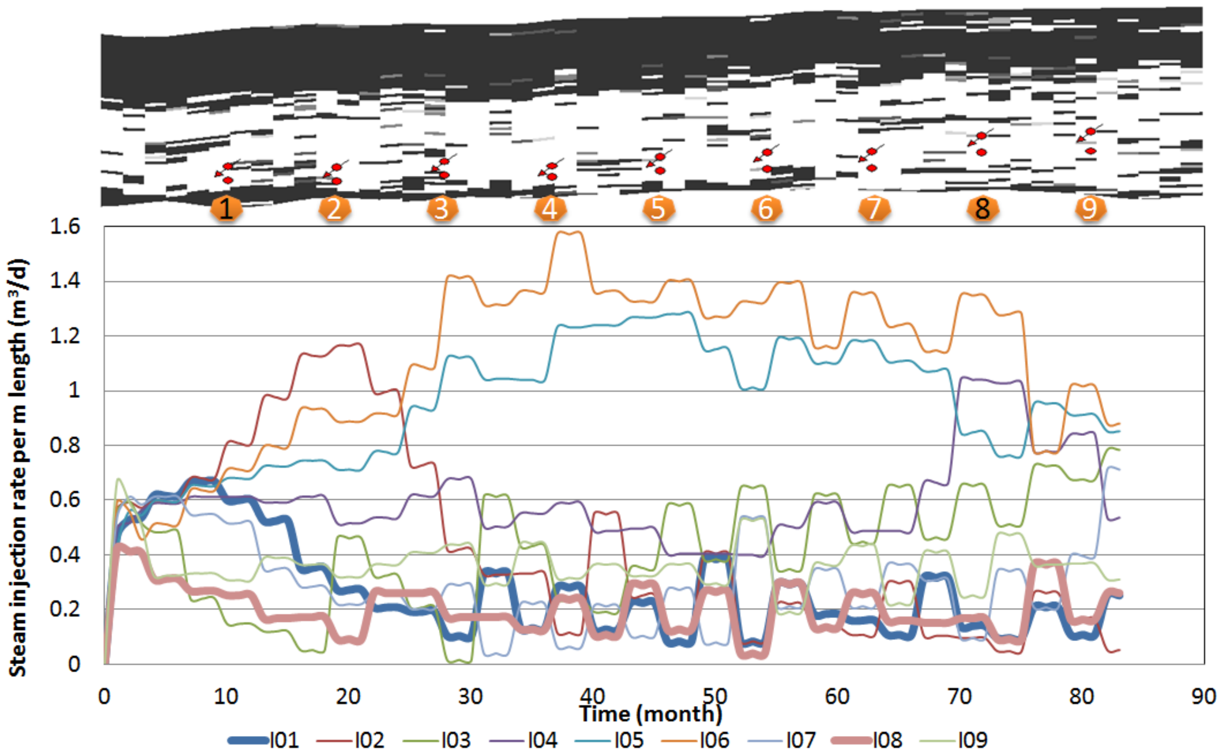

Figure 4-12: PID Case II steam injection rates and vertical permeability distribution: Wellpairs 1 and 8 rates are bolded.

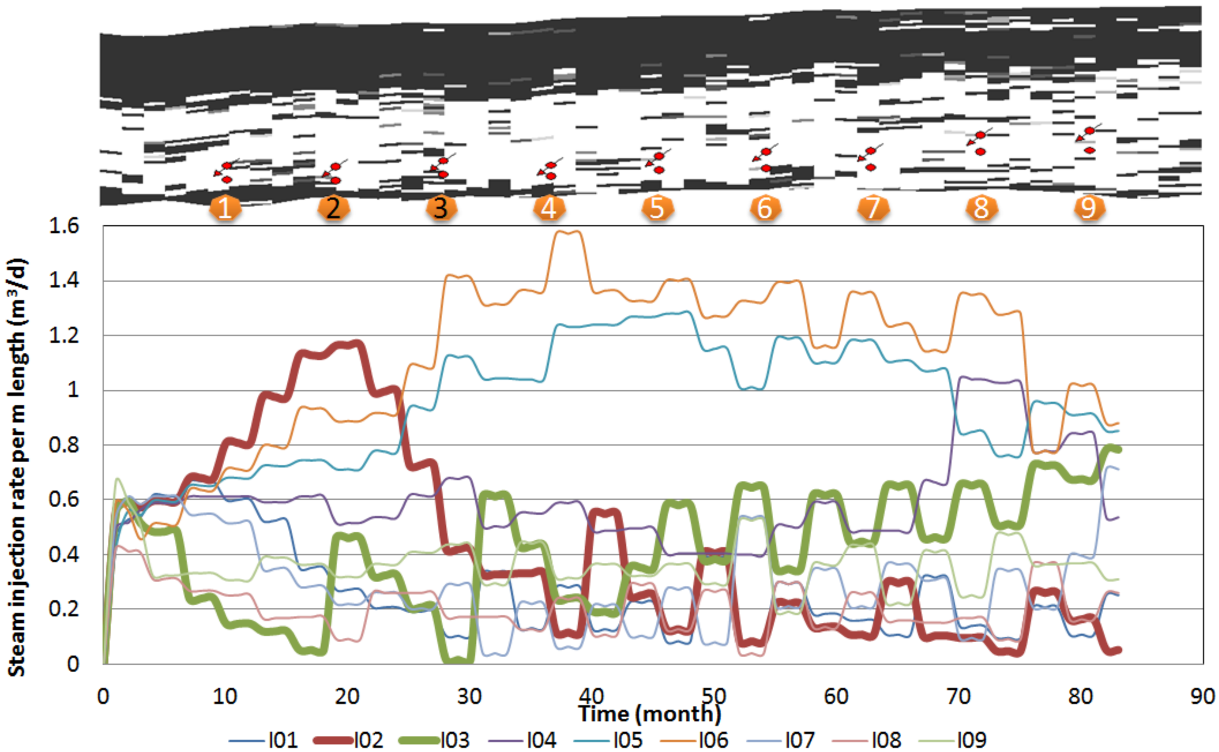

Figure 4-13: PID Case II steam injection rates and vertical permeability distribution: Wellpairs 2 and 3 rates are bolded.

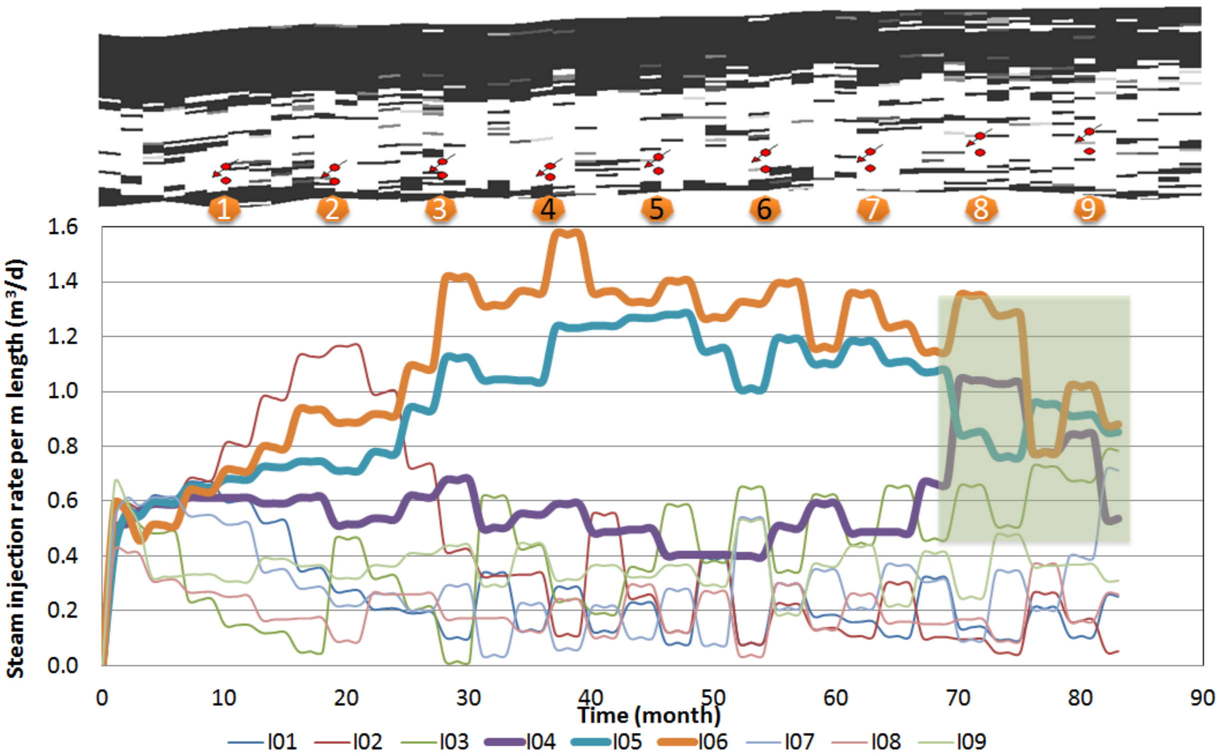

Figure 4-14: PID Case II steam injection rates and vertical permeability distribution: Wellpairs 4, 5, and 6 rates are bolded.

Wellpairs 5 and 6 have high production index which results from the lower amounts of shale barriers and relatively higher oil saturation near to the wellpairs. After 70 months of operation, the steam chambers of these three wellpairs merge but before that time, Wellpair 4 has a distinctive rate trend which is different from that of Wellpairs 5 and 6. After the chambers merge, the Wellpair 4 steam injection rate surges to that of Wellpairs 5 and 6. After the chambers merge, there is essentially only one steam chamber surrounding the three wellpairs. In terms of control, this could be an adverse factor. Since after chambers merge, discrete steam injection into each wellpair loses accuracy since the injected steam would more easily flow to regions surrounding Wellpairs 5 and 6. Also, the obtained iSOR for each well pair would no longer reflect the local heterogeneity but instead represent the overall heterogeneity of the extended region surround the three wellpairs.

On the other hand, merging of steam chambers can be beneficial. For example, the early merging of the steam chambers surrounding Wellpairs 5 and 6 allows the steam injected at 5 to flow over the shale barriers in the near Wellpair 6 region thus providing access to oil above the barrier. With steam injected from 5, the steam chamber growth in the 6 region is accelerated. In addition, most cold spots between I05 and I06 are swept due to the early coalescence of the steam chambers.

4.4 Conclusions

The results of this chapter show that PID control algorithm, given a fixed pad steam rate constraint, dynamically distributes steam to multiple wellpairs, according to the production index of each well pair. Thus, on pad-scale, the utilization of given steam would be maximized and better thermal efficiency is achieved. The results also reveal that the instantaneous steam-to-oil ratio provides an excellent signal to measure the steam injectivity, oil mobilization and drainage, and oil storage in the context of a heterogeneous reservoir.

Chapter Five: **Conclusions and Recommendations**

The conclusions are as follows:

1. PID feedback control can be used to shift the steam-to-oil ratio to target value in SAGD. This has important implications for improvements of greenhouse gas emissions since the amount of fuel consumed is directly tied to the steam requirement. Furthermore, less steam use per unit volume of oil produced implies lower water consumption. Thus, PID control offers a means to reduce the environmental intensity of SAGD.
2. The instantaneous steam-to-oil ratio (iSOR) provides a signal that measures the injectivity of the steam, the storage and mobilization of oil, the heterogeneity of the reservoir, and the oil drainage rate. It is the ratio of the daily amount of steam injected (expressed as cold water equivalent) to the volume of oil produced. The results suggest that greater attention should be paid to the iSOR. In most operations, the cumulative steam-to-oil ratio is the most observed energy efficiency measure but this gives an integrated and smoothed out version of the steam-to-oil ratio that potentially masks the daily (and short time scale) evolution of the process.
3. The automated controlled case where there is no constraint on the total steam injection rate to the pad (PID Case I) exhibits a decreasing injection pressure trend which is consistent with previous research and ongoing SAGD field operations. However, since the amount of steam injected into the formation declines as the operation proceeds, the amount of oil recovered suffers.
4. The PID control algorithm for the case when the total pad steam rate is fixed (PID Case II) dynamically distributes steam to multiple wellpairs according to the production index of each well pair and yields improvements of the overall steam-to-oil ratio. Since the amount of steam injected into the pad is constant through time, the volume of oil produced from the pad does not suffer.
5. The study provides a detailed work flow for PID controlled SAGD operation in which the iSOR is used to guide steam injection rate, so as to achieve target cSOR in the long run.

The recommendations are as follows:

1. The control algorithm must be tested on three-dimensional models to verify that it can handle the response in systems with three-dimensional heterogeneity.
2. The combination of PID control using the subcool temperature difference and instantaneous steam-to-oil ratio should be investigated. Also, the use of thermocouple or 4D seismic data to monitor steam conformance should be included in the control strategy.
3. Alternative controllers to the PID controller should be evaluated for improved performance of the controller.

References

Araki M., 2009. *Control Systems, Robotics, and Automation*. Vol. II. PID Control

Astrom K., Hagglund T. 1995. *PID Controllers: Theory, Design, and Tuning.* Instrument Society of America. ISBN 1-55617-516-7

Banerjee S., Abdelfatah T., Nguyen H., 2013. Benefits of Passive Inflow Control Devices in a SAGD Completion. Paper SPE 165478 presented at the SPE Heavy Oil Conference Canada. Calgary, Alberta, Canada. 11-13 June 2013

Christophe B. 2012. *Designing Control Loops for Linear and Switching Power Supplies: A Tutorial Guide*. Artech House. ISBN 978-1608075577

Stuart B. 1984. Nicholas Minorsky and the automatic steering of ships. IEEE Control System Magazine 4. 10-15. 1984. ISSN 0272-1708

Stuart B. 1993 *A History of Control Engineering* 1930-1955. IET. pp. 48. ISBN 978-0-86341-299-8

Bois A., Tec C. Mainguy M., 2013. Importance of Thermal Consolidation of Shale During SAGD Process. Paper SPE 150420 presented at the SPE Heavy Oil Conference and Exhibition. Kuwait City, Kuwait. 12-14 December 2011

Butler, R.M. 1997. *GravDrains's Blackbook: Thermal Recovery of Oil and Bitumen*. GravDrain Inc. Calgary, Alberta. ISBN 0-9682563-0-9

Banerjee S., Abdelfattah T., Nguyen H., 2013. Benefits of Passive Inflow Control Devices in a SAGD Completion. Paper SPE 165478 presented at the SPE Heavy Oil Conference Canada. Calgary, Alberta, Canada. 11-13 June 2013

Clark H.P., Ascanio F.A., Kruijsdijk V., Chavarria J.L, Zatka M.J., Williams W., Yahyai A., Shaw J., Bedry M., 2010. Method to Improve Thermal EOR Performance Using Intelligent Well Technology: Orion SAGD Field Trial. Paper SPE 137133 presented at the Canadian Resources & International Petroleum Conference. Calgary, Alberta, Canada. 19-21 October 2010

CMG 2011 Computer Modelling Group STARS™ User Manual, Version 2011. Calgary, Alberta, Canada.

Card C. C., Chakrabarty N., Gates I. D. 2006 Automated Global Optimization of Commercial SAGD Operations. Paper 2006-157 is presented at the Petroleum Society 7th Canadian International Petroleum Conference. Calgary, Alberta, Canada. 13-15 June 2006

ConocoPhillips. 2007-2013. ERCB Annual Update: Surmont Project. In-Situ Process Reports, Alberta Energy Resources Conservation Board, Calgary, Alberta. 2007-2013.

Ezeuko C.C., Wang J., Sen A., Gates I.D., 2011. A New Perspective on Tracking Energy Transfer in SAGD during Three-Dimensional Numerical Field-Scale Simulations. SPE paper 150692 is presented at the SPE Heavy Oil Conference and Exhibition, Kuwait City, Kuwait. 12-14 December 2011

Energy Resources Conservation Board. 2012. ST98-2012 Alberta's Energy Reserves 2011 and Supply/Demand Outlook 2012-2021. ISSN 1910-4235

Fustic M., Bennet B., Hubbard S. M., Huang H., Oldenburg T., Larter S. 2012. Impact of reservoir heterogeneity and geohistory on the variability of bitumen properties in the Athabasca Oil Sands. Canada. In Hein F. J., Leckie D., Larter S., Suter J., eds., Heavy oil and oil sand petroleum systems in Alberta and beyond: *AAPG Studies in Geology*., v. 64, 42 pp.

Franklin. Et al. 2002. *Feedback Control of Dynamic Systems* (4th ed.). New Jersey: Prentice Hall. ISBN 0-13-032393-4

Gotawala D. and Gates I.D. 2009. SAGD Subcool Control With Smart Injection Wells. Paper SPE 122014 presented at the SPE EUROPEC/EAGE Annual Conference and Exhibition, Amsterdam, The Netherlands, 8-11 June 2009

Gotawala D. and Gates I.D. 2012. A Basis for Automated Control of Steam Trap Subcool in SAGD. SPE J.

Graham J., Olson J., Pinguet B., Abraham A. 2012. The Benefits of Multiphase Flow Meters in SAGD for Production Optimization and Allocation Measurements. Paper SPE 157915 presented at the SPE Heavy Oil Conference Canada. Calgary, Alberta, Canada. 12-14 June 2012

Graham G. 2001. *Control System Design.* Prentice Hall. ISBN 0-13-958653-9

Guyaguler B., Papadopoulos A.T., Philpot J.A. 2009. Feedback Controllers for the Simulation of Field Processes. Paper SPE 118969 presented at the SPE Reservoir Simulation Symposium, Woodlands, Texas, USA. 2-4 February 2009

Hubbard S.M., Smith D.G., Nielsen H., Leckie D.A., Fustic M., Spencer R.J., Bloom L. 2011. Seismic geomorphology and sedimentology of a tidally influenced river deposit, Lower Cretaceous Athabasca oil sands, Alberta, Canada. The American Association of Petroleum Geologists. V. 95, No. 7, PP. 1123-1145.

Hyanpour M., Chen Z., 2013. A New Approach for Designing Steam Splitters and Inflow Control Devices in Steam Assisted Gravity Drainage. Paper SPE 165487 presented at the SPE Heavy Oil Conference Canada. Calgary, Alberta, Canada. 11-13 June 2013

Li W., Mamora D.D., Li Y., Qiu F. 2011. Numerical Investigation of Potential Injection Stratefies to Reduce Shale Barrier Impacts on SAGD Process. Paper presented at the SPE Western Regional Meeting. Anaheim, California, USA. 25-28 May 2010

Kuo B., C., 1991. *Automatic Control Systems* (6^{th} ed.). New Jersey: Prentice Hall. ISBN 0-13-051046-7

Medina M., 2013. Design and Field Evaluation of Tubing Deployed Passive Outflow Control Devices in SAGD Injection Wells. Paper 165563 presented at the SPE Heavy Oil Conference Canada. Calgary, Alberta, Canada. 11-13 June 2013

Shin H., Choe J. 2009. Shale Barrier Effects on the SAGD Performance. Paper SPE 125211 presented at the SPE/EAGE Reservoir Characterization and Simulation Conference. Abu Dhabi, UAE. 19-21 October 2009

Su Y., Wang J. Y., Gates I.D., 2012. SAGD Well Placement in Ultra-Defined Point Bar Deposit. Paper SPE 157857 presented at the SPE Heavy Oil Conference. Calgary, Alberta, Canada 12-14 June 2012

Stone T., Guyaguler B., Bailey W.J., Damas C.E.P., Naccache P.F., Morton A. 2010. Dynamic SAGD Well Flow Control Simulation. Paper CSUG/SPE 138054 presented at the Canadian Unconventional Resources & International Petroleum Conference. Calgary, Alberta, Canada. 19-21 October 2009

Stone T., Brown G., Guyagular B., Bailey W.J., Law D.H.S. 2011. Practical Control of SAGD Wells with Dual Tubing Strings. Paper CSUG/SPE 149352 presented at the Canadian Unconventional Resources Conference. Calgary, Alberta, Canada. 15-17 November 2011

Stone T., Damas C.E.P., Woiceshyn G., Law D.H.S., Brown G., Olapade P., Bailey W.J. 2013. Advanced Wellbore Simulation of Flow Control Devices With Feedback Control for Thermal Operations. Paper SPE 163594 presented at the SPE Reservoir Simulation Symposium. Woodlands, Texas, USA. 18-20 February 2013.

Stone T., Law D.H.S., Bailey W.J. 2013. Control of Reservoir Heterogeneity in SAGD Bitumen Processes. Paper PSE 165388 presented at the SPE Heavy Oil Conference Canada. Calgary, Alberta, Canada. 11-13 June 2013

Stalder J., 2013 Test of SAGD Flow-Distribution-Control Liner System in the Surmont Field, Alberta, Canada. Journal of Canadian Petroleum Technology.

Schlumberger 2012 Petrel User’s Manual.

William L., S., ed. 1996. *The Control Handbook.* New York. CRC Press. ISBN 978-0-8493-8570-4

Xie J., Jones, S. W., Mattews C. M., Wagg B. T., 2007. Slotted liner design for SAGD wells. *World Oil*. Pg. 67-75. June 2007

Yang, G., Butler, R.M. 1992. Effects of reservoir heterogeneities on heavy oil recovery by steam-assisted gravity drainage. *The Journal of Canadian Petroleum Technology* 31 (8): 37-43